รายงานวิจัยฉบับสมบูรณ์

โครงการ การศึกษาการสร้างและการพัฒนาที่สมบูรณ์ของเซลล์สืบพันธุ์เพศผู้และขบวนการขดแน่นของใยโครมาตินในหนูพุกใหญ่

MALE GERM CELL MATURATION AND CHROMATIN CONDENSATION OF THE ASIAN BANDICOOT RAT (*BANDICOTA INDICA*)

โดย

รองศาสตราจารย์ ดร. ประพีร์ เศรษฐรักษ์

และ

นางสาว ภควดี วรวิทยาวงศ์

ธันวาคม 2547

สัญญาเลขที่ BGJ/37/2543

รายงานวิจัยฉบับสมบูรณ์

โครงการ การศึกษาการสร้างและการพัฒนาที่สมบูรณ์ของเซลล์สืบพันธุ์เพศผู้และขบวนการขดแน่นของใยดินในหนูพุกใหญ่

MALE GERM CELL MATURATION AND CHROMATIN CONDENSATION OF THE ASIAN BANDICOOT RAT (*BANDICOTA INDICA*)

คณะผู้วิจัย

1. รองศาสตราจารย์ ดร. ประพีร์ เศรษฐรักษ์
   ภาควิชากายวิภาคศาสตร์ คณะวิทยาศาสตร์
   มหาวิทยาลัยมหิดล
2. นางสาว ภควดี วรวิทยาวงศ์
   นักศึกษาปริญญาเอก ภาควิชากายวิภาคศาสตร์
   คณะวิทยาศาสตร์ มหาวิทยาลัยมหิดล

สนับสนุนโดยสำนักงานกองทุนสนับสนุนการวิจัย

ACKNOWLEDGEMENT

This work was supported by the Thailand Research Fund, BGJ/37/2543 and Royal Golden Jubilee (RGJ) Ph.D. Program Grant No. PHD/0119/2542

ABSTRACT

Project Code : BGJ/ 37/ 2543

Project Title : Male Germ Cell Maturation and Chromatin Condensation of the Asian Bandicoot Rat (*Bandicota indica*)

Investigator : Assoc. Prof. Prapee Sretarugsa, Miss Pakawadee Worawittayawong. Department of Anatomy, Faculty of Sciences, Mahidol University

E-mail Address : scpsr@mahidol.ac.th and pkwd18@yahoo.com

Project Period : 4 Years

Bandicoot rat, *Bandicota indica* is one of the rodent species that commonly occurs in the rice fields of Thailand. It causes considerable damage to the rice fields crops and is thus of considerable economic importance to the country. The knowledge of its reproductive biology could be useful for controlling number of the animals. The aims of this study are, therefore: 1) to investigate the cycle of seminiferous epithelium by light microscopy; 2) to study the organization and chromatin condensation of germ cells during spermiogenesis by electron microscopy; 3) to localize the basic nuclear proteins during spermiogenesis by immunocytochemistry and immunoelectron microscopy; 4) to characterize the sperm basic nuclear proteins profile by acid urea triton-X gel electrophoresis.

Seminiferous tubules of *B. indica* could be characterized into nine stages based on the morphological changes of spermatogenic cells along with the pattern of cellular association. This seminiferous cycle was considerable of heterogenous type, i.e., more than one cellular association pattern could be found in a cross section of seminiferous tubule. During maturation process, epididymal sperm exhibited more than seven types of head morphology as assessed by propidium iodide staining. Further attempt was launched to study the nucleoprotein components in the sperm nuclei that modulate chromatin condensation. Immunocytochemical analysis clearly demonstrated that histones remained throughout late spermiogenesis. This histone remnant was not detected within the nuclear vacuoles. Histones were also present in epididymal sperm as demonstrating by acid urea gel. It was also apparent that there were transition protein (TP) and protamines in epididymal sperm, however, the amount of TP proteins seem to be much higher than protamine as compared by the intensity of Coomassie Blue staining. These results were in marked contrast to other mammals studied so far, where protamine was shown to be a predominant basic protein in mature sperm. The functional implication of the abundance of TP and lower amount of protamines need further investigation.

Keywords : germ cell association, seminiferous epithelium, chromatin condensation, spermiogenesis, Bandicota indica

บทคัดย่อ

รหัสโครงการ : BGJ/ 37/ 2543

ชื่อโครงการ : การศึกษาการสร้างและการพัฒนาที่สมบูรณ์ของเซลล์สืบพันธุ์เพศผู้ของหนูพุกใหญ่

ชื่อนักวิจัย : รศ. ดร. ประพีร์ เศรษฐรักษ์ และ น.ส. ภควดี วรวิทยาวงศ์

E-mail Address : scpsr@mahidol.ac.th and pkwd18@yahoo.com

ระยะเวลาโครงการ : 4 ปี

หนูพุกใหญ่ *Bandicota indica* จัดอยู่ในพวกสัตว์แทะ (rodent) ที่พบได้ในนาข้าว หนูพวกนี้เป็นตัวการที่สำคัญที่ทำลายพืชเศรษฐกิจในไร่นา ซึ่งมีผลกระทบไปถึงเศรษฐกิจที่สำคัญของประเทศ การศึกษาหาความรู้ทางด้านชีววิทยาของระบบสืบพันธุ์ของหนูพุกใหญ่นี้น่าจะเป็นประโยชน์ในการควบคุมจำนวนประชากรของสัตว์ประเภทนี้ได้ในกรณีที่มีจำนวนมากเกินไป วัตถุประสงค์ในการศึกษาครั้งนี้คือ 1. ศึกษาวงจรของเซลล์สืบพันธุ์ในหลอดสร้างอสุจิโดยกรรมวิธีจุลทรรศน์ธรรมดา 2. ศึกษาการจัดเรียงตัวและการขดตัวของเส้นใยโครมาตินของเซลล์สืบพันธุ์ในช่วงของการพัฒนาที่สมบูรณ์โดยกรรมวิธีจุลทรรศน์อิเล็คตรอน 3. หาตำแหน่งและการกระจายตัวของโปรตีนในนิวเคลียสของอสุจิในช่วงการพัฒนาขั้นท้าย ๆจนถึงขั้นสมบูรณ์โดยวิธีอิมมูโนซัยโตเคมิสตรี (immunocytochemistry) และอิมมูโนอิเล็กตรอน (immunoelectron microscopy) 4. เพื่อหาลักษณะเฉพาะของโปรตีนที่เกิดขึ้นในนิวเคลียสของอสุจิโดยการแยกโปรตีนด้วยกระแสไฟฟ้า

การจัดเรียงตัวของเซลล์สืบพันธุ์ภายในหลอดสร้างอสุจิของหนูพุกใหญ่สามารถแบ่งได้เป็น 9กลุ่ม ตามความสัมพันธ์ของเซลล์สืบพันธุ์ขั้นต่าง ๆที่จัดเรียงตัวกันในระหว่างการสร้างเซลล์อสุจิ ในภาพตัดขวางของหลอดสร้างอสุจิพบเซลล์สืบพันธุ์มีการจัดเรียงตัวมากกว่าหนึ่งกลุ่ม ซึ่งแตกต่างกับพวกหนู rat หรือหนู mouse แต่จะคล้ายกับในคน ในขบวนการสร้างเซลล์สืบพันธุ์พบว่ารูปร่างหัวของเซลล์อสุจิจากอิพิดิไดมิส มีมากกว่า 7 ชนิด เมื่อศึกษาด้วยการย้อมด้วย propidium iodide จากการวิเคราะห์ด้วย อิมมูโนซัยโตเคมิสตรี พบว่าโปรตีนฮิสโตนยังคงมีอยู่ในนิวเคลียสของเซลล์สืบพันธุ์ขั้นท้าย ๆจนถึงขั้นที่พัฒนาสมบูรณ์ แต่ไม่พบโปรตีนชนิดนี้ในช่องว่างที่อยู่ในนิวเคลียส ยิ่งไปกว่านั้น เมื่อศึกษาด้วยเจลอิเล็กโตรโฟเรซิส พบว่าโปรตีนฮิสโตนยังมีอยู่ในนิวเคลียของเซลล์อสุจิที่ได้จากท่ออิพิดิไดมิส และยังพบโปรตีนทรานสิชั่น และโปรตีนโปรตามีน เมื่อเปรียบเทียบความเข้มข้นของสีย้อม Coomassie Blue ดูเหมือนปริมาณของโปรตีนทรานสิชั่นมีมากกว่าโปรตีนโปรตามีน จากผลการทดลองนี้ แสดงให้เห็นว่าหนูพุกใหญ่ มีความแตกต่างจากสัตว์เลี้ยงลูกด้วยนมอื่น ๆที่มีโปรตีนโปรตามีนเป็นโปรตีนหลักสำคัญในหัวอสุจิที่เจริญเต็มวัย การที่นิวเคลียสของอสุจิของหนูพุกใหญ่มีปริมาณโปรตามีนค่อนข้างต่ำ จากการศึกษาขณะนี้ยังไม่สามารถหาคำอธิบายได้ ซึ่งควรจะต้องศึกษาเพิ่มเติมต่อไป

CONTENTS

CONTENTS (CONT.)

LIST OF TABLES

Table **Page**

LIST OF FIGURES

Figures **Page**

LIST OF FIGURES (CONT.)

Figures **Page**

INTRODUCTION

Southeast Asia lies in the tropical zone and was once largely covered by rain forest. Much of the land has now been cleared for agriculture and other activities associated with humans. The mammals of Southeast Asia include a number of rain forest species together with a few that have taken advantage of the agricultural land that has been developed. Typical Southeast Asian (including Thailand) large mammals include elephants, tigers and various primates like gibbons etc. however the two families that contain the greatest number of species are the bats and rodents. Many species of Thai rodents occur in forests but a few are now common in rice fields. These species cause considerable damage to the rice field crops and are thus of considerable economic importance to the country. In addition these species have the potential to spread diseases to humans and in a few cases they are a source of food to at least some rural communities. The rodent species that commonly occur in the rice fields of Thailand are *Rattus argentiventer*, *Mus caroli*, *Mus cervicolor* and two species of bandicoot rats, *Bandicota indica* and *Bandicota savilei* (Boonsong and McNeely, 1977). All these 5 species occur commonly in at least parts of Thailand and all are members of the rodent family Muridae within in the subfamily Murinae. The relationships between the species within the Murinae are not well known but there is some evidence that the species of *Bandicota* are closely related to *Rattus*.

Within the genus *Bandicota*, there are three well recognized species *B.indica, B.savilei, and B.bengalensis*. The two former species occur in Thailand whereas the third is common in India, Burma and was also introduced onto Penang Island many years ago.

B.indica is particularly widespread in Thailand (Boonsong and McNeely, 1977). It's body size considerably exceeds that of *B.savilei* and it does, at times, do considerable damage to the rice crops. It thus needs to be controlled periodically. It is an aggressive animal on which relatively little biological work has, to date, been performed. A knowledge of its reproductive biology could, thus, be useful in both breeding the species for human consumption and for apply immunocontraceptive techniques for controlling numbers of animals when they are overabundant. For

applying the latter technique a knowledge of sperm and egg biology may be useful so that sperm-egg binding could be prevented.

LITERATURE REVIEW

In sexually mature, adult, males of most mammalian species germ cell production occurs in a highly regulated and organized way with the resultant spermatozoa having a uniform, and species-specific, shape. In species such as the laboratory rat and mouse, as well as in farm animals, the maturing germ cells within the testicular seminiferous epithelium are organized into a series of characteristic cell associations of various maturational stages that occupy the entire cross-sectional area of a seminiferous tubule. At any one point along a tubule, there is a change in the cell associations over time with the length of time it takes to pass through all of the cell associations resulting in a cycle of the seminiferous epithelium (Leblond & Clermont, 1952; Hess, 1990; Russell *et al.*, 1990). Furthermore, along the length of a tubule at any one time, different cell associations are present with the consequence that a wave of the seminiferous epithelium occurs (Perey *et al.*, 1961). In the human testis however, the germ cell organization is quite different as cross-sections of the seminiferous tubules display multiple cell associations including some that have an atypical composition of germ cell developmental stages (Clermont, 1964; Heller and Clermont, 1964). Moreover, adjacently located cell associations do not precede or follow each other consecutively in the cycle of the seminiferous epithelium (Heller and Clermont, 1964), although some, but not all, workers believe that a spiral wave is present (Schulze & Rehder, 1984; Johnson, 1994a). Tubule cross-sections with more than one cell association or stage of the cycle of seminiferous epithelium are also common in some other primates including apes and New World monkeys (Smithwick *et al.*, 1996; Weinbauer *et al.*, 2001; Wistuba *et al.*, 2003). Germ cell production in humans is also less efficient than that in laboratory rats (Johnson, Petty and Neaves, 1980; Johnson *et al.*, 2000) with apoptosis occurring in spermatogonia and primary spermatocytes as well as in spermatids (Sinha Hikim *et al.*, 1997, 1998). Additionally, in humans, unlike in common laboratory rodents, the final form of the spermatozoon is

highly pleiomorphic with some sperm having nuclear vacuoles (Bedford *et al.*, 1973; Fawcett, 1975).

Cell associations within the testes have been described for various rodent species besides common laboratory mice and rats, including hamsters (Clermont and Trott, 1969; Oud and de Rooij, 1977), prairie voles (Schuler and Gier, 1976), field voles (Grocock and Clarke, 1975, 1976), bank voles (Grocock and Clarke, 1976), grey squirrels (Tait and Johnson, 1982), mole rats (Redi *et al.*, 1986), Asian gerbils (Bilaspuri & Kaur, 1994), viscachas (Munoz *et al.*, 1998), capybaras (Paula *et al.*, 1999), lesser bandicoot rats, (Sinha Hikim *et al.*, 1985), plains rats (Peirce and Breed, 1987), and hopping mice (Peirce and Breed, 1987). In all of these species, with the exception of the hopping mouse *Notomys alexis* (Peirce and Breed, 1987), a similar germ cell organization to that of the laboratory rat and mouse was found to occur.

A study of the sperm morphology of the three species of Asian bandicoot rats, genus *Bandicota*, has shown that, whereas lesser bandicoot rats have a similar sperm morphology to that of laboratory rats, this is not the case for the greater bandicoot rat, *B. indica* where a very different, and highly variable, sperm head and nuclear morphology is present (Breed, 1993, 1998, 2004).

Sperm Morphology of Placental Mammals

For a new individual to be formed the spermatozoon has to enter the female reproductive tract and travel to the site of fertilization. Prior to sperm-egg fusion the spermatozoon has to first penetrate the glycoprotein coats that surround the ovulated egg. Mammalian spermatozoa have several unique features that are not present in other vertebrate groups and it has been suggested that these features relate to the challenges that the spermatozoon faces in reaching the egg and, in particular, for penetrating the surrounding egg coats (Bedford 1991). These peculiar features include (1) a bilaterally flattened sperm head, (2) keratinoid, disulfide bonding, within, and between, the protamines to which the DNA is bound in the sperm nucleus, (3) the site of sperm oolemma fusion by way of the molecules that are localized on the plasma membrane that overlies the equatorial segment of the acrosome.

The spermatozoon is formed within the testes after the completion of two meiotic divisions and the transformation of a spermatid by a process called spermiogenesis.

We will first describe the dynamics of sperm production in the testis, then the morphological events that take place during spermiogenesis (Clermont et al., 1993).

Sperm Production Within the Testis

Spermatozoa are produced within seminiferous tubules of the testis by a process called spermatogenesis. This process is highly regulated with the number of sperm produced being determined by the rate at which germ cell maturation occurs and by the number and length, of the seminiferous tubules. Within the seminiferous tubules germ cell maturation gradually occurs at a species specific rate with the length of time for the germ cells to pass through meiosis and spermiogenesis occurring in a very controlled manner. It is usually found that, in the tubules, certain germ cell maturational stages coincide with each other. As a consequence of this it is generally possible to recognize particular germ cell associations where these particular stages always coincide. Germ cell maturation proceeds at a particular site within the narrow and highly coiled seminiferous tubules, each of which has a central fluid-filled lumen that is lined by the epithelium composed of germ cells and somatic cells, Sertoli cells, which support and nourish the germ cells (Lombardi, 1998). These germ cell associations change over time and, by determining the percentage of a particular germ cell association, it is possible to determine how long it takes for cells to pass through particular maturational stages relative to that of the other stages. The duration of the cycle of the seminiferous epithelium is found to be remarkably constant and characteristic for a given species, for example, in mice: 8.6 days (Oakberg, 1956), in sheep: 10.4 days (Ortavant, 1954, 1956), in rats: 12.9 days (Hilscher, 1964), in monkeys: *Macaca fascicularis*: 9.3 days (Dang, 1971) and *Macaca mulatta*: 10.5 days (Clermont and Antar, 1973; de Rooij *et al.*, 1986), and in men: 16.0 days (Heller and Clermont, 1963) Furthermore, by determining the consistency of particular germ cell maturational stages within a particular cell association, the preciseness, or otherwise, of the control of the process of germ cell maturation can be ascertained (Peirce and Breed, 1987; Clermont *et al.*, 1993; Clermont and Trott, 1969; Hess *et al.*, 1990). The

stages or cell associations of the cycle of seminiferous epithelium are characterized by the changes in shape of spermatid nuclei, acrosomal changes, the maturation and meiotic stages of spermatocytes, and relative positions of germ cells, particularly spermatids, within the epithelium (Curtis, 1918; Roosen-Runge and Giesel, 1950; Ortavant, 1959; Amann, 1962; Grocock and Clarke, 1975). There are 6 cell associations in man (Clermont, 1963), 8 cell associations in Australian rodents: *Pseudomys australis* and *Notomys alexis* (Peirce and Breed, 1987), and in albino rat (Roosen-Runge and Giesel, 1950), 9 cell associations in common marmoset: *Callithrix jacchus* (Holt and Moore, 1984), 13 stages in musk shrew: *Suncus murinus* (Kurohmaru *et al.*, 1994) and 14 stages of the cycle of seminiferous epithelium in laboratory rat (Leblond and Clermont, 1952).

Spermatogenesis

This process, spermatogenesis, is a complex, continuous process that takes place in the seminiferous tubules which are formed by the epithelial cells that lie against basal lamina of the tubules and the germ cells. The process begins with spermatogonia, which develop from primordial male germ cells. Spermatogonia undergo mitotic division into primary spermatocytes, which then undergo first and second meiotic divisions which results in reduction of the chromosome number by half so that haploid cells are formed. The first meiotic division gives rise to secondary spermatocytes and then the second meiotic division occurs to form spermatids. All of these developing germ cells organize themselves in the way that layers of the later developmental stage are closer to the lumen. At the basal lamina of the seminiferous tubules, two types of diploid spermatogonia can be distinguished; type A and type B spermatogonia. Type A spermatogonia have paler nuclear staining with haematoxylin, and they undergo mitosis frequently thus continuously maintain a population of precursor cells. Type B spermatogonia eventually form and then divide further to form primary spermatocytes. Primary spermatocytes undergo morphological changes that in which chromosome pairing. The stage of this process can be used as criteria to subdivide the primary spermatocytes into leptotene, zygotene, pachytene, and diplotene based upon their nuclear appearance. Pachytene spermatocytes are ended by their relatively large size, especially their nuclei, which occupy most of the cell

volume. Their chromatin appears as condensed threadlike structures. The life time of pachytene spermatocytes is longer than that of other stage of the primary spermatocytes. Therefore, they are the major primary spermatocyte population consistency existing above the layer of spermatogonia. During prophase of meiosis I, duplication of the DNA of primary spermatocytes takes place. DNA becomes double stranded. Exchanging the DNA fragments through crossing over of sister chromatids, followed by their separation at the end of meiosis I, results in reduction of DNA and chromosome number of primary spermatocytes by half, so that haploid secondary spermatocytes are formed. Rapid division of secondary spermatocytes through meiosis II results in spermatid formation, in which their DNA is reduced by half to that of secondary spermatocytes (Ravindranath *et al.*, 2003).

Spermiogenesis

Once the germ cells have completed the two meiotic divisions a small round cell is formed, the spermatid, that gradually transforms into a spermatozoon. During this time a radical reorganization of the intracellular organelles takes place. The major events of spermiogenesis include: 1) formation of the acrosome, 2) formation of the sperm tail, 3) condensation of the chromatin and transformation of the nuclear shape, and 4) loss of the majority of cytoplasm. These morphological changes based upon the characteristics of the acrosome formation and nuclear transformation. The following is a brief summary of these events.

(1) Formation of the acrosome

One of the first changes that is observed is the budding of small vesicles from the Golgi apparatus. These vesicles travel to the apical pole of the nucleus where they fuse together to form an acrosomal cap that progressively spreads over the anterior pole of the nucleus. Further vesicles arise from the Golgi and empty their contents into the acrosomal vesicle that progressively enlarges. It forms a prominent structure over the nucleus, the acrosomal cap. Major differences occur between species in the size of the acrosomal cap but there are, nevertheless, almost universely two functional regions that develop: they are (1) the principle segment, that undergoes vesiculate at the time of the acrosome reaction, and (2) the equatorial segment that stabilizes the overlying

plasmalemma for fusion with the oolemma at the time of fertilization (Bedford, 1982; Yanagimachi, 1994).

(2) Formation of the sperm tail

At the same time as the acrosome is forming 2 centrioles come to the lie at the opposite pole of the nucleus. One, the distal centriole, starts to give rise to a flagellum that progressively elongates and forms the sperm tail. As this process proceeds the germ cell starts to elongate and it rotates so that the developing tail protrudes into the lumen. Peripheral to the elongating flagellum another series of microtubules occur, the manchette, and, as the germ cell becomes polarized, the mitochondria migrate to come to lie around the flagellum within the manchette- this region eventually becomes the mid piece of the sperm tail.

(3) Condensation of the chromatin and transformation of the nuclear shape

The spermatid nucleus is, initially, a spherical structure within which a haploid set of chromosomes occurs. As maturation proceeds the nucleus becomes markedly reduced in volume. Histones become removed and are replaced initially by transitional proteins (TP) which are subsequently replaced by protammines (Balhorn, 1989; Hecht, 1989; Meistrich *et al.*, 1994). Coinciding with the changes in the intranuclear proteins, the DNA becomes very tightly packaged by forming complexes with the basic amino acid, arginine, of the protamine molecules. Interestingly, unlike histones that are highly conserved between species, there is much variation in the amino acid sequence of the protamines that occurs between species. Furthermore, in some species, two types of protamines, P1 and P2, occur whereas in others only P1 protamine is present. The reason for this is not known.

It has been suggested that the final arrangement of the chromatin is in the form of a toroidal structure (Balhorn, 1982). In human and primates, the fine granular chromatin of early spermatids gradually turned into coarser and denser bodies which eventually coalesce to form the compact homogenous mass in the mature spermatozoa (Holstein and Roosen-Runge, 1981; Allen *et al.*, 1997; Balhorn *et al.*, 1999). In most rodents the highly coiled 30 nm chromatin fibers are transformed into larger and straightened, 40-50 nm fibers that arranged in parallel during the early acrosomal phase (Balhorn *et al.*, 1999; Wanichanon *et al.*, 2001). These chromatin fibers fuse into the larger fibers with about 100 nm in width. The large fibers are completely fused to form the compact

chromatin (Ward and Coffey, 1991; Wanichanon *et al.*, 2001). Alternatively, in *Rana tigerina*, the process of chromatin condensation is similar to the heterochromatin in the somatic cells where 30 nm fibers are coalesced together into a dense mass in spermatozoa without changing their initial size and nucleosomal organization (Manochantr *et al.*, 2004).

In most mammals during spermiogenesis, the DNA in the haploid male germ cells becomes progressively condensed by the replacement of the histones with transition proteins (TP) and these transition proteins are being replaced by basic nuclear proteins called protamines which are highly enriched in arginine and also the cysteine residues which forms strongly disulfide (S-S) crosslinks (Balhorn *et al.*, 1984; Goldberg, 1977) between the adjacent protamine molecules and further stabilizing a highly compactness structure of chromatin by inter and intra molecular covalent disulfide bonds between protamines (Bedford and Calvin, 1974). Thus, protamines with strong disulfide cross-links, are believed to play a major role in the complete condensation in the mature spermatozoa in mammals (Bedford and Calvin, 1974; Balhorn *et al.*, 1999). The degree of chromatin package in mature sperm of various species depends on the amount of histones being replaced by protamines. Rat spermatozoa have a higher degree of chromatin condensation than in human spermatozoa. This is probably due to the higher amount of disulfide cross links of protamines and lower percentage of histones remaining in the rat spermatozoa. It is well-known that the nuclear DNA in somatic cells forms nucleosomes which are composed of core dimeric histones; H2A, H2B, H3, and H4, forming the octamer proteins that are the repeated structural unit of the chromatin (Kornberg, 1999). These nucleosomes are joined together by histone H1 binding to the linker DNA. It is shown that the chromatin forms beads on a string conformation linked with DNA to further form the coiled solenoid pattern of 30 nm fibers. This appearance of chromatin organization may also be found in early steps of spermatids which have suggested the presence of the nucleohistones in the nucleus. Chromatin organization during mid and late spermatids has been shown the replacing of histones by transition proteins and protamines respectively. Thus, the DNA in sperm nucleus can be tightly packed in a very small volume to protect itself from damage during sperm transportation in the

female reproductive tract (Balhorn, 1982). However, there is the evidence suggesting that the modes of chromatin condensation between species varies.

(4) Loss of the majority of cytoplasm

During the time the sperm tail is forming, the excess cytoplasm moves toward the tail, forming a cytoplasmic body, called the residual body. Most of the residual bodies are then endocytosed by Sertoli cells, leaving a minor part, termed cytoplasmic droplet, attached to the tail.

In spite of the commonality of changes during spermiogenesis in all mammals, the eventual morphology of the spermatozoon shows considerable diversity between species. In most (primates, ungulates, carnivores etc.) the sperm head shape is spatulate with a bilaterally flattened nucleus being capped by a more or less symmetrical acrosome. By contrast, in most rodents, the morphology of the spermatozoon is remarkably different and also shows considerably variation between species.

Sperm Morphology of Rats and Mice

In species of *Rattus* and *Mus* (including the species that occur in the rice fields of Thailand) as well as the common lab rodents, the house mouse *Mus musculus* and the norway rat *Rattus norvegicus*, the sperm head is hook shaped or falciform. Transmission electron microscopy (TEM) has shown that, within this structure, there is uniformly very condensed chromatin in the nucleus which extends into the apical hook. In sperm of these species the acrosome is highly asymmetrical and lies along the upper convex and lateral surfaces of the nucleus with the equatorial segment occurring along the midlateral surface of the sperm head. There is, in addition, a small accessory segment that occurs along the concave surface of the apical hook (Lalli and Clermont, 1981). Between the acrosome and nucleus there is extensive cytoskeletal material which also extends beyond the apical tip of the nucleus as a perforatorium (Lalli and Clermont, 1981; Oko and Clermont, 1988; Oko *et al.*, 1990). The sperm tail attaches to the head on the lower concave surface.

Sperm Morphology of *Bandicota indica*

An early light microscopical study indicated that the sperm morphology of *B.bengalensis* was similar to that of *Rattus*. This was followed up by a TEM investigation of the sperm head of this species in which it was found that the nucleus was uniformly electron dense and that, like in the sperm of the lab rat, it extended into the apical hook and form a sickle shape, a pear shape in man, and a paddle shape in domestic animals. As with the lab rat, the acrosome mainly occurs over the convex and upper lateral surface of the sperm nucleus with the thinner, equatorial segment, running as a band across the lateral surface of the sperm head. Also the cytoskeletal material that occurs within the subacrosomal space extends beyond the nucleus toward the apical tip of the sperm head. One difference from the lab rat sperm found is that there are two, rather one, ridges of subacrosomal material running along the convex nuclear surface (Breed, 1998).

The other two species of *Bandicota* have a totally different sperm morphology from that of *B.bengalensis*. In these the sperm head morphology shows considerate similarity between the two species but this sperm morphotype is remarkably different from that of all other rats and mice so far described, and even all other mammalian species. In these species, *B.savilei* and *B.indica*, the overall shape of the sperm head is globular or pyriform and there is also much variability evident (Breed, 1993).

TEM has shown that in these species of *Bandicota* there is a relative small sperm nucleus in which there are large nuclear vacuoles present, and, in addition, there is considerable variability in the apical nuclear region. The acrosome of these sperm is very large indeed and is, like the nucleus, more or less spherical in cross-section. Another very unusual feature is the apparent absence of an equatorial segment to the acrosome (Breed, 1993, 1998). Extending caudal to the acrosome is a short postacrosomal dense lamina which terminates well anterior to the caudal pole of the nucleus to which the sperm tail attaches. The cytoskeletal region sperm head is only modestly developed with a narrow space being presented between the acrosome and nucleus. There is no indication of a perforatorium being present in the sperm head of these animals, whereas preliminary observations suggest that chromatin condensation during spermiogenesis also differs markedly from that of lab rats (Breed, 1993, 1998).

These unusual morphological features of the sperm head of B.indica and B.savilei strongly suggest that the way the chromatin condenses, and the process by

which the sperm passes through the egg coats and fuses with the egg at fertilization differ markedly from that of the other rodent species and perhaps even most other mammals. Consequently a more detailed study of male germ cell formation, structural organization and function is required to better understand the reproductive biology of these animals.

OVERALL OBJECTIVES

To study the cell associations in the seminiferous tubules and the pattern of chromatin condensation of germ cells during spermiogenesis in *Bandicota indica*.

SPECIFIC OBJECTIVES

1. To study the stages of the cycle of seminiferous epithelium in *B. indica*
2. To investigate the organization of chromatin in germ cells during spermiogenesis by transmission electron microscopy.
3. To localize the distribution of nuclear proteins during spermiogenesis.
4. To characterize the sperm basic nuclear proteins.

MATERIALS AND METHODS

1. To Study the Stages of the Cycle of Seminiferous Epithelium in *B. indica*

Rationale: *In sexually mature, adult, males of most mammalian species germ cell production occurs in a highly regulated and organized way with the resultant spermatozoa having a uniform, and species-specific, shape. In laboratory rat and mouse, including hamsters (Clermont and Trott, 1969; Oud and de Rooij, 1977), and lesser bandicoot rats (Sinha Hikim et al., 1985), the germ cells within the seminiferous epithelium are organized into the characteristic cell associations of various maturational stages that occupy the entire cross-sectional area of a seminferous tubule. However in the human, the germ cell organization is quite different as cross-sections of the seminiferous tubules display multiple composition of germ cell developmental stages (Clermont, 1963; Heller and Clermont, 1964). A study of the sperm morphology of the lesser bandicoot rats have a similar sperm morphology to that of laboratory rats, this is not the case for the greater bandicoot rat, B. indica where a very different, and highly variable, sperm head and nuclear morphology is present (Breed, 1993, 1998, 2004). Due to this highly divergent sperm head shape and the fact that these sperm, like those of humans, shows a high degree of pleiomorphism, we, in this study, ask a related question; "What is the organisation of the seminiferous epithelium?"*

Light Microscopic Study for Germ Cell Association

Animals:

Greater Bandicoot rats, *B. indica*, were collected in Thailand from near Maesod, Tak Province in October 2001 (n=22, 11 females, 11 males), in Supanburi, and Nakornrachasima province in January 2003-2004 (n=21, 10 females, 11 males). After returning the animals to the laboratory at Mahidol University, Bangkok, they were anaesthetised and their sex, weight and reproductive condition was determined. In the 2001 sample, two of the 11 females were pregnant and two of the 11 males had sperm in the cauda epididymides, whereas in the 2003-2004 sample seven of the 10

females were pregnant, another had recently ovulated, and all 11 males had sperm in the cauda epididymides.

Tissue Preparation:

From the males with sperm, small pieces of one testis and epididymis were removed and rapidly fixed in 3% glutaraldehyde/3% paraformaldehyde made up in 0.1M phosphate buffer, pH 7.4, whereas the other testis was fixed whole using the same fixative. The small pieces of testes were post-fixed in 1% osmium, dehydrated and embedded in epoxy resin. Larger pieces of fixed tissue were removed from the whole testis, dehydrated and embedded in paraffin wax. From the epoxy resin-embedded testis samples, 0.5 to 1 μm thick plastic sections were cut and stained with toluidine blue. From the paraffin-embedded blocks, 6-8 μm thick sections were cut and stained with either H & E or PAS and haematoxylin.

Organization and Frequency of Stages of the Seminiferous Epithelium:

The testicular seminiferous epithelium in both epoxy-embedded and paraffin sections was analysed for the two animals with sperm collected in 2001 and four of the males collected in 2003. Nine cell associations were characterised, based on the appearance of the younger generation of spermatids within the seminiferous epithelium. The relative frequencies of the different cell associations, and the number of tubular cross-sections displaying more than one cell association, were determined in epoxy sections by scoring at least 130 tubular cross-sections from at least 3 different locations within the testis for each male.

Sperm Morphology:

For assessing the pleiomorphism in the sperm head nuclei, cauda sperm from four of the animals collected in January 2003 were placed on glass slides and then stained with dilute propidium iodide. The slides were viewed with an Olympus BH epifluorescent microscope using a 515 nm excitation filter and an IFK 90 nm barrier filter with an absorption wavelength of 535 nm and an emission wavelength of 617 nm. Photographs of the nuclei of cauda epididymal sperm were taken using an Olympus C-4040 zoom digital camera and 196 to 327 sperm randomly counted from each of these individuals and allocated to the various nuclear morphotypes.

2. To Investigate the Organization of Chromatin in Germ Cells during Spermiogenesis by Transmission Electron Microscopy.

Rationale: *During mammalian spermiogenesis, the haploid male germ cells undergo the morphological transformations leading to the formation of mature spermatozoa. One of the most changes involves the remodeling of the dispersed chromatin into a highly condensed chromatin. The reorganization of the packaging chromatin coincides with two patterns of chromatin condensation (Ward et al., 1989; Balhorn et al., 1999). Firstly, the replacement of the testis specific nuclear proteins, histones, by lysine-rich proteins termed transition proteins. Secondly, these transition proteins are being replaced by spermatid basic nuclear proteins rich in arginine and cysteine called protamines (Balhorn, 1989; Meistrich et al., 1994) which occurs at a time when the nucleus is highly condensed. Therefore, the question arises; "How is the chromatin condensed in the sperm of Bandicota indica?"*

2.1 Conventional Transmission Electron Microscopic Study

Small pieces of the tissues were fixed immediately in a solution containing 3% glutaraldehyde and 3% paraformaldehyde in 0.1M phosphate buffer saline (PBS) to which 2.5% PVP 40 has been added, pH 7.4 at 4 °C, for overnight, and then washed with 0.1M phosphate buffer. Specimens were post-fixed in 1% osmium tetroxide in the same buffer, at 4 °C, for 1 hour. Subsequently, the specimens were washed with the same buffer, dehydrated sequentially by passing through a graded series of ethanol and finally embedded in epoxy TAAB resin. Semithin (1um) and thin (60-90 nm) sections with an interference color of silver to silver-gold were cut using an ultramicrotome fitted with glass knives. Thin sections were picked up on uncoated 200 mesh copper grids, air dried and stained sequentially with 2% uranyl acetate in 70% alcohol in the dark and lead citrate, then observed in a Phillips CM100 transmission electron microscopy.

2.2 Phosphotungstic Acid Staining (PTA)

Pieces of testis were fixed for 4 hr at 20 °C in 4% glutaraldehyde in 0.1M PBS, pH 7.4. They were washed in 0.2M phosphate buffer, and then in distilled water before

dehydrated by passing through increasing concentrations of ethyl alcohol (30-100%). *En bloc* staining with 3% phosphotungstic acid (Courtens and Loir, 1981; Dadoune, 1991) in 100% ethyl alcohol for 16 hr at 20 °C was followed by washing in ethyl alcohol for 2 hr and embedding in Epon. Ultrathin sections were examined without counterstaining then observed by Phillips CM 100 TEM.

3. To Localize the Distribution of Nuclear Proteins during Spermiogenesis.

Rationale: *During the chromatin condensation, we have followed the fine structural distribution of histones, transition proteins, and protamines by means of specific antibodies with the ultrastructural immunogold localization. Our aim is to define the spermatid phases where the protein substitution takes place and to correlate them with the morphological changes during the sperm maturation.*

3.1 Immunocytochemistry

The sections obtained from testes fixed with Bouin's were deparaffinized in xylene twice for 5 minutes each time. The tissue was hydrated in the following graded ethanol series (100%- 70%) 3 minutes in each. The residual picric acid (one ingredient of Bouin's fixative) was removed from the tissue sections by immersing the slide in 70% ethanol containing 1% of Saturated Lithium carbonate ($LiCO_3$) for 5 minutes. Then the endogenous peroxidase activity was abolished by immersing the tissue sections in 70% ethanol containing 1% H_2O_2 for 5 minutes. The slides were placed in distilled water containing 0.1M glycine for 5 minutes to block free aldehyde groups in the testes sections. A drop of 1% TritonX-100 in 0.1M PBS was added to the slide to permeabilize the plasma membrane for 15 minutes, after that, blocking non-specific staining with 50 um. of 4% BSA in PBS for 15 minutes. Sections were then incubated with one each of 30 um. of histone H1, H3 or protamine in 0.1M PBS in humidified chamber at room temperature for 90 minutes. The concentration of three primary antibodies was 1: 100, 1: 300, and 1: 100 respectively. For control sections, the tissues were added 50 um. of 0.1M PBS instead of antibody.

The tissue sections were washed twice in TWBS (PBS containing 0.05% Tween 20 which was mild detergent) for 5 minutes each time to remove unbound

antibody. To incubate the sections with secondary antibodies, goat anti-rabbit IgG conjugated with Horseradish peroxidase (HRP) at 1: 360 for histone, and goat anti-mouse-HRP at 1: 250 for protamine, for 90 minutes. The tissue sections were then washed again in the same TWBS twice for 5 minutes each time. The final reaction products were achieved by incubating the tissue sections for 10 minutes in 50 ml of PBS containing 0.03%H_2O_2, 0.3%$NiCl_2$, and 0.05% diaminobenzidine tetrahydrochloride (DAB) pH 7.4. The tissue sections were then washed in distilled water and uncounter-stained. The sections were dehydrated by passing the sections through the graded ethanol series (70%-100%) for 3 minutes in each. Then they were immersed in xylene two times for 5 minutes each and mounted with Permount. The sections were observed under the light microscope, and photos taken by Nikon digital camera DXM 1200.

3.2 Immunogold Electronmicroscopy

In this study, the following polyclonal antibodies raised in rabbits were used:

- Either whole anti-histone antibodies to H2A, H2B, H3, or H4 (different antisera) or to peptide 1-20 of H2A and 85-102 of H4. These antibodies were donated by S. Muller in France to Assoc. Prof. W. G. Breed.
- Transition protein 1 (TP1) and transition protein 2 (TP2) were donated by R.J. Oko in Canada to Assoc. Prof. W. G. Breed.

All antibodies were used for localization of these proteins in the spermatids, testicular sperms and sperm in the cauda epididymis of the bandicoot rat.

LR-white resin embedded ultrathin sections (60-90 nm. thick) of bandicoot rat testes were cut with diamond knife using an ultramicrotome and mounted on formval coated 100 mesh nickel grids. The grids were floated on drops of the various solutions. The sections were first quenched for aldehydes by placing on drop of 0.01 M glycine solution in 0.1 M Tris buffer saline (TBS), pH 7.4 for 20 min at room temperature, and blotted on filter paper. The sections were then placed on 1% normal goat serum (NGS) in TBS with 0.5 % Tween 20 for 20 min to block non-specific binding. After blotting the grids on filter paper, the sections were then placed overnight at 4 °C on drops of primary antibodies (the dilutions of 1:10 for histones, and 1:5 for transition proteins) diluted with 1% NGS in TBS with 0.5% Tween 20. Next, they were rinsed 6 times by

passing through drops of TBS with 1% NGS only (no Tween 20), 5 min on each drop, followed by blotting on filter paper after last drop of rinsed solution. The grids were then incubated on an appropriate secondary antibodies conjugated with 10 nm gold particles made up to 1:20 dilution for 1 hr, followed by extensive rinsing in TBS with 1% NGS 6 times, 5 min for each drop, and washed in a series of distilled waters. The grids were then air dried and stained with uranyl acetate for 1 1/2 min in the dark and observed under CM100 Philips transmission electron microscope.

4. To Characterize the Sperm Basic Nuclear Proteins.

Rationale: *After several attempts to correlate the appearance of the spermatid nuclear proteins with the precise structural phase of the chromatin condensation have been made, we've found that the replacement of histones by transition proteins and finally replaced by protamines leading to the highly condensed chromatin in bandicoot rat was different of what it does in other mammalian rodents. There was no specific phase where the sperm nuclear proteins have been replaced and most of the histones are still remained in mature spermatozoa. So in this study we investigate the profile of the sperm nuclear basic proteins of B. indica which destroys the rice field and effects to the economic in agricultural matters, commonly found in Thailand.*

Biochemical Studies of the Basic Nuclear Proteins

4.1 Isolation of Sperm Nuclei

The animals were injected overdose of Nembutal (pentobarbitone sodium). After opening up the body cavity the cauda spermatozoa were isolated from semen by centrifugation at 600g for 10 min in normal saline, and then resuspended in SMT solution (250 mM sucrose, 2 mM $MgCl_2$, and 10mM Tris-HCl, pH 7.4), then centrifuged at 600g for 10 min. They were demembranated with 0.5% Triton X-100 in SMT solution for 10 min at room temperature. After incubation, they were centrifuged at 1500g for 10 min, washed again with SMT solution and centrifuged at 1500g for another 10 min. Now there were only the nuclei of spermatozoa in the pellets. The reducing agent (5M guanidine HCl, 0.5M Tris-HCl pH 8.5, 0.28M β-mercaptoethanol, and 10mM DTT) was added for 30 min with homogenizer or sonicator.

4.2 Isolation of Testicular Cells Nuclei

After removal of the testes from the animals, they were immediately placed on ice and all of the following steps were performed at 4 °C. Testes were decapsulated and chopped into small pieces, filtered by 4 layers of gauze and homogenized gently in 5 volume of homogenized buffer (0.31M sucrose, 3mM $MgCl_2$, 5mM potassium phosphate pH 6.0, 0.05% Triton X-100, 0.1mM PMSF) using a hand homogenizer (PMSF was added immediately just before homogenization). The homogenate was filtered through four layers of gauze and centrifuged at 600g for 10 min. The pellets were then suspended in cold distilled water containing 0.1mM PMSF to demembrane the cells. After centrifugation at 1500g for 10 min, the pellet was resuspended in the MP solution (5mM $MgCl_2$, 5mM sodium phosphate, pH 6.5) using micropipette and centrifuged at 1500g for 10 min to collect the pellet fractions (Platz *et al.*, 1975). The reducing agent (5M guanidine HCl, 0.5M Tris-HCl pH 8.5, 0.28M β-mercaptoethanol, and 10mM DTT) was added for 30 min with homogenizer or sonicator.

4.3 Extraction of Basic Nuclear Proteins by Using HCl Extraction

After incubation the cauda spermatozoa and testicular nuclei (4.1 and 4.2) with the reducing agent, 0.33 ml of 1N HCl per volume of the solution was added to make the solution 0.25N HCl, and then 1.0 ml of 0.25 N HCl per volume of the solution was added and allowed to stand on ice for 1 hr with occasional homogenization. The solution was centrifuged at 12,000g for 10 min and the supernatant was collected. The pellet was re-extracted with 1.0 ml of 0.25N HCl, centrifuged, and the supernatants were combined with those collect earlier. Proteins from the pooled extracts were precipitated by adding 0.33 ml of 80% TCA per 1 ml of extracted solution, and the solution was allowed to stand on ice for 60 min. the precipitate was recovered by centrifugation at 12,000g for 10 min, washed with cold (-70 °C) acidified acetone (200 ml of acetone plus 0.1 ml of 12N HCl), washed with cold (-70 °C) acetone, and then air dried by opening the lids of each eppendorf (Platz *et al.*, 1975).

4.4 Electrophoretic Separation of Basic Nuclear Proteins by Acid Urea Triton X-100 Polyacrylamide Gel Electrophoresis (AUT-PAGE) and Immunoblotting

AUT-PAGE

Basic nuclear proteins were electrophoretically separated and compared on slab gels containing 17% acrylamide, 2.5M urea, 6mM Triton X-100, and 5% acetic acid (Zweidler, 1978). Proteins samples were dissolved in sample buffer (1-2 mg/ml), 9M urea, 0.9N acetic acid, 5% mercaptoethanol, and 0.2% pyronine-G, heated for 1 min in boiling water bath to unfold polypeptide chains and reduce the disulfide linkages. 2.5µl of sample solution was loaded into each well, and stacked neatly at the bottom of the well. Electrophoresis was carried out at 120 volts at constant voltage with alternating the current for 1 hr or until the front-dye reached to the bottom of the gel. The gel was stained with protein binding dye i.e. 0.125% Coomassie Brilliant Blue R-250, in 50% methanol and 10% acetic acid for 1 hr, followed by destaining I in 50% methanol and 10 % acetic acid, 5% methanol and 7% acetic acid for 2 hrs and overnight for destaining II (Laemmli, 1970). The last step was repeated by changing the destained solution until the background was completely colorless. The gels were dried onto cellophane paper for longer storage.

Immunoblotting

The specificity of anti-protamine antibody was assessed by immunoblotting as followed. Total basic nuclear proteins from testicular nuclei, spermatozoa nuclei, and chick erythrocytes were separated in 17% AUT-PAGE as previously described. Proteins were transferred onto nitrocellulose membrane (with 0.45 um pore size) positioned at the cathode side of the gel, using 0.9 N acetic acid, pH 2.3, as the transfer buffer, at 400 mA for 2 hrs. Following tranfer, the proteins on nitrocellulose membranes were visualized by brief staining with 0.5% Ponceaus S in distilled water, while the gels were stained in Coomassie blue to determine the efficiency of transfer. The membrane were incubated in the primary antibodies at the dilution of 1:10.000 for 1 hr, followed by washing with 10 mM Tris-buffered saline, pH 7.4 containing 0.1% Tween-20. The secondary antibody, HRP-conjugated goat anti-mouse IgG, was added

at the dilution of 1:20,000 for 40 min, washed with 10 mM Tris-buffered saline, pH 7.4 containing 0.1% Tween-20. Finally, the membranes were washed with 10 mM Tris-buffered saline, pH 7.4. The membranes were visualized in the solution of 0.03% 3,3',4,4'- tetraamine biphenyl DAB in 50 mM Tris, pH 7.4, containing 0.1% H_2O_2. The reaction was terminated by rinsing the membranes in several changes of distilled water. The membranes were dried at room temperature and kept in plastic bags in the dark.

RESULTS

1. To Study the Stages of the Cycle of Seminiferous Epithelium in *B. indica*

The body weights of the two 2001 individuals studied in detail with sperm were 655 g and 561 g. The average paired testes weight 2,105 mg, whereas in the 2003 sample mean (±SE) body weight was 489 ±55g and paired testes weight 2,098 ± 287mg (n=7). Since these testes weights are similar to those of mature male greater bandicoot rats caught previously (Breed & Taylor, 2000), and some females in both the 2001 and 2003 samples were pregnant, it is assumed that the males investigated were sexually mature.

Stages of the Cycle of the Seminiferous Epithelium

The classification system used to determine the germ cell associations was that based on the morphological appearance of the younger generation of spermatids in the cell associations with Stage I beginning at the completion of the second meiotic division (see Russell *et al.*, 1990). The cycle of the seminiferous epithelium was divided into 9 cell associations or stages based on spermatid characteristics. In cycle Stages I – III one generation of pachytene primary spermatocytes and two generations of spermatids were present, whereas Stages IV – VIII had two generations of primary spermatocytes but only one generation of spermatids. Stage IX was characterized by the presence of meiotic figures in the older population of spermatocytes or by the presence of secondary spermatocytes.

Morphology and organization of the germ cells of the various cycle stages as seen in the toluidine blue-stained epoxy sections are described below (see Fig. 6 for summary). The cell associations were also identified in PAS and haematoxylin-stained paraffin sections, however cellular preservation and detail were not as good as in the plastic sections and thus the latter were used for describing the cell associations. Type A spermatogonia were present in all cell associations; they were flattened cells displaying extensive cytoplasmic contact with the basement membrane of the

seminiferous tubule and had an ovoid nucleus that occupied a major portion of the cell.

Stage I was defined by the presence of small round spermatids without a visible Golgi complex or acrosomal vesicle (Fig. 1a). Type A and occasional intermediate spermatogonia or spermatogonia undergoing mitosis were present at the base of the seminiferous epithelium. The nuclei of intermediate spermatogonia were characterised by patches of heterochromatin around the nuclear envelope (Fig. 1a) whereas those of type A spermatogonia contained little heterochromatin. Pachytene primary spermatocytes had chromatin condensed into thick strands and, above them several layers of early spermatids with round nuclei were present. Situated between, and above, the round spermatids were groups of elongated spermatids in which there were intensely stained nuclei with acrosomes that were generally oriented towards the basement membrane (Fig. 1a).

Stage II was defined by the presence of round spermatids with a Golgi complex adjacent to the nucleus. Acrosomal vesicles or granules were present within the spermatid cytoplasm, but had little contact with the nuclear envelope (arrow – Fig. 1b). Intermediate spermatogonia were present. Round, pachytene primary spermatocytes contained large central, round nuclei with condensed, tightly packed, chromosomes. Early spermatids with central round nuclei were located above the pachytene primary spermatocytes and elongated late spermatids were present, with some of the nuclei having an apical extension (arrowhead – Fig. 1b) or an indented nuclear envelope (asterisk – Fig. 1b). The acrosomes of late spermatids were stained lighter than the nuclei and generally remained oriented toward the basement membrane.

Stage III was characterised by enlargement of the acrosome of the round spermatids. During this stage, the acrosome was round, attached to the anterior pole of the nucleus and spread over about 15° of the nuclear surface (Fig. 1c). Type B spermatogonia were present and characterised by having nuclei with an ovoid to round profile that displayed intensely stained chromatin along the nuclear envelope (arrowhead – Fig.

1c). There were 2 to 3 layers of pachytene primary spermatocytes that had round, heterochromatic, nuclei. Several layers of early round spermatids were located above the pachytene primary spermatocytes and along their nuclear envelopes in some regions there was intensely stained chromatin (Fig 1c, arrow). The round spermatids were oriented in various directions, in some the acrosome was directed towards the basement membrane whereas in others it faced the lumen (Fig. 1c). In all round spermatids, the acrosome stained strongly with toluidine blue. Late spermatids had their heads located close to the luminal surface of the seminiferous epithelium. In these cells the chromatin was highly condensed and abundant residual bodies were present around the perimeter of the lumen of the seminiferous tubule (Fig. 1c) suggesting the shedding of considerable amounts of germ cell cytoplasm at this time.

In **Stage IV** the acrosome of the early spermatids was larger than that observed in Stage III and, in some cases, it had become somewhat oval in shape. It extended from 15° to about 45° over the nuclear surface. The spermatid nuclei were mostly round, with intensely stained chromatin along the nuclear envelope (arrow – Fig. 1d) although, in some, the nuclear envelope was flattened beneath the acrosome. These spermatids were located close to the lumen and oriented in various directions. During this stage, mitosis of Type B spermatogonia to form preleptotene primary spermatocytes occurred. The nuclei of the latter cells were generally round in shape, and contained lightly stained fine chromatin threads. Pachytene primary spermatocytes were larger than preleptotene primary spermatocytes and were irregular in shape. Late spermatids had been released into the lumen and were generally not evident although abundant residual bodies could still be seen close to the tubule lumen.

Stage V was characterised by spermatids having an acrosome that was crescent shaped and covered about a quarter of the anterior surface of the nucleus (Fig. 2a). Their nuclei were round or slightly ovoid with lightly stained chromatin. Many residual bodies remained near the luminal surface during this stage. The acrosome, which had reached its maximum size, was very intensely stained and in most cases oriented towards the basement membrane. Preleptotene primary spermatocytes, which were round with central nuclei and lightly stained chromatin, were generally present,

whereas the pachytene primary spermatocytes, that were also present, had round nuclei with dense heterochromatin.

Some of the spermatids of **Stage VI** had nuclei that were a little bilaterally elongated. They were located near the lumen and had homogeneously stained chromatin. The acrosome was intensely stained and oriented toward the base of the tubule. In these cells the cytoplasm had migrated posteriorly (arrow – Fig. 2b) resulting in the acrosome being generally close to the plasma membrane. Leptotene primary spermatocytes occurred which were round cells with large round nuclei and tightly packed threads of chromatin. Either pachytene, or occasionally diplotene, primary spermatocytes were present and generally ovoid in shape. Their nuclei were round and contained conspicuous chromatin threads.

In **Stage VII,** the spermatid nuclei were reduced in size compared with those in Stage VI and they stained more strongly with toluidine blue. They were generally oriented toward the basal lamina and the chromatin was condensed along the nuclear envelope (arrow – Fig. 2c). The acrosome covered the anterior region of nucleus and was deeply stained. Leptotene primary spermatocytes contained round central nuclei with thicker chromatin threads. Diplotene primary spermatocytes were irregular in shape, had spherical nuclei, and were larger in diameter than the pachytene primary spermatocytes at the previous stage. Their chromatin was loosely packed and most of the nucleus was only weakly stained (Fig. 2c).

Stage VIII had spermatids that were elongated and had more strongly stained chromatin than in the previous stage. They were embedded in recesses of the cell membrane of the Sertoli cells and oriented toward the basal lamina. Nuclear vacuoles could be seen (arrowhead – Fig. 2d). Most of the late spermatids had nuclei with apical extension(s) (arrows – Fig. 2d), and acrosomes that were lightly stained. Leptotene and diplotene primary spermatocytes had similar morphologies to those of Stage VII.

Stage IX began with the diplotene spermatocytes undergoing meiosis to form early round spermatids and ended with the completion of the second meiotic division (Fig. 3). Zygotene primary spermatocytes were present and round in shape; the strongly stained nuclei showed more tightly packed chromatin than those of leptotene primary spermatocytes. The late spermatids were elongated and located near the lumen, and their chromatin had condensed along the nuclear envelope. The acrosome was strongly stained.

Frequencies (%) of the Stages of Cycle of the Seminiferous Epithelium

The frequency of each of the nine cell associations is presented in Table 1. The total number of seminiferous tubule cross sections counted was 1230 from six animals, two of which were collected in 2001 and the other four in 2003. Stage II occurred most often, with an average frequency of 28.5% (range 11.1 – 41.6%), whereas Stage VIII was the least frequent, and was observed in only three of six animals with a range of 1 – 3.7%. In three males (Bi 2-003, Bi 5-001, Bi 14-001) Stage II was the most frequent, whereas Stage V was the most common in Bi 7-003, Bi 8-003 and Bi 11-003. Although some variation in the most frequent cell associations was found between animals, in all cases Stages VII, VIII and IX each comprised <10% of the total number of tubule cross sections and Stage I never exceeded 12% of the total.

In 140 out of 1230 tubule cross-sections examined, more than one cell association was present in the tubule cross section (Fig. 4). Such tubule cross-sections occurred with an average frequency of 11.4% (range 6.8 – 19.1% for the different individuals). The most common mixed cell associations in the tubule cross sections were either Stages I and IX, V and VI, or III and IV, but many combinations of cell associations (see Figs. 4a –4d) were found to occur occasionally. Three, or even four, stages were present in a single cross section in 14 of the tubule cross-sections examined, e.g. in Bi 2-003 there were Stages V, VI and IX in one tubule cross section (see Fig. 4a).

In 141 out of the 1230 tubule cross sections examined there was at least one germ cell population that was different from that normally seen within the cycle stage,

with the result that atypical cell associations were present. Such associations occurred in an average of 11.5% (range 2.3-22.7%) of tubules examined for a particular individual. Animals Bi 8-003, Bi 11-003, and Bi 14-001 all had >15% tubule cross-sections with atypical cell associations (Table 1). Most abnormalities were associated with cell association IV. Normally in this stage there is no highly condensed spermatid population close to the lumen as recent release of spermatozoa had generally occurred. However, in some tubule cross sections, late spermatids were still present, and preleptotene primary spermatocytes were absent. In other cases of atypical cell associations a generation of germ cells was absent from the typical cell association (e.g. in Stage III where there were no late spermatids in the cross section of one tubule), or development of a spermatid population appeared to be delayed with respect to the other germ cell types present. For example, Step 9 spermatids generally occurred in Stage IX when the older generation of spermatocytes was undergoing the meiotic divisions, but in a few tubule cross-sections more immature spermatids were seen to occur in conjunction with the meiotic figures.

Nuclear pleiomorphism of mature spermatozoa

Fluorescent microscopy, after staining with the DNA dye propidium iodide, indicated a range of different nuclear shapes occurred, the most frequent of which are shown in Figure 5. Table 2 shows the frequency of the 7 different nuclear morphotypes that were most commonly seen. It is clear that in all individuals a range of different nuclear shapes were evident. In Bi 4-003 and Bi 7-003 morphotype 1 was the most frequent, whereas in Bi 6-003 morphotype 2 predominated, whereas in Bi 11-003 morphotype 3 was by far the most common.

2. To Investigate the Organization of Chromatin in Germ Cells during Spermiogenesis by Transmission Electron Microscopy.

Chromatin Condensation during Spermiogenesis as Revealed by Conventional TEM and PTA Staining Methods

2.1 Conventional TEM Study

Spermiogenesis took place in several successive phases based upon the principal morphogenetic events which occurred as development proceeds. In this study a description of the development of the sperm head within the context of four divisions, or phases, of spermiogenesis in bandicoot rat is given.

(1) Initial or Golgi Phase

During the initial phase of spermiogenesis, proacrosomal granules derived from the Golgi apparatus appeared in the spermatid cytoplasm and fused to form a single large acrosomal granule which became associated with the nuclear envelope (Figs. 7a-7b) which surrounded a round vesicular nucleus (N) with a little heterochromatin condensed along its inner surface. Chromatin threads with diameter of 15-23 nm located throughout the nucleus, and a layer of 28-52 nm dense material occurred along the nuclear envelope. The pattern of chromatin arrangement showed a ray of star pattern with about 5 small fibrils around an electron dense granule. These star-like patterns connected to each other to form a pack, or network, of chromatin. A prominent Golgi apparatus was evident together with adjacent proacrosomal granules (G). The Golgi apparatus situated on the luminal side of, and adjacent to the nucleus, defining the future anterior nuclear pole (Fig. 7a). Numerous small, electron dense, proacrosomal granules appeared between the Golgi apparatus and the nucleus. Some of the proacrosomal granules fused together to form bigger ones, each of which contained electron dense material in their granules. A single large proacrosomal granule developed and finally associated with the anterior pole of the nucleus (Fig. 7b).

(2) Cap Phase

This phase was characterized by the attachment of a large acrosomal granule to the nucleus. It increased in size and gradually spread over the anterior pole of the

nucleus (Figs. 7c-7d). The changes in acrosomal size and shape were identified this phase of spermiogenesis. The development of acrosomal granule resulted in slight indentation of the nuclear envelope above which a huge acrosome, with electron dense material, occurred. The chromatin in the spermatid nucleus showed increased condensation close to the nuclear envelope (Fig. 7c). Nuclear envelope had an increased indentation above which a large spherical acrosome, with homogeneous electron dense material, occurred (Fig. 7d). Within the spermatid nucleus there was a thin region of condensed electron dense chromatin just beneath the acrosome as well as condensed chromatin close to other regions of the nuclear envelope. The chromatin was more homogeneous than in early of this phase (Fig. 7c).

(3) Acrosome Phase

A reorientation of the nucleus, modification of nuclear shape and the attached acrosome which was about one-third of the nucleus were characterised this phase (Figs. 7e-7f, and 8a). The acrosome (Ac) had become oval shape and laterally bi-flattened and still had homogeneous, electron dense, material. The nucleus (N) still showed indentation due to the acrosome and the chromatin now showed localized foci of highly, electron dense material, and thin threads of chromatin radiated from the foci. These regions of electron dense material tended to be more abundant in the peripheral parts of the nucleus (Fig. 7f). Also the condensed chromatin had become displaced from the nuclear envelope. There was a small area of dispersed chromatin between the electron dense chromatin and the nuclear envelope. At this phase there were 3 different types of chromatin organization. There were (1) thin threads of chromatin that were radiated from the 15-18 nm in diameter chromatin foci, (2) 39-48 nm foci in diameter, and (3) variable sized chromatin granules ranging from 35-79 nm located centrally (Fig. 8a). The anterior pole of each spermatid had become close to a process of Sertoli cell cytoplasm and cellular reorientation had occurred. Nucleoli were not observed in this phase. An array of microtubules of the manchette (M), which extended posteriorly from the perinuclear ring (pr), ensheathed the posterior approximate two-thirds of the elongating spermatid (Fig. 7f). A postacrosomal dense lamina (PADL) could be seen just above the perinuclear ring. The proximal centriole (C) occurred in a recess in the nuclear membrane, the implantation fossa (IF) (Fig. 7f).

The inner membrane of the nuclear envelope that was closed to the implantation fossa was thickened by dense material. A tail (T) of elongating spermatid was observed.

(4) Maturation Phase

Spermatids had entered the final form, or maturation, phase of spermiogenesis which was characterised by the completion of the chromatin condensation (Figs. 8b-8f). In addition to developing an extremely electron dense nucleus its gradually acquired the size and shape of the mature sperm. The acrosome (Ac) still contained electron dense material and was now indented posteriorly by a small nuclear extension (Fig. 8c) and there were two regions of differing electron dense material appearing in the acrosome (Figs. 8d-8f). The chromatin was very largely made up of 46-117 nm. granules and of threads of condensed chromatin (Fig. 8c). A small region of electron lucent material still occurred between the condensed chromatin and nuclear envelope especially posteriorly. Peripheral to the nucleus and passing from the nuclear ring posteriorly the microtubules of the manchette (M) were still present. The shape of the nucleus was more elongated than before. As spermatid progressed through this phase, the chromatin in the nucleus (Fig. 8e) now had an extensive area of homogeneous electron dense material although in addition conspicuous electron lucent regions together with some electron dense granules with size of 52-111 nm in diameter occurred. The overall nuclear shape was more elongated and more condensed further with some nuclear vacuoles containing spherical dense granules with 73-148 nm (Fig. 8f). At the conclusion of the condensation process the nucleoplasm was uniformly dense except for the presence of the nuclear vacuoles and some translucent areas.

2.2 Phosphotungstic acid (PTA) stained chromatin

For determining the present and distribution of lysine rich protein in the nuclear spermatids were stained with PTA. The results showed that in early spermatids the chromatin in the nucleus generally lightly stained with PTA (Fig. 10a). However the chromatin underlying the acrosome (Ac) stained strongly with PTA (Fig. 10b) as did some of the chromatin lying closed to the rest of the nuclear envelope. The next developmental stage the chromatin was lightly stained with PTA (Fig. 9c). The chromatin generally was lightly stained (Fig. 9d) except for a small area where a group of granules stained strongly PTA about 0.1 um in diameter. The chromatin stained more strongly with PTA which had an appearance of three dimensional meshwork (Fig. 10a) and also there were localized areas of strongly PTA stained material within the nucleus. With further maturation of the spermatids (Fig. 10b) the nucleus mainly had poorly stained PTA material except for the peripheral rim of chromatin and one to three regions in the anterior part of the nucleus which were strongly stained with PTA. Most of the nucleus (N) had negatively stained except for the peripheral rim, extended anterior region of nucleus, and near the basal plate (Fig. 10c).

In the acrosome (Ac) most of the acrosomal material did not stained with PTA except for a small localized area closed to the nuclear envelope. Between the PTA stained acrosomal material and the nucleus there was a thin region, subacrosomal space (SAS), of strongly stained PTA material.

3. To Localize the Distribution of Nuclear Proteins during Spermiogenesis.

3.1 Immunocytochemistry

Light micrographs of portions of seminiferous tubules immunostained with anti-H1 antibody (Fig. 11A and 11B). A positive staining pattern wass visualized at the base of the seminiferous tubule which referred to the spermatogonia. Some of them showed intensely immunoperoxidase reactivity (Fig. 11A, inserted a), somes were not. Pachytene spermatocytes (P) and spermatids were unreactive (arrow). A variable staining pattern was depicted among different seminiferous tubule depended on stage of cycle of seminiferous epithelium (Fig. 11B). Late spermatids showed dense reactivity of DAB reaction product within the spermatid nuclei (Fig. 11B, inserted b). Small amounts of spermatogonia cell type were positive staining (arrow). No reactivity of DAB reaction was found in primary spermatocytes (P).

Immunoreactivities of anti-H3 antibody of *Bandicota indica* seminiferous tubules (Fig. 11C and 11D). Pachytene spermatocytes showed highly reactivity throughout their nuclei (Fig. 11C, inserted c2) and also the spermatogonia (Fig. 11C, arrow), whilst round spermatids (Fig. 11C, inserted c1) showed immunoreactivity at the periphery of nuclei. Intense reactions of DAB product were present in late spermatids (Fig. 11D, arrows). Discontinuous thin rims as well as the occasional blebs of reaction product were present at the edge of round spermatid nuclei (Fig. 11D, arrow in inserted d). Spermatogonia and pachytene spermatocytes were unreactive.

Light micrographs of seminiferous tubules immunoperoxidase stained with anti-protamine antibody and the control (Fig. 11E and 11F). Fig.11E was a control section. Anti-protamine P2B antibodies reacted only in late spermatids (Fig. 11F, inserted f1, f2). Others were unreactive. The positively nuclear extension reactivity showed in late spermatids (Fig. 11F, inserted f2 arrow).

3.2 Immunogold Electronmicroscopy

Antibody to anti-histone H2A raised in rabbits: Popeye saignee 10 were used. In the condensing chromatin very light gold labeling was evident. However in the

condensed chromatin there was a greater abundance of gold particles although where there were nuclear vacuoles no labeling occurred. The labeling was spread throughout the chromatin (Fig.12).

With the anti- H2B antibody raised in rabbit Firmin saignee 27 again light labeling over dispersed chromatin was evident with a little increase over the electron dense chromatin even though no labeling occurred over the acrosomal region or other cytoplasmic regions of the spermatid (Fig.13).

Antibody to anti-histone H3 raised in Tristan saignee 9 again showed sparse labeling over the dispersed chromatin but heavy labeling over the condensed chromatin, although there was virtually no labeling over the acrosome (Fig.14).
With the anti-H4 raised in Cologne saignee 7 antibody there was again little labeling over the dispersed chromatin but dense labeling over the condensed chromatin although none over the nuclear vacuoles (Fig.15).

With antibodies to TP1 and TP2 abundant labeling was clearly evident over the condensed chromatin but the nuclear vacuoles were conspicuous in there total absent of any labeling (Fig.16).

4. To Characterize the Sperm Basic Nuclear Proteins.

Acid Urea Triton X-100 Polyacrylamide Gel Electrophoresis (AUT PAGE) and Immunoblotting

For this study, we used two standard markers; 1: chick erythrocytes as a standard marker for histones and 2: salmon protamine for protamine marker. Human, laboratory rat, and laboratory mouse spermatozoa were also co-electrophoresed with experimental samples (Fig. 17). Testes of these species were also done in the purpose to evaluate any the different patterns of histones between spermatogenic cells in the testes and mature spermatozoa in the cauda epididymis.

In bandicoot rats, the pattern of histones in the testes showed 4 different bands of H2A, H3, H2B, and H4 whilst in spermatozoa represented the same level of histone bands as in the testes but there were less amount of vary histones in mature spermatozoa because its paler staining with Coomassie Blue (Fig. 17). Moreover, in spermatozoa there was a major band located between the pack of histone bands and the protamine at the bottom. We assumed that this major band could be a transition protein or protamine-like protein in bandicoot spermatozoa. Further studies will be done to confirm for this expectation.

To proof the bioreactivity to antibody against protamine, the protamine in human and mouse spermatozoa has been detected by immunoblotting with anti-protamine antibody (Fig. 17, lane a and b). The positive immunoreactivity at the position of protamine was found in both species suggesting that this antibody had high specificity to its antigen which is suitable for immunohistochemistry and immunoblotting. Unfortunately, we have not yet proved the presence of protamine in bandicoot spermatozoa by immunoblotting. However, using AUT PAGE, the presence of protamine band of bandicoot spermatozoa was gaged by the same mobility as human and mouse spermatozoa. In the near future, we plan to load the higher concentration of proteins in bandicoot spermatozoa in order to detect by immunoblotting technique.

Table 1

Number and frequency (%) of each germ cell association in seminiferous tubule cross sections of Greater Bandicoot Rats

ANIMAL No.	Number and frequency (%) of tubules with typical cell associations									Total no. with typical cell associations	No. with atypical associations (%)	No. with multi-stage associations (%)
	I	II	III	IV	V	VI	VII	VIII	IX			
Bi 5-001	25(11.2)	65(29.0)	36(16.1)	45(20.1)	21(9.4)	8(3.6)	4(1.8)	0	20(8.9)	224	18(6.5)	34(12.3)
Bi 14-001	22(11.9)	77(41.6)	36(19.5)	23(12.4)	19(10.3)	6(3.2)	1(0.5)	0	1(0.5)	185	62(22.7)	26(9.5)
Bi 2-003	26(11.4)	76(33.3)	25(11.0)	47(20.6)	15(6.6)	14(6.1)	4(1.8)	3(1.3)	18(7.9)	228	6(2.3)	32(12.0)
Bi 7-003	10(9.8)	21(20.6)	14(13.7)	20(19.6)	22(21.6)	11(10.8)	0	1(1.0)	3(2.9)	102	12(8.5)	27(19.1)
Bi 8-003	7(6.5)	12(11.1)	16(14.8)	16(14.8)	26(24.1)	24(22.2)	2(1.9)	4(3.7)	1(0.9)	108	22(15.5)	12(8.3)
Bi 11-003	11(10.8)	20(19.6)	17(16.7)	12(11.8)	25(24.5)	10(9.8)	6(5.9)	0	1(1.0)	102	21(15.9)	9(6.8)
Total (mean)	101(10.6)	271(28.5)	144(15.2)	163(19.1)	128(13.5)	73(7.7)	17(1.8)	8(0.8)	44(4.6)	949	141(11.5)	140(11.4)

Table 2

Numbers of sperm nuclei in the various different shape categories shown in Fig. 5 for four individual Greater Bandicoot Rats

ANIMAL No.	N*	SPERM NUCLEAR SHAPES (see Fig. 5)**						
		1	2	3	4	5	6	7
Bi 4-003	289	92 (32%)	55 (19%)	29 (10%)	14 (5%)	35 (12%)	12 (4%)	52 (18%)
Bi 6-003	186	13 (7%)	73 (39%)	0	56 (30%)	26 (14%)	9 (5%)	9 (5%)
Bi 7-003	327	108 (33%)	0	26 (8%)	56 (17%)	26 (8%)	36 (11%)	75 (23%)
Bi 11-003	276	41 (15%)	14 (5%)	215 (78%)	0	6 (2%)	0	0

N* Total number of sperm counted for each individual
** Numbers refer to head shape shown in Fig. 5

Figs. 1-3. The stages of the cycle of seminiferous epithelium in *B. indica* as shown in plastic sections stained with toluidine blue. Fig 1a-1d = Stages I – IV, Fig 2a-2d = Stages V – VIII, and Fig 3 = Stage IX respectively. Abbreviations: A, In, B = A, intermediate, and B spermatogonia; Pl = preleptotene primary spermatocyte; L = leptotene primary spermatocyte; Z = zygotene primary spermatocyte; P = pachytene primary spermatocyte; D = diplotene primary spermatocyte; M-II = Meiosis II; 1-12 = steps of spermatid maturation. All scale bars = 10 μm.

Fig.1

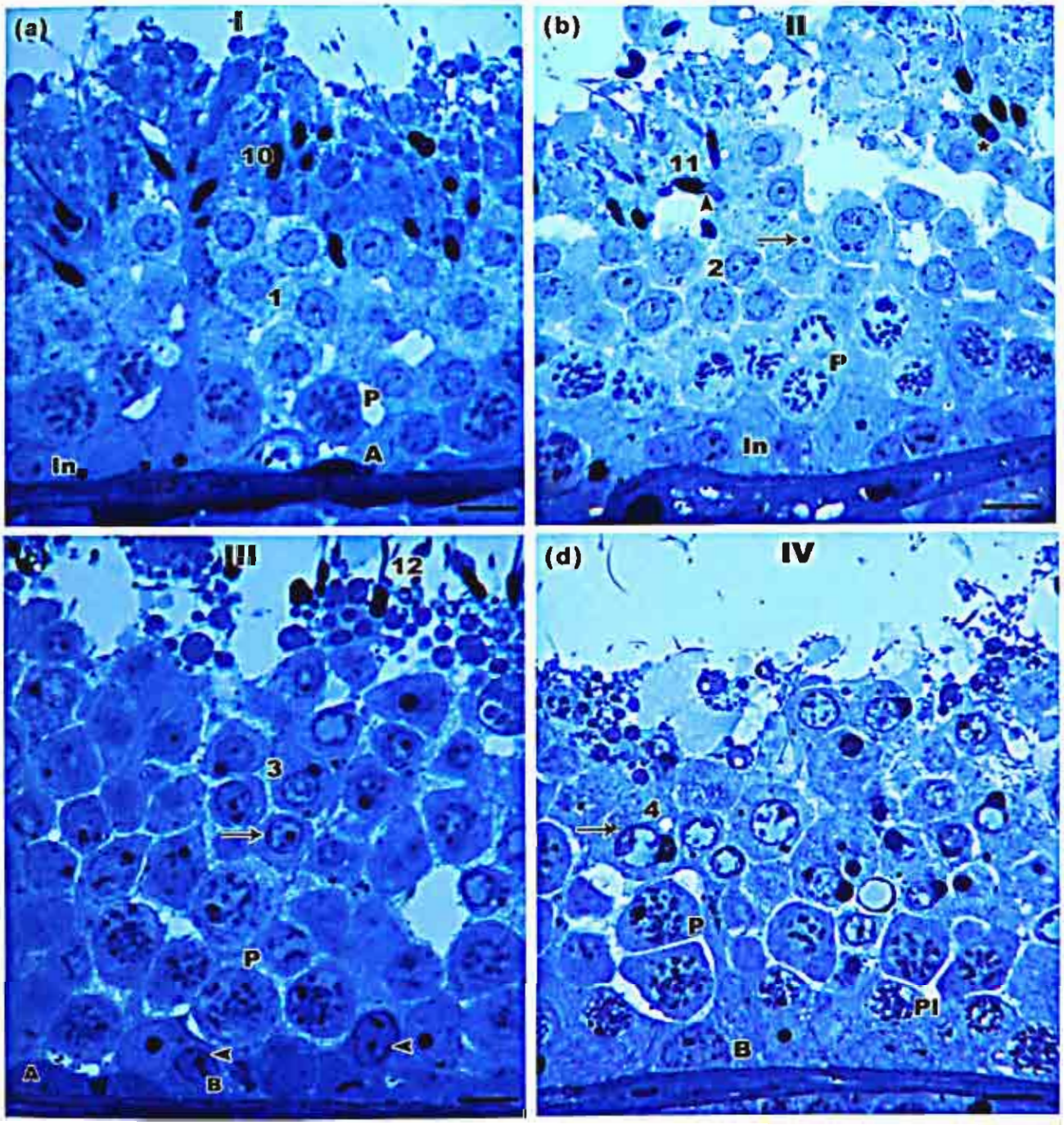

Figs. 1-3. The stages of the cycle of seminiferous epithelium in *B. indica* as shown in plastic sections stained with toluidine blue. Fig 1a-1d = Stages I – IV, Fig 2a-2d = Stages V – VIII, and Fig 3 = Stage IX respectively. Abbreviations: A, In, B = A, intermediate, and B spermatogonia; Pl = preleptotene primary spermatocyte; L = leptotene primary spermatocyte; Z = zygotene primary spermatocyte; P = pachytene primary spermatocyte; D = diplotene primary spermatocyte; M-II = Meiosis II; 1-12 = steps of spermatid maturation. All scale bars = 10 μm.

Fig.2

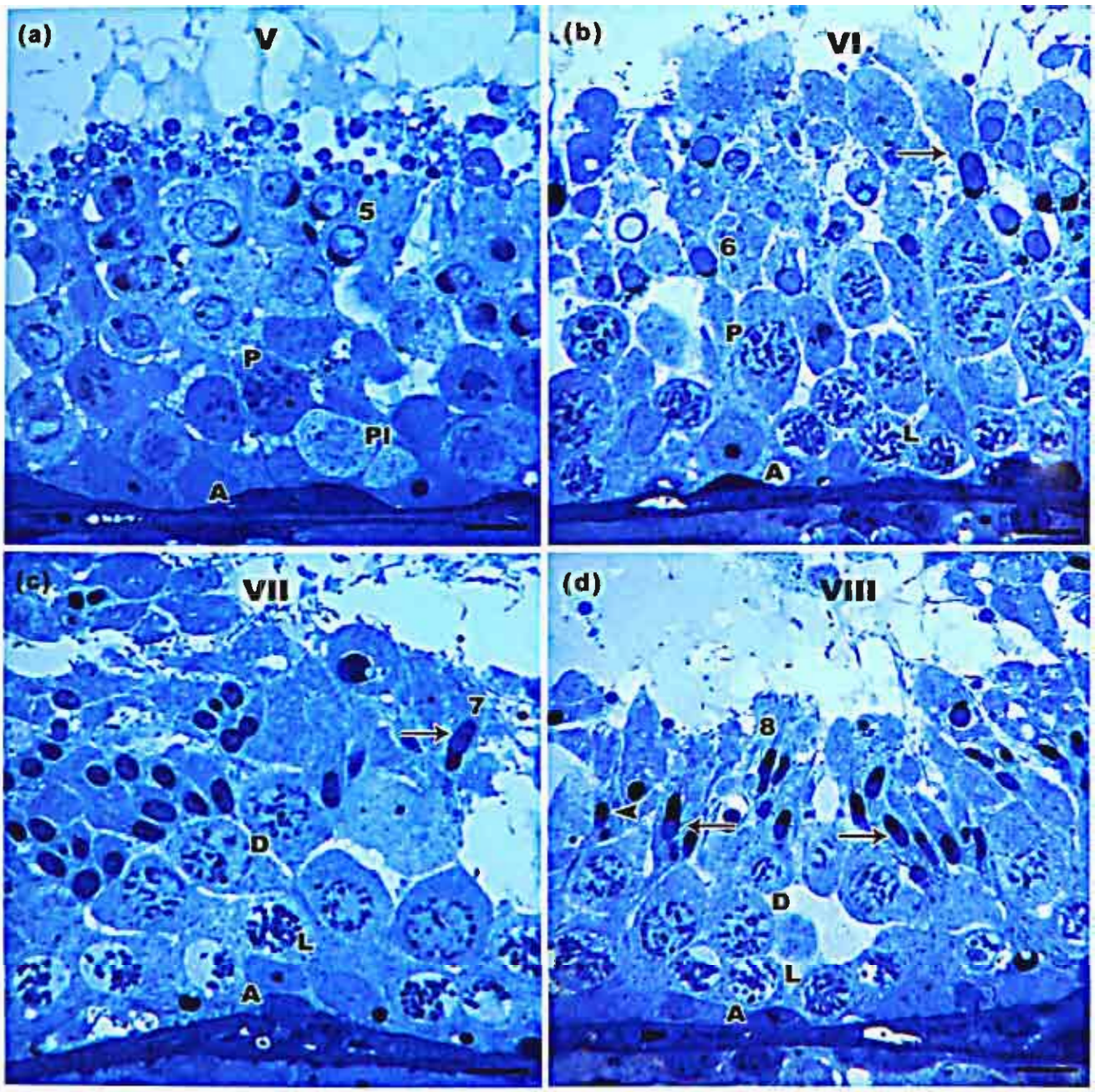

Figs. 1-3. The stages of the cycle of seminiferous epithelium in *B. indica* as shown in plastic sections stained with toluidine blue. Fig 1a-1d = Stages I – IV, Fig 2a-2d = Stages V – VIII, and Fig 3 = Stage IX respectively. Abbreviations: A, In, B = A, intermediate, and B spermatogonia; Pl = preleptotene primary spermatocyte; L = leptotene primary spermatocyte; Z = zygotene primary spermatocyte; P = pachytene primary spermatocyte; D = diplotene primary spermatocyte; M-II = Meiosis II; 1-12 = steps of spermatid maturation. All scale bars = 10 μm.

Fig.3

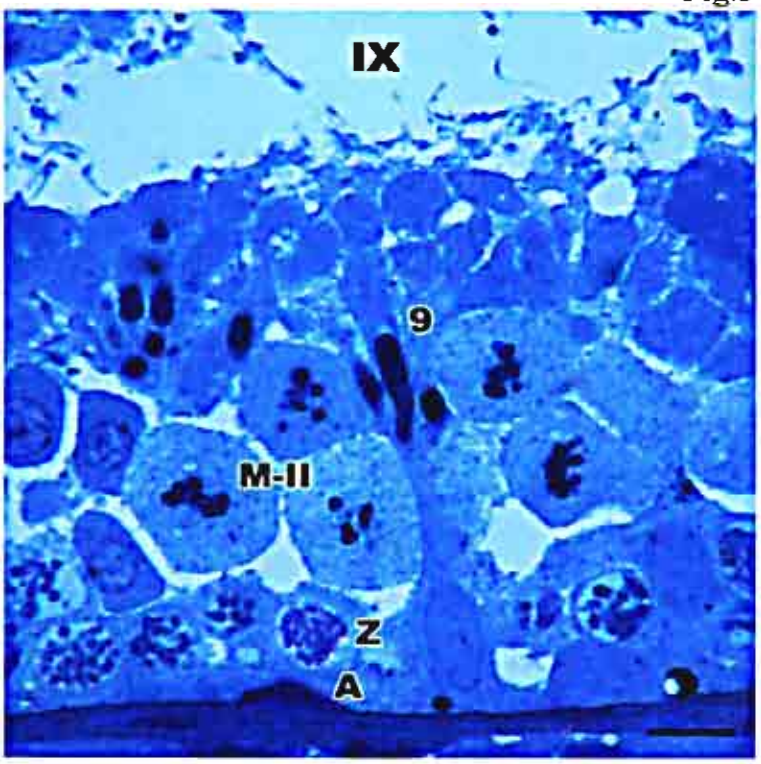

Fig. 4. Seminiferous tubules of *B. indica* testis containing more than one cell association in the same cross-section (a) Stages V, VI, and IX, (b) Stages III and IV, (c) Stages II and VI, (d) Stages III, IV and IX, (e) Atypical cell association of Stage VII and M-II (meiosis II), and (f) Atypical cell association of Stage I and VII. All scale bars = 25 μm.

Fig.4

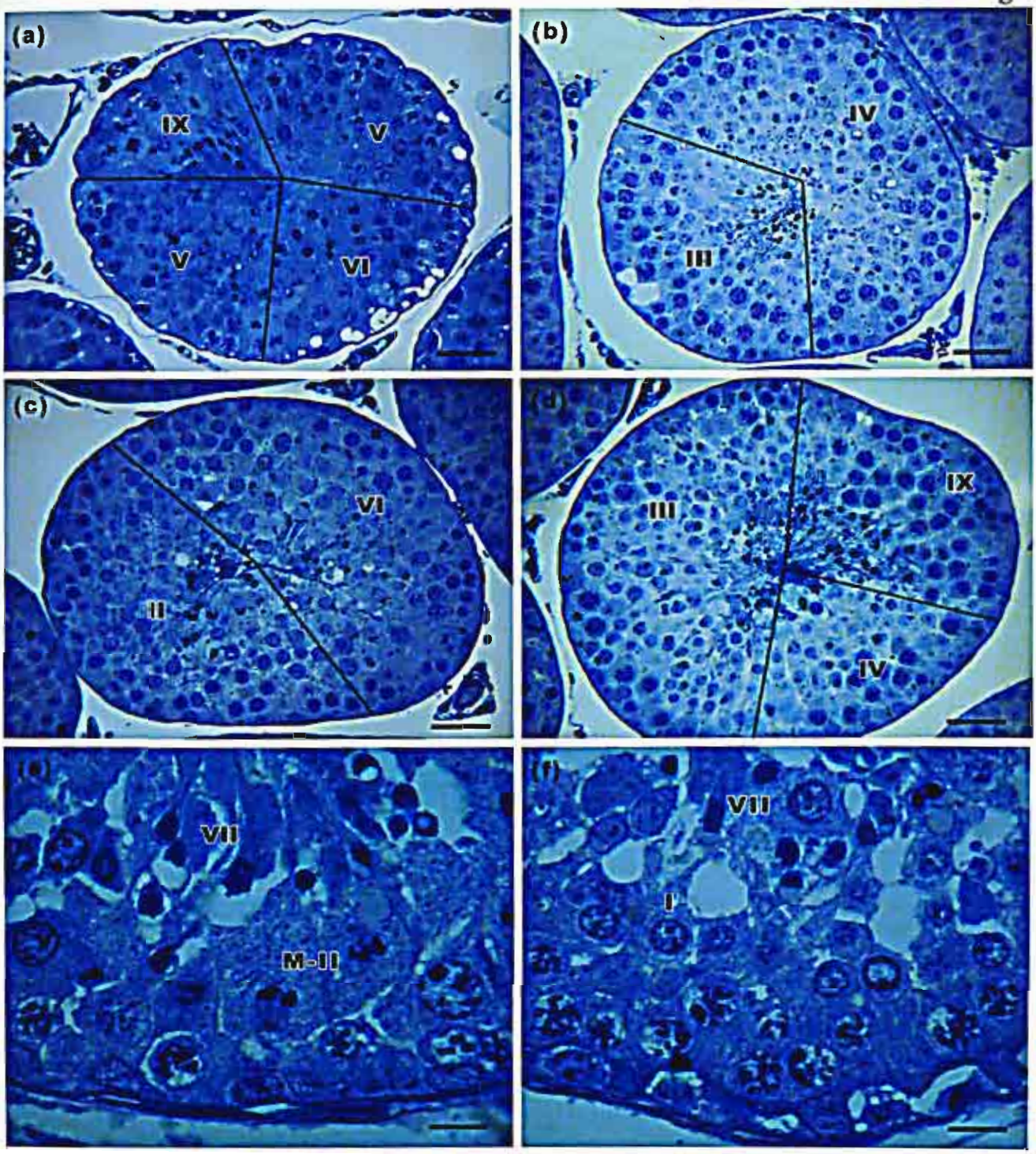

Fig. 5. Fluorescence microscopy of nuclei of cauda epididymal sperm from *B. indica* adult male stained with propidium iodide showing highly variable nuclear shape. Scale bar = 2.8 μm.

Fig.5

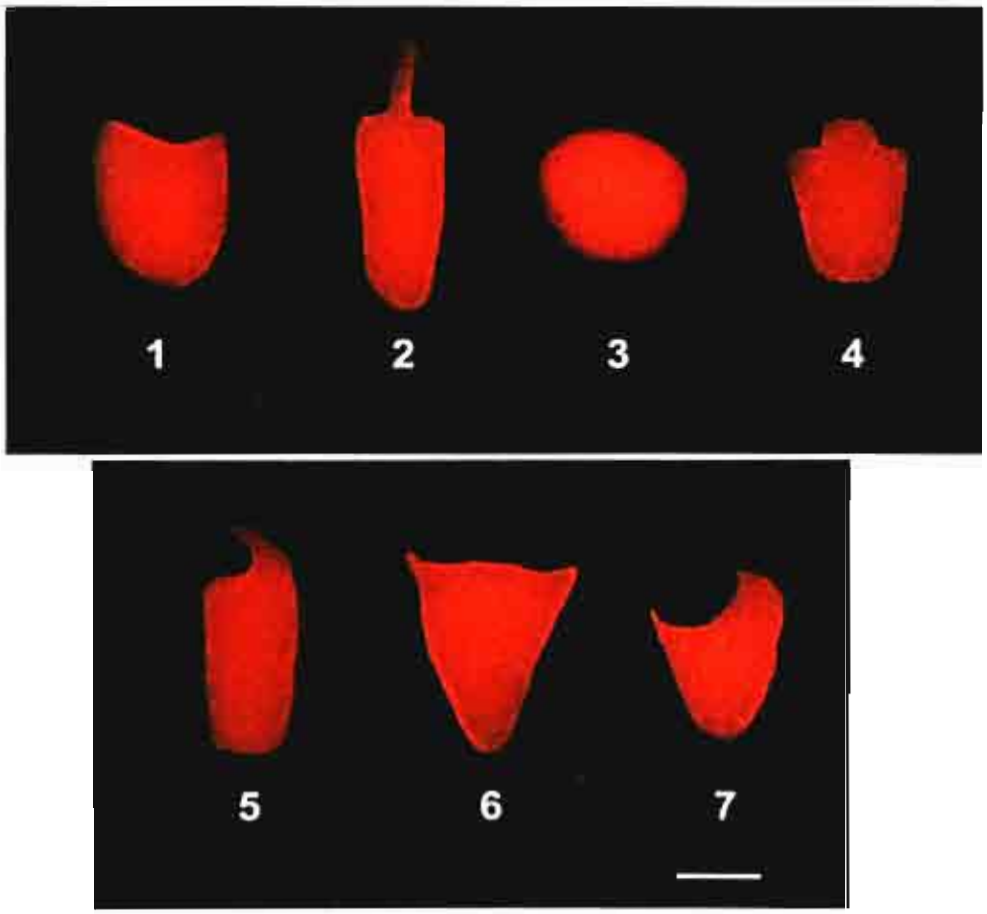

Fig. 6. A map of the stages of the cycle of seminiferous epithelium in *B. indica*, showing the phases of germ cell development. Type A spermatogonia have been omitted. Abbreviations: In, B = intermediate, and B spermatogonia; PL = preleptotene, L = leptotene, Z = zygotene, P = pachytene, D = diplotene primary spermatocytes; M-II = meiosis II; 1-12 = steps of spermatid maturation (for more details see text and Figs 1 - 3).

Fig.6

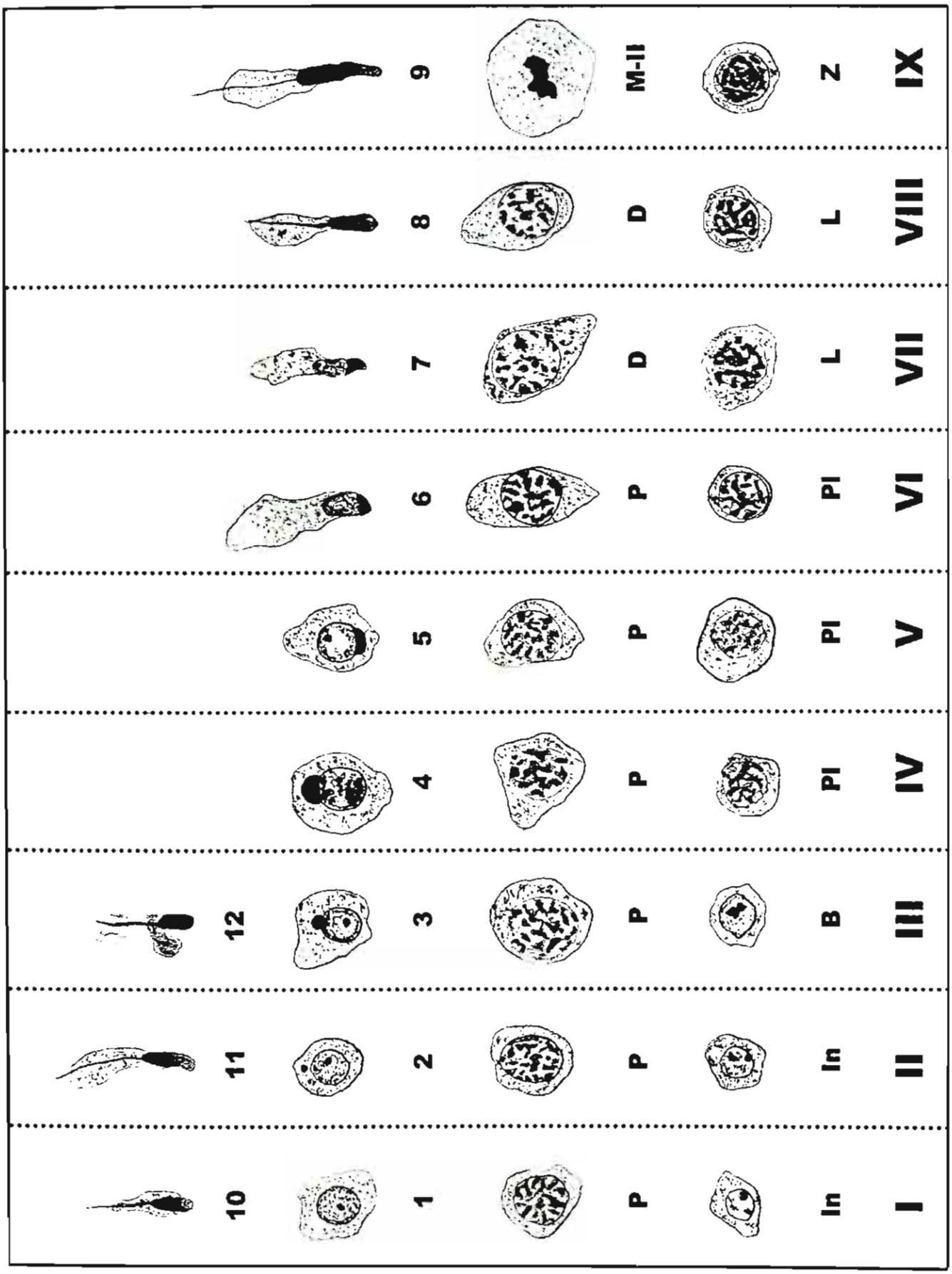

Figs. 7-8. Transmission electron micrographs of four successive phases based upon the principal morphologenetic events which occurred as development proceeds. Fig. 7a-7b = Initial or Golgi phase showed numerous small, electron dense proacrosomal granules (G) appearing between the Golgi apparatus and nucleus (N). Chromatin threads with 15-23 nm in diameter located throughout the nucleus. Fig. 7c-7d = Cap phase a large acrosomal granule attached to the nuclear membrane to form an acrosome (Ac) over the anterior pole of nucleus (N). Thin region of condensed electron dense chromatin just beneath the acrosome (Fig. 7d-arrow) as well as close to other regions of the nuclear envelope (Fig. 7c-arrow). Fig. 7e-7f, and 8a-8c = Acrosome phase the acrosome became oval shape with homogeneous, electron dense material. Shape of nucleus had bi-laterally flattened with gradually condensed chromatin diameter of 39-48 nm foci and chromatin granules ranging from 35-79 nm in diameter located centrally (Fig. 8a-arrow). Fig. 8d-8f = Maturation phase chromatin developing an extremely electron dense nucleus with 46- 117 nm granules in the nucleus and showing the spherical electron dense granules with 73- 148 nm in the nuclear vacuoles (NV) (Fig. 8e-8f-arrow). Abbreviations: PADL = postacrosomal dense lamina, M = manchette. IF = implantation fossa, pr = perinuclear ring, and T = tail. All scale bars = 1 um. and 2 um for Fig. 7f.

Fig.7

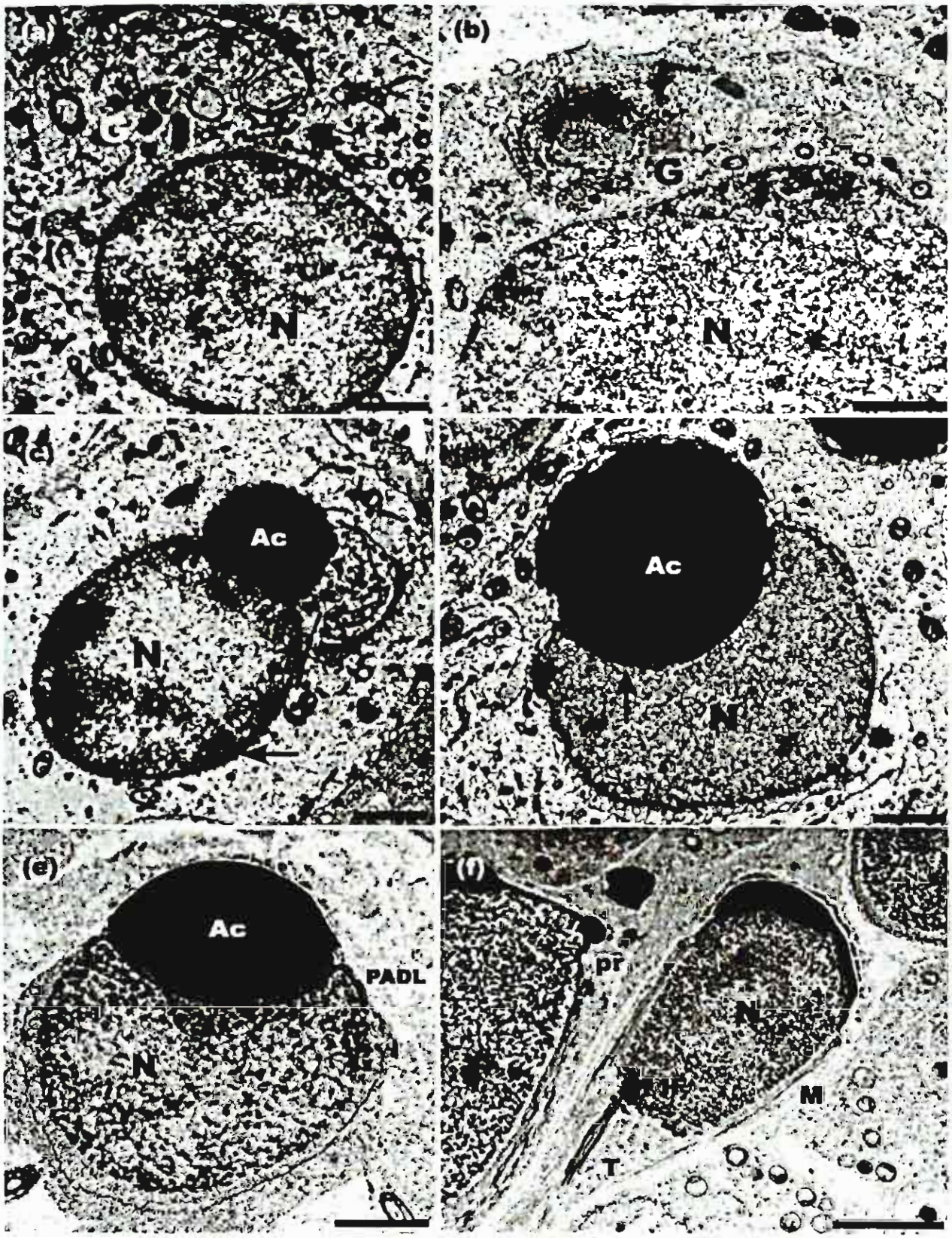

Figs. 7-8. Transmission electron micrographs of four successive phases based upon the principal morphologenetic events which occurred as development proceeds. Fig. 7a-7b = Initial or Golgi phase showed numerous small, electron dense proacrosomal granules (G) appearing between the Golgi apparatus and nucleus (N). Chromatin threads with 15-23 nm in diameter located throughout the nucleus. Fig. 7c-7d = Cap phase a large acrosomal granule attached to the nuclear membrane to form an acrosome (Ac) over the anterior pole of nucleus (N). Thin region of condensed electron dense chromatin just beneath the acrosome (Fig. 7d-arrow) as well as close to other regions of the nuclear envelope (Fig. 7c-arrow). Fig. 7e-7f, and 8a-8c = Acrosome phase the acrosome became oval shape with homogeneous, electron dense material. Shape of nucleus had bi-laterally flattened with gradually condensed chromatin diameter of 39-48 nm foci and chromatin granules ranging from 35-79 nm in diameter located centrally (Fig. 8a-arrow). Fig. 8d-8f = Maturation phase chromatin developing an extremely electron dense nucleus with 46- 117 nm granules in the nucleus and showing the spherical electron dense granules with 73- 148 nm in the nuclear vacuoles (NV) (Fig. 8e-8f-arrow). Abbreviations: PADL = postacrosomal dense lamina, M = manchette. IF = implantation fossa, pr = perinuclear ring, and T = tail. All scale bars = 1 um. and 2 um for Fig. 7f.

Fig.8

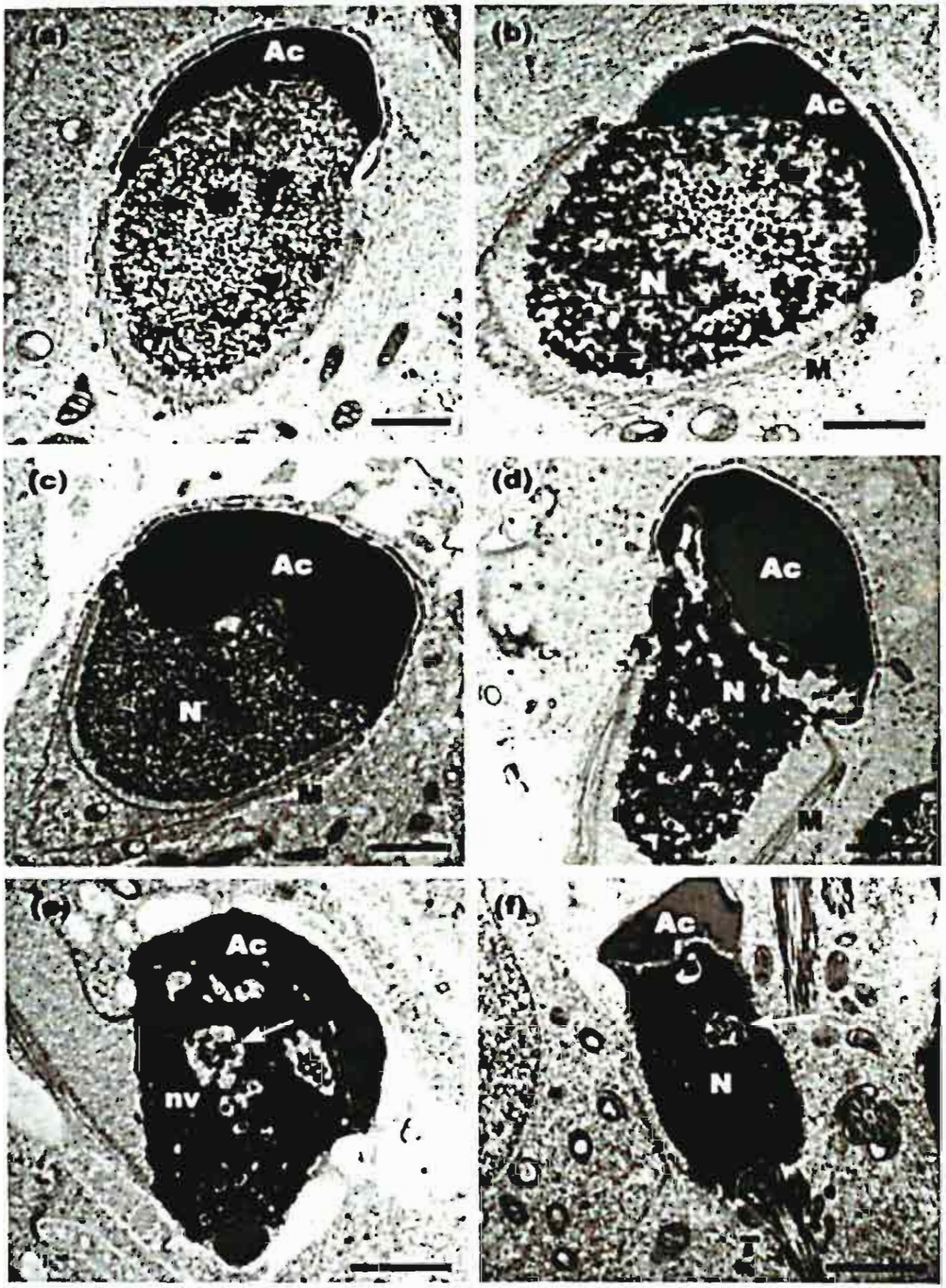

Figs. 9-10. Phosphotungstic acid (PTA) stained detecting lysine rich protein in the nuclear chromatin. Early spermatid generally lightly stained chromatin (Fig. 9a), however chromatin lying close to nuclear envelope as well as did some chromatin underlying the acrosome (Ac) stained strongly (Fig. 9b-arrow). Small area of group of chromatin granules had positively stained (Fig. 9c, 9d-arrow). PTA strongly stained material localized within the nucleus (N) and an area underneath the acrosome (Fig. 10a-arrow). With further maturation of spermatid nucleus had poorly stained PTA except for the peripheral nuclear rim (Fig. 10b-arrow), anterior part of nucleus (N) (Fig. 10b-arrowhead), and near the basal plate (Fig. 10c-arrow). Acrosomal material did not stained with PTA except for a small localized area closed to nuclear envelope (Fig. 9c-arrow). Between acrosome and nucleus there was a thin region, subacrosomal space (SAS) stained strongly. Abbreviations: PADL = postacrosomal dense lamina. All scale bars = 1 um. and 0.5 um for Fig. 10a.

Fig.9

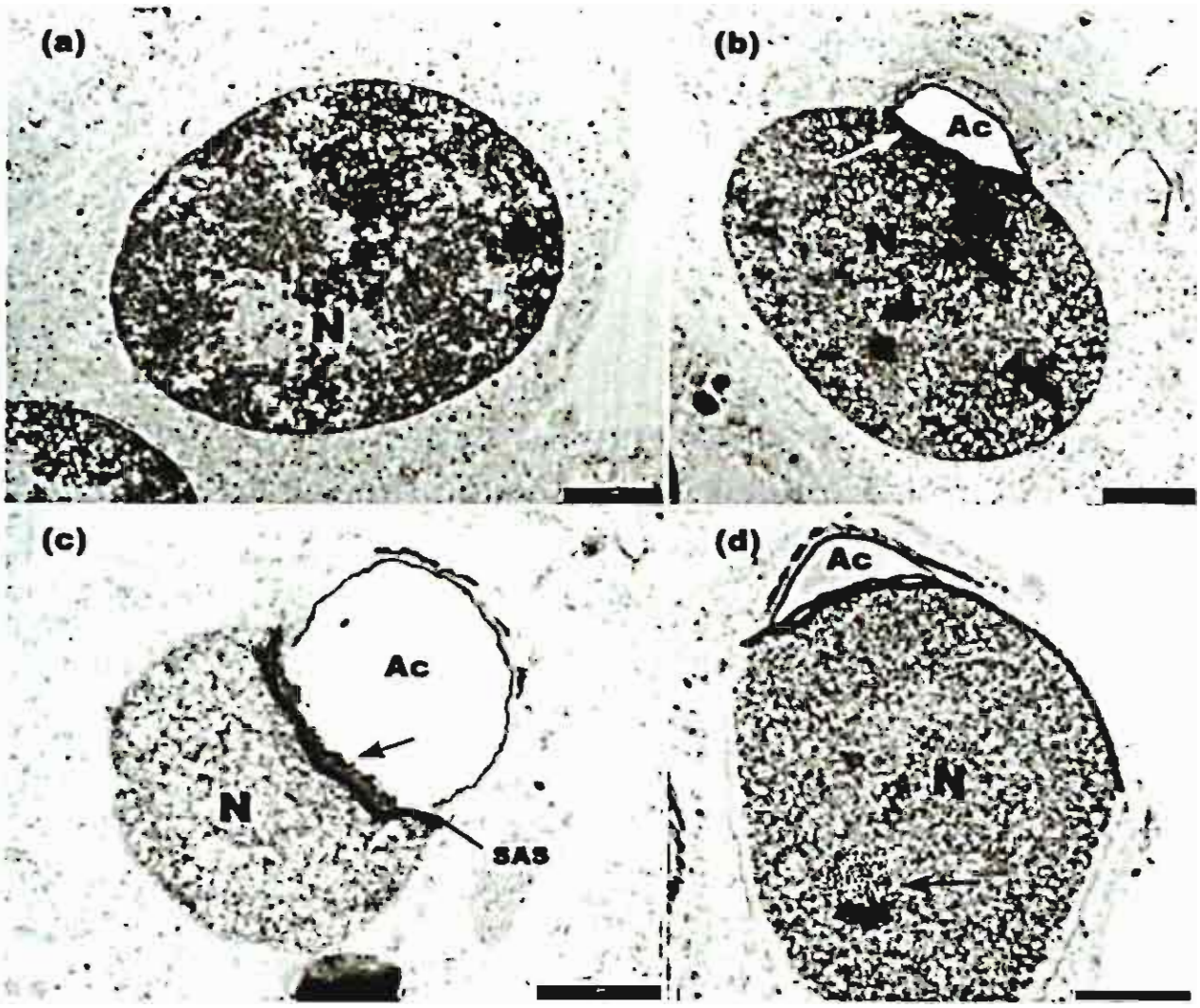

Figs. 9-10. Phosphotungstic acid (PTA) stained detecting lysine rich protein in the nuclear chromatin. Early spermatid generally lightly stained chromatin (Fig. 9a), however chromatin lying close to nuclear envelope as well as did some chromatin underlying the acrosome (Ac) stained strongly (Fig. 9b-arrow). Small area of group of chromatin granules had positively stained (Fig. 9c, 9d-arrow). PTA strongly stained material localized within the nucleus (N) and an area underneath the acrosome (Fig. 10a-arrow). With further maturation of spermatid nucleus had poorly stained PTA except for the peripheral nuclear rim (Fig. 10b-arrow), anterior part of nucleus (N) (Fig. 10b-arrowhead), and near the basal plate (Fig. 10c-arrow). Acrosomal material did not stained with PTA except for a small localized area closed to nuclear envelope (Fig. 9c-arrow). Between acrosome and nucleus there was a thin region, subacrosomal space (SAS) stained strongly. Abbreviations: PADL = postacrosomal dense lamina. All scale bars = 1 um. and 0.5 um for Fig. 10a.

Fig.10

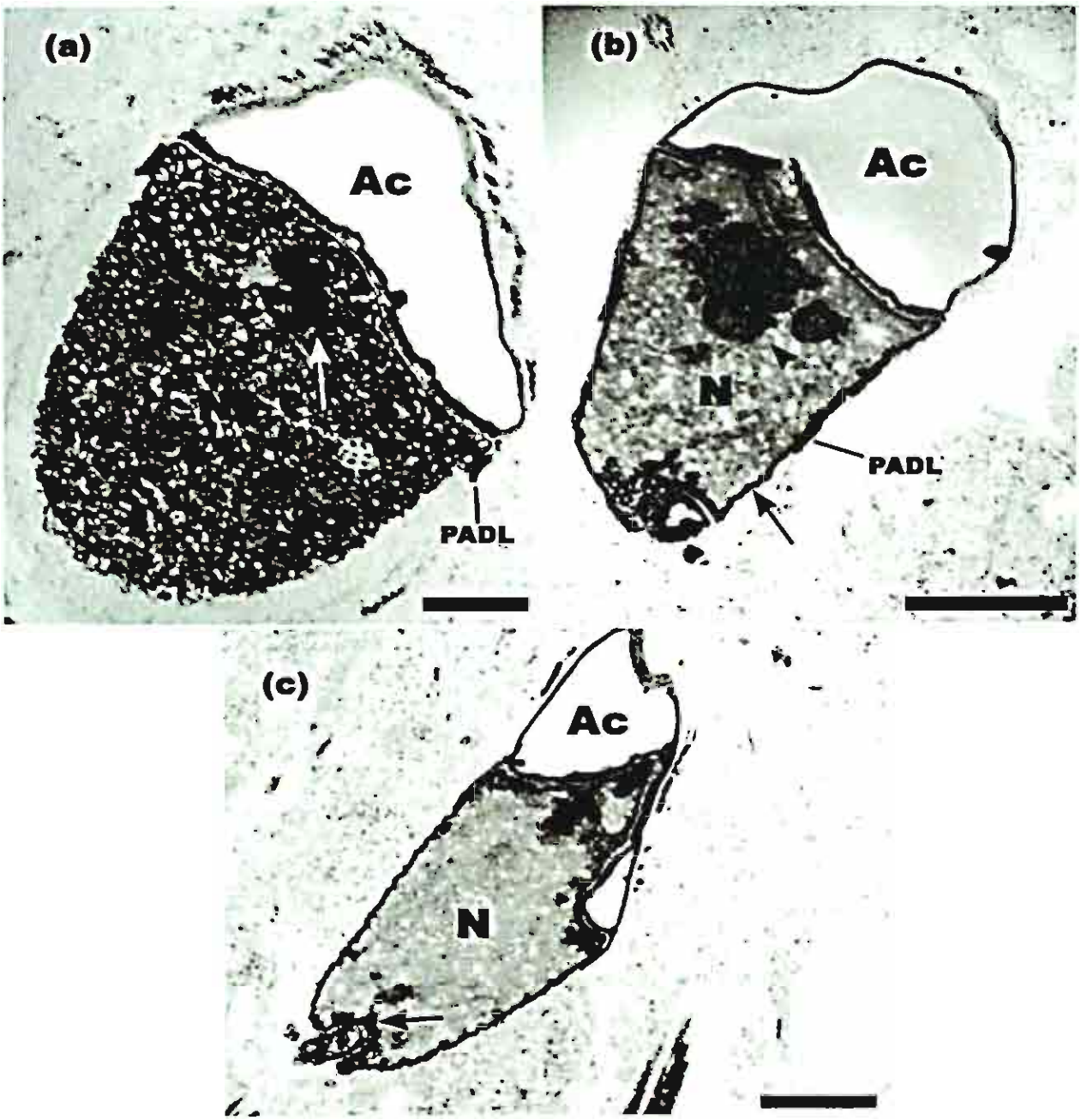

Fig. 11. Light micrographs of paraffin sections of seminiferous tubules immunostained with anti-H1 antibody. A positive staining pattern was visualized at the base of the seminiferous tubule which referred to the spermatogonia. Some of them showed intensely immunoperoxidase reactivity as in Fig. 11A-inserted a, some were not. Pachytene spermatocytes (P) and spermatids are unreactive (Fig. 11A-arrow). A variable staining pattern was depicted among different seminiferous tubule depends on stage of cycle of seminiferous epithelium. Late spermatids showed dense immunoreactivity within the spermatid nuclei as in Fig. 11B-inserted b. Small amounts of spermatogonia cell type are positive staining (Fig. 11B-arrow). No immunoreactivity was found in primary spermatocytes (P). Immunoreactivities of anti-H3 antibody of *B.indica* seminiferous tubules (Fig. 11C, 11D). Pachytene primary spermatocytes showed highly reactivity throughout their nuclei as in Fig. 11C-inserted c2 and also the spermatogonia (Fig. 11C-arrow), whilst round spermatids (inserted c1) showed immunoreactivity at the periphery of nuclei. Intense reactions of anti-H3 antibody presented in late spermatids (Fig. 11D-arrows). Discontinuous thin rims as well as the occasional blebs of reaction product were present at the edge of round spermatid nuclei (Fig. 11D-arrow in inserted d). Spermatogonia and pachytene spermatocytes were unreactive. Light micrographs of seminiferous tubules immunoperoxidase stained with anti-protamine antibody and the control. Fig. 11E was a control section. Fig.11F anti-protamine P2B antibodies reacted only in late spermatids (inserted f1, f2). Others were unreactive. Inserted f2 showed the positively nuclear extension reactivity in late spermatids (Fig. 11F-arrow).

Fig.11

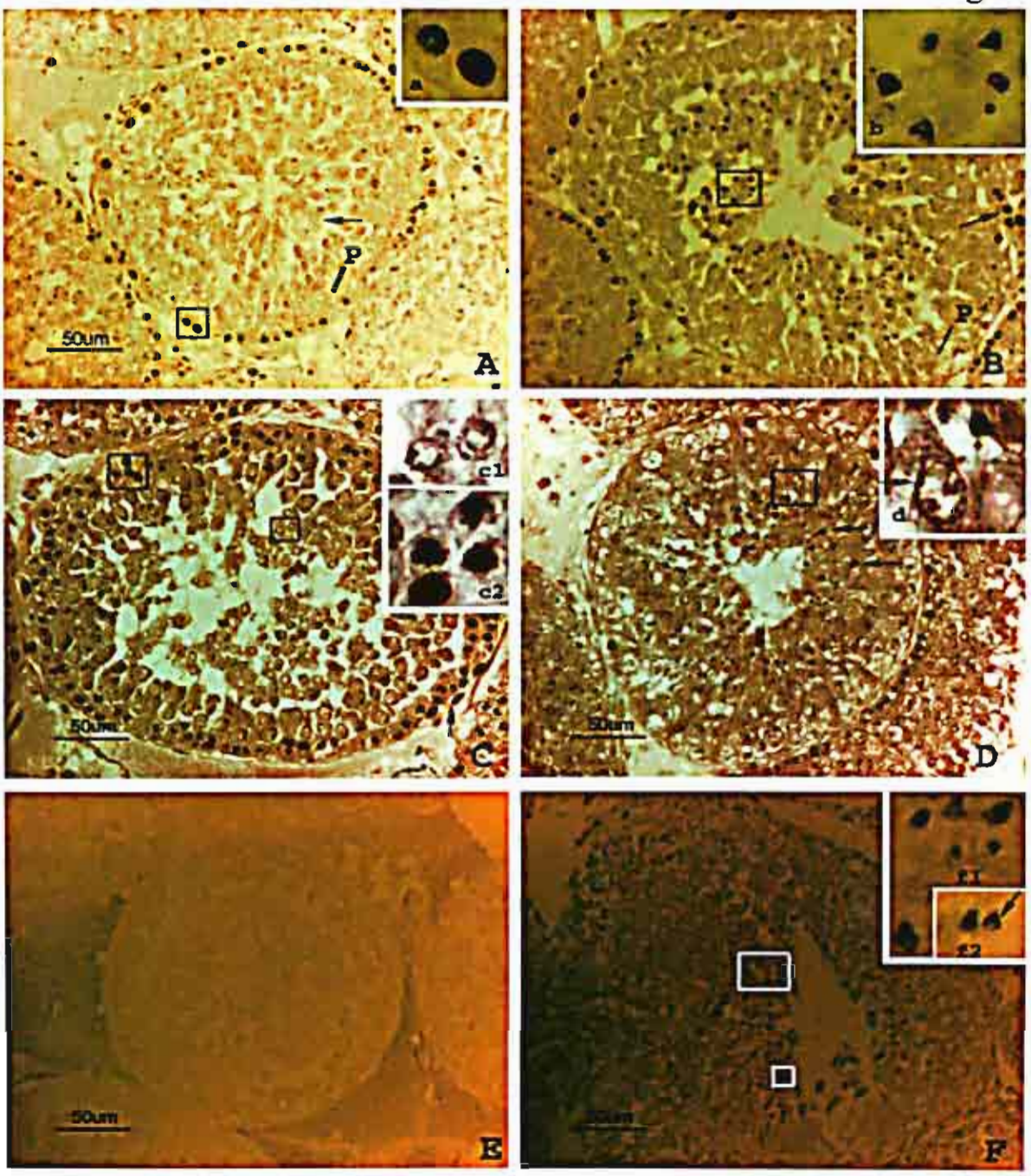

Fig. 12. Transmission electron micrographs (TEM) of gold labeled of spermatid nuclei (a, b, c, and f) and cauda epididymides (d, e) using anti-histone H2A antibody. A number of gold particles were more in nuclei of cauda spermatozoa (d, e) than those in spermatids (a, b, c) but no labeling occurred in nuclear vacuoles (nv) (f). Bar represents 1 um. in fig. (a), 200 nm in fig. (f), and 500 nm in fig. (b-e).

Fig.12

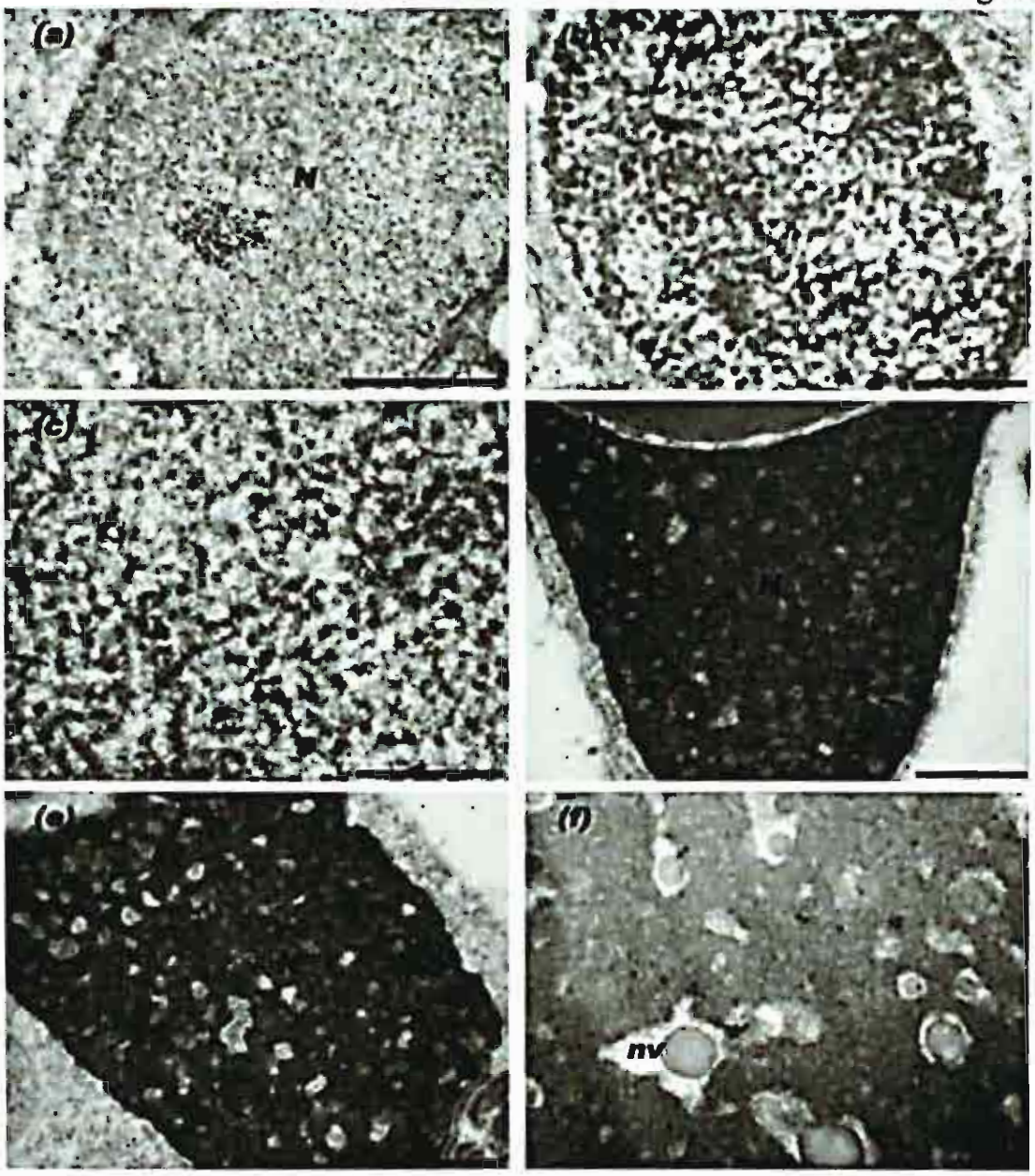

Fig. 13. Immunoelectron micrographs of spermatids and mature sperms stained with anti-histone H2B. A small amount of gold particles were observed in spermatids (a-d), while a slightly increased gold particles in mature sperms (e, f). There is no labeling over the acrosomal region (Ac), nuclear vacuoles (nv), and in part of cytoplasm. Bar represents 200 nm in fig. (e), and 500 nm in fig. (a-d, f).

Fig.13

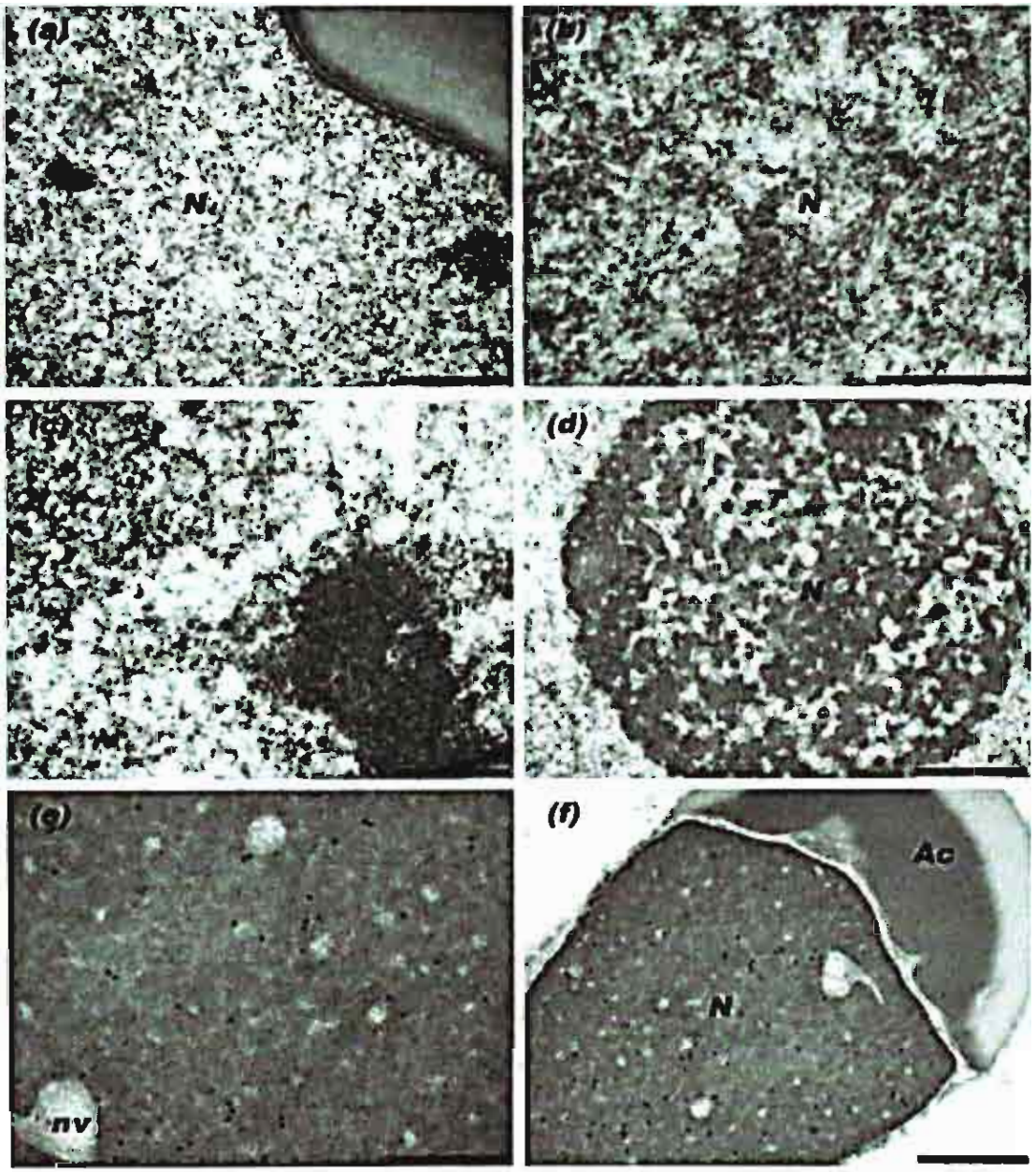

Fig. 14. Immunoelectron micrographs of spermatids and mature sperms stained with anti-histone H3 showing sparse labeling over the dispersed chromatin (a, b), but heavy labeling occurred over condensed chromatin (c, d) in cauda sperm. In the acrosome (Ac) and nuclear vacuoles (nv) showed no labeling (e, f). Bar represents 200 nm in fig. (a, f), and 500 nm in fig. (b-e).

Fig.14

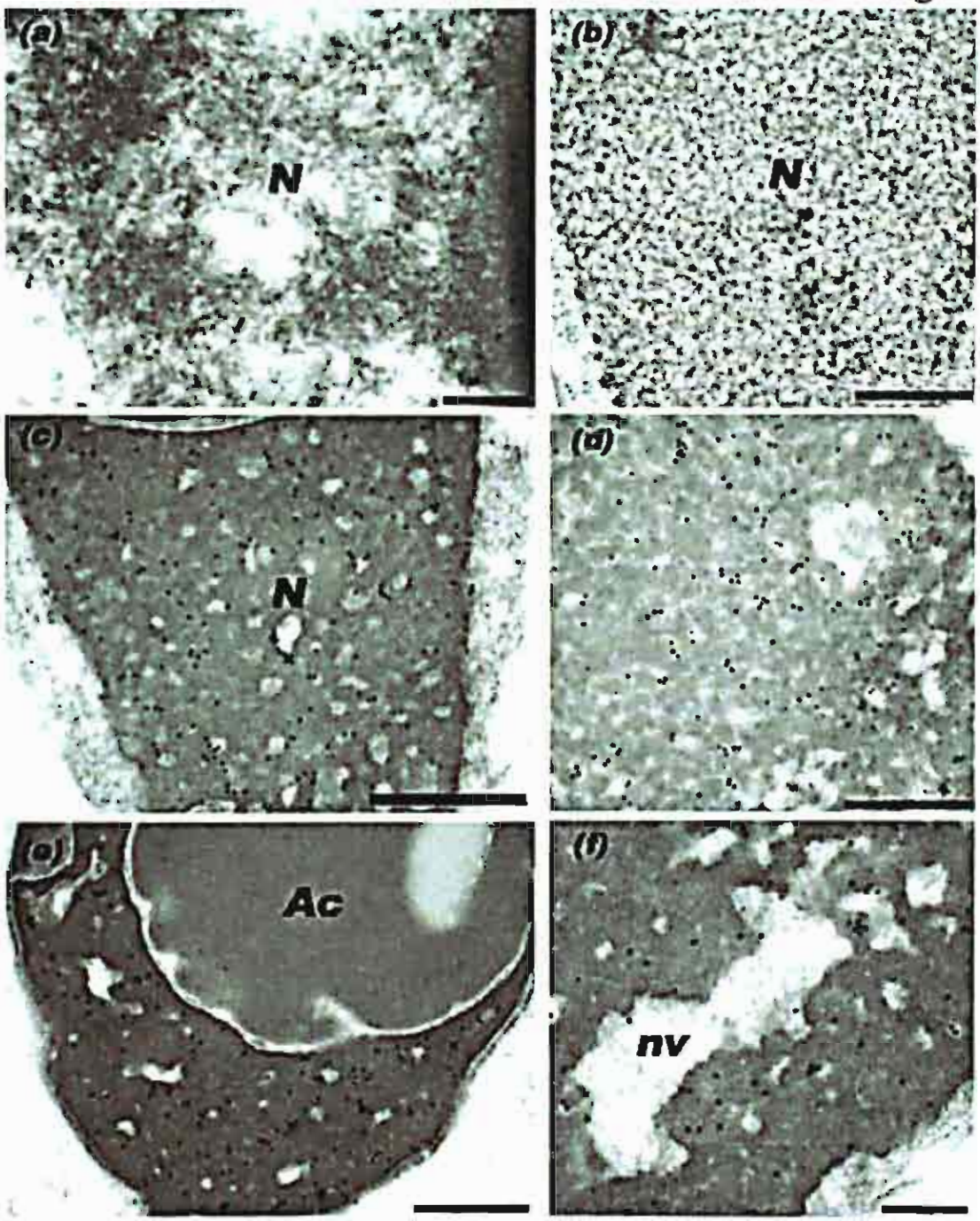

Fig. 15. Immunoelectron micrographs of spermatids and mature sperms stained with anti-histone H4. It showed little labeling over the chromatin in the testicular spermatids (a, b) but more labeling over condensed than uncondensed chromatin (c, d, e), the nuclear vacuoles (nv) showed no labeling (f). Bar represents 1 um. in fig. (b), 200 nm in fig. (e), and 500 nm in fig. (a, c-d, f).

Fig.15

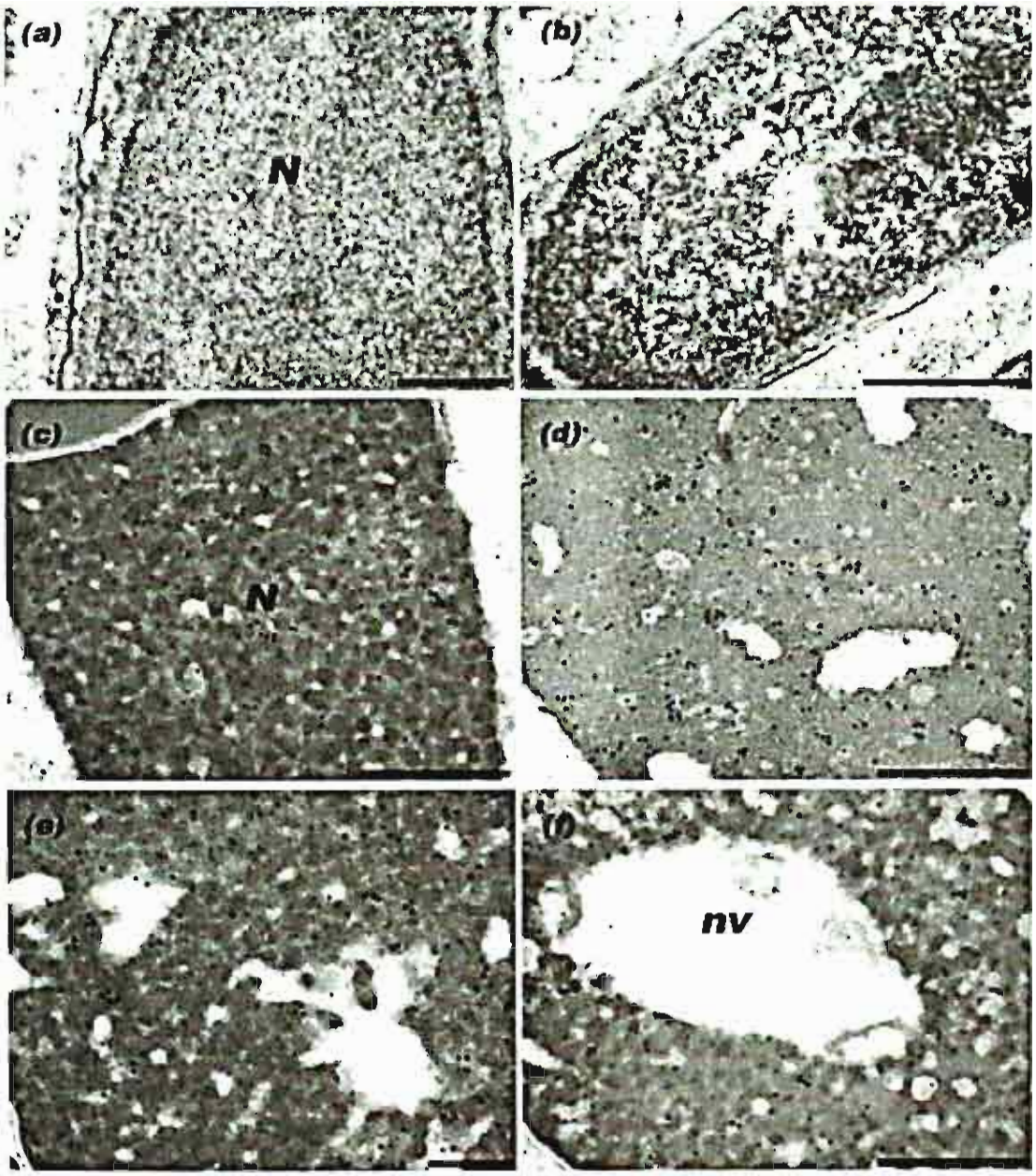

Fig. 16. Gold labeling of transmission electron micrographs using anti-transition proteins TP1 (b-f) and TP2 (a) antibodies. Abundant labeling was clearly evident over the condensing chromatin and also over the condensed chromatin (a-d) but the nuclear vacuoles were conspicuous in their total absent of any labeling (e, f). Bar represents 1 um. in fig. (b, c), 200 nm in fig. (f), and 500 nm in fig. (a, d, and e).

Fig.16

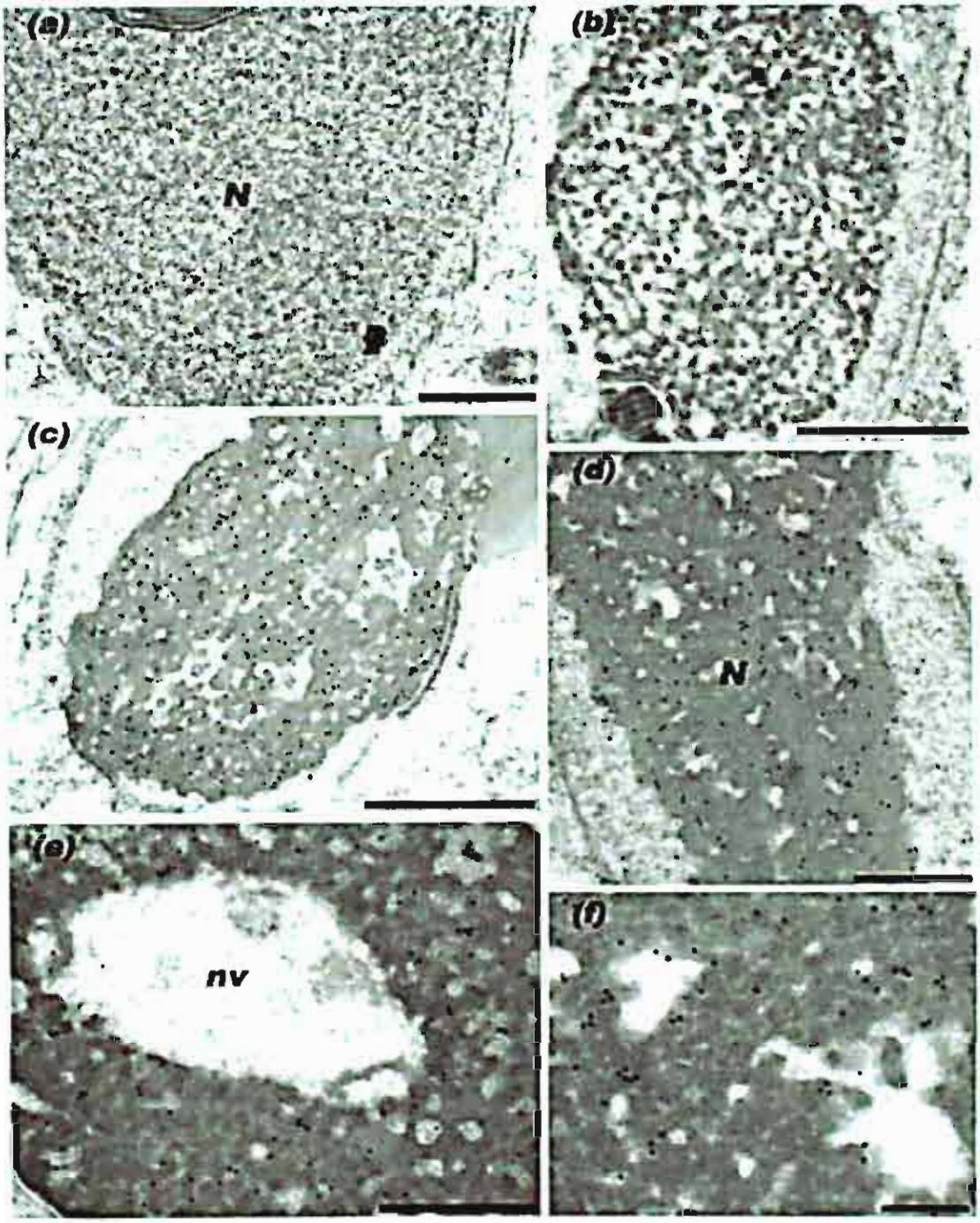

Fig. 17. AUT-PAGE (17%) analysis of the basic nuclear proteins from spermatozoa nuclei of human, *B. indica*, lab rat, and lab mouse (lane 2-5) comparing with the nuclei of testicular cells of *B. indica*, lab rat, lab mouse (lane 6-8), and salmon protamine (lane 9) respectively. Basic nuclear proteins from chick erythrocytes were used as a standard marker (lane 1). Extracted proteins were applied to each well and electrophoresed from top (+) to bottom (-). Each lane showed the Coomassie Blue-stained bands displaying all fractions of histones (H), transition proteins or protamine-like (PL), and protamines (P). Lane a and b = basic nuclear proteins from human and mouse spermatozoa demonstrated the specificity of anti- protamines antibody analyzed by Western blotting.

Fig.17

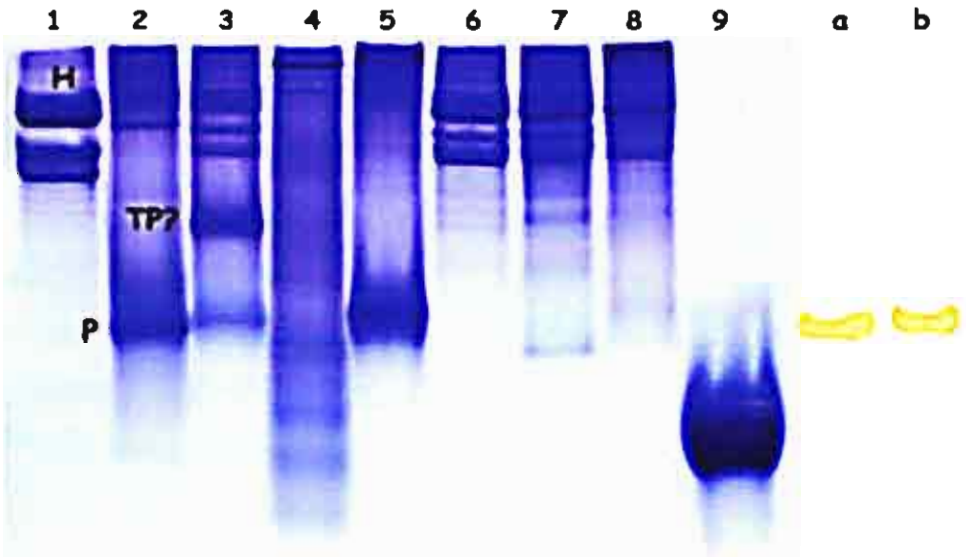

CONCLUDING REMARKS AND DISCUSSION

Stages of the Seminiferous Epithelium

Characteristics of each cell type were described in detail in this study. The criteria used were cell size and their appearance, the presence of marking organelles such as Golgi body, acrosomal granule, and the condensation of chromatin fibers corresponding with the reduced size of nuclei. As the sperm cell developed and differentiated, Golgi body became visible at stage II. Meanwhile, the acrosomal granule was initially formed in in this stage. This acrosomal granule then contacted with nuclear membrane and it finally became elongated along the nuclear shape. Nuclear chromatin gradually packed tighter and tighter in correlation with the slimmer and small head as the spermatogenic cell became more mature.

Morphological characteristics of spermatogenic cells along with the pattern of cellular association were further used as the criteria to establish seminiferous cycles which were consisted of nine stages. These cellular associations were considerable of heterogenous type and closely similar to that of humans, namely, more than one seminiferous cycle could be found in a cross section of the tubule.

After production in the testis, the sperm of most mammals must be translocated into epididymis to undergo the post-testicular modification in order to gain more fertilizing ability. During this sperm "maturation" process, epididymal sperm are still considerably heterogenous in certain degree depending on species. As assess the sperm head morphology by propidium iodide staining, sperm of *B. indica* revealed a higher degree of heterogeneity among other rodent species. In this context, there were at least seven types of head morphology was notified in bandicoot epididymal sperm.

This study thus showed that this species of bandicoot rat, *B. indica*, has several features of the germ cell organization in the testis that differ from that of the laboratory rat and lesser bandicoot rats. In some regards they showed some similarity to that of humans, apes and New World primates (Chowdhury & Steinberger, 1976; Johnson *et al.*, 1992; Johnson, 1994a; Smithwick *et al.*, 1996; Wistuba *et al.*, 2003). Greater bandicoot rats have previously been found also to have highly derived and pleiomorphic cauda epididymal sperm populations (Breed, 1993, 1998) and, in the

present study, the pleiomorphic nature of the sperm nuclei was also confirmed. Furthermore, previous transmission electron microscope studies have shown nuclear vacuoles were sometimes present in late spermatids, testicular spermatozoa, and epididymal spermatozoa and that there was a variable response between the spermatozoa in chromatin dispersion when cauda spermatozoa are incubated in detergents (Breed, 1998). Therefore, the present observations, together with those made previously, indicated that some of the processes of germ cell maturation and the final form of the sperm of the greater bandicoot rat showed some similarity to the situation in humans (Bedford *et al.*, 1973; Fawcett, 1975).

In conclusion, the greater bandicoot rat, that was a common and widespread species throughout much of southeast Asia (Corbett & Hill, 1992; Musser & Carleton, 1993), may turn out to be a useful model for investigations on the processes controlling spermatogenesis and sperm form due to the lack of tight synchrony in both germ cell maturation and final sperm form that occurs. Andrologists in southeast Asia may thus have a very useful model for probing questions on the regulatory processes of male germ cell morphogenesis and maturation both of which are extremely poorly understood phenomena at the present time (Sharp, 1994).

We have published one paper from these data in International Journal of Andrology (see the attached document).

Chromatin Condensation during Spermiogenesis

Although it has been known that the nuclear chromatin undergo high degree condensation during germ cell differentiation, mediating through the replacement of histones with a higher positive charged basic nuclear proteins, termed transition protein and protamine. Sperm of *B. indica* possessed a wide variety of head morphology, therefore, it would be interested to see the pattern of basic nuclear proteins and their localization in developing and differentiated germ cells.

Information of immunohistochemical analysis clearly demonstrated that the remaining of histones in late differentiated spermatids, and protamine was found mainly in late differentiated spermatid. This histone remnant was not coincident with

the presence of many nuclear vacuoles as was addressed by immunoTEM. Question is still remained whether what materials make up of the nuclear vacuoles and why there is still a considerably high level of histone in late differentiated germ cells in *B. indica*? We further confirmed that during germ cell development in the testis, there seem to be a gradual decrease of total histone proteins (observed by the intensity of Coomassie Blue staining when compared to epididymal sperm). Histones were also present in epididymal sperm in considerably high level. It was also apparent that there were transition protein and protamine in epididymal sperm, however, the amount of TP proteins seem to be much higher than protamine. This result was somewhat discrepancy to other mammals studied where protamine was shown to be a predominant basic protein in mature sperm. The onset of transition proteins and protamine was still unclear at the moment and need further investigation.
The experiments will be repeated before any firm conclusion is drawn.

We are preparing in manuscript for publication (about molecular level of chromatin condensation in B. indica) and will be submitted to Biology of Reproduction or Molecular Reproduction and Development.

REFERENCES

Allen, M. J., Bradbury, E. M., & Balhorn, R. (1997). AFM analysis of DNA-protamine complexes bound to mica. Nucleic Acids Research, 25, 2221-2226.

Amann, R. P. (1962). Reproductive capacity of dairy bulls. IV. Spermatogenesis and testicular germ cell degeneration. American Journal of Anatomy, 110, 69-78.

Balhorn, R. (1982). A model for the structure of chromatin in mammalian sperm. Journal of Cell Biology, 93, 298-305.

Balhorn, R., Weston, S., Thomas, C., & Wyrobek, A. J. (1984). DNA packaging in mouse spermatids. Synthesis of protamine variants and four transition proteins. Experimental and Cell Research, 150, 298-308.

Balhorn, R. (1989). Mammalian protamine: Structure and molecular interactions. In K. W. Adolph (Ed.), Molecular biology of chromosome function (pp. 366-395). New York: Springer Verlag.

Balhorn, R., Cosman, M., Thornton, K., Krishnan, V. V., Corzett, M., Bench, G., et al. (1999). Protamine mediated condensation of DNA in mammalian sperm. In C. Gagnon (Ed.), The male gamete: From basic science to clinical applications (pp. 55-70). Vienna: Cache River Press.

Bedford, J.M, Bent, M.J. & Calvin, H. (1973) Variations in the structural characters and stability of the nuclear chromatin in morphologically normal human spermatozoa. Journal of Reproduction and Fertility, 33, 19-29.

Bedford, J. M., & Calvin, H. I. (1974). The occurrence and possible functional significant of -S-S- crosslinks in the sperm, with particular reference to eutherian mammals. Journal of Experimental Zoology, 188, 137-158.

Bedford, J. M. (1982). Fertilization. In C. R. Austin & R. V. Short (Eds.), Reproduction in mammals: Germ cells and Fertilization (2 ed., Vol. 1, pp. 128-163). Cambridge: Cambridge University Press.

Bedford, J. M. (1991). The Coevolution of Mammalian Gametes. In B. S. Dunbar & M. G. O'Rand (Eds.), A Comparative Overview of Mammalian Fertilization (pp. 3-39). New York: Plenum Press.

Bilaspuri, G.S. & Kaur, R. (1994) Spermatogenic cells and stages of the seminiferous epithelial cycle in the Indian Gerbil Field Rat, Tatera indica. Reproduction Fertility and Development, 6, 699-704.

Boonsong, L., & McNeely, J. A. (1977). Mammals of Thailand. In (pp. 397-427). Ladprao, Bangkok: Kurusapha.

Breed, W.G. (1993) Novel organisation of the spermatozoon in two species of murid rodents from Southern Asia. Journal of Reproduction and Fertility, 99, 149-158.

Breed, W.G. (1998) Interspecific variation in structural organisation of the spermatozoon in the Asian Bandicoot rats. Bandicota species (family Muridae). Acta Zoologica, 79, 277-285.

Breed, W. G., & Taylor, J. (2000). Body mass, testis mass, and sperm size in murine rodents. Journal of Mammalogy, 81, 758-768.

Breed, W. G. (2004) The spermatozoon of Eurasian murine rodents: its morphological diversity and evolution. Journal of Morphology, 261, 52-69.

Chowdhury, A.K. & Steinberger, E. (1976) A study of germ cell morphology and duration of spermatogenic cycle in the baboon Papio anubis. Anatomical Record, 185, 155-170.

Clermont, Y. (1963). The cycle of the seminiferous epithelium in man. American Journal of Anatomy, 112, 35-51.

Clermont, Y. & Trott, M. (1969) Duration of the cycle of the seminiferous epithelium in the mouse and hamster determined by means of 3H-thymidine and radioautography. Fertility and Sterility, 20, 805-817.

Clermont, Y., & Antar, M. (1973). Duration of the cyle of the seminiferous epithelium and the spermatogonial renewal in the monkey Macaca arctoides. American Journal of Anatomy, 136, 153-166.

Clermont, Y., Oko, R., & Hermo, L. (1993). Cell biology of mammalian spermiogenesis. In C. Desjardins & L. L. Ewing (Eds.), *Cell and Molecular Biology of the Testis* (pp. 332-376). New York: Oxford University Press.

Corbett, G. B., & Hill, J. E. (1992). The mammals of the Indomalayan Region:A Systematic Review. In Natural History Museum Publications (pp. 488). Oxford: Oxford University Press.

Courtens, J. L., & Loir, M. (1981). A cytochemical study of nuclear changes in boar, bull, goat, mouse, rat, and stallion spermatids. Journal of Ultrastructure Research, 74, 327-340.

Curtis, G. M. (1918). The morphology of the mammalian seminiferous tubule. American Journal of Anatomy, 24, 339-394.

Dadoune, J. P. (1991). Cytochemical variations in the nucleolus during spermiogenesis in man and monkey. Cell and Tissue Research, 264, 167-173.

Dang, D. C. (1971). Dure'e du cycle de l'e'pithe'lium se'minife're du singe crabier, Macaca fascicularis. Annales de Biologie Animale, Biochimie, Biophysique, 11, 373-377.

de Rooij, D. G., van Alphen, M. M. A., & van de Kant, H. J. G. (1986). Duration of the cycle of the seminiferous epithelium and its stages in the rhesus monkey (Macaca mulatta). Biology of Reproduction, 35, 587-591.

Fawcett, D.W. (1975) The Mammalian spermatozoon. Developmental Biology, 44, 394-436.

Golberg, R. B., Geremia, R., & Bruce, W. R. (1977). Histone synthesis and replacement during spermatogenesis in the mouse. Differentation, 7, 167-180.

Grocock, C.A. & Clarke, J.R. (1975) Spermatogenesis in mature and regressed testes of the vole (Microtus agretis). Journal of Reproduction and Fertility, 43, 461-470.

Grocock, C.A. & Clarke, J.R. (1976) Duration of spermatogenesis in the vole (Microtus agrestis) and bank vole (Clethrionomys glareolus). Journal of Reproduction and Fertility, 47, 133-135.

Hecht, N. B. (1989). Mammalian protamine and their expression. In L. Hnilica, G. Stein & J. Stein (Eds.), Histones and other basic nuclear proteins (pp. 347-373): Boca Raton: CRC Press.

Heller, C. G., & Clermont, Y. (1963). Spermatogenesis in man: an estimate of its duration. Science, 140, 184-186.

Heller, C. G., & Clermont, Y. (1964). Kinetics of germinal epithelium in man. Recent Prog. Horm. Res., 20, 545-575.

Hess, R. A., Schaeffer, D. J., Eroschenko, V. P., & Keen, J. E. (1990). Frequency of the stages in the cycle of the seminiferous epithelium in the rat. Biology of Reproduction, 43, 517-524.

Hilscher, W. (1964). Beitrage zur Orthologie und Pathologie der 'Spermatogoniogenese' der Ratte. Beitrage zur pathologischen Anatomie und allgemeinen Pathologie, 130, 69-132.

Holstein, A. F., & Roosen-Runge, E. C. (1981). *Atlas of human spermatogenesis.* Berlin: Grosse Verlag.

Holt, W. V., & Moore, H. D. M. (1984). Utrastructural aspects of spermatogenesis in the common marmoset (Callithrix jacchus). Journal of Anatomy, 138(1), 175-188.

Johnson, L., Petty, C.S. & Neaves, W.B. (1980) A comparative study of daily sperm production and testicular composition in humans and rats. Biology of Reproduction 22, 1233-1243.

Johnson, L., Chaturvedi, P. K., & Williams, J. D. (1992). Missing generations of spermatocytes and spermatids in seminiferous epithelium contribute to low efficiency of spermatogenesis in humans. Biology of Reproduction, 47, 1091-1098.

Johnson, L. (1994a) A new approach to study the architectural arrangement of spermatogenic stages revealed little evidence of a partial wave along the length of human seminiferous tubules. Journal of Andrology, 15, 435-441.

Johnson, L., Varner, D.D., Roberts, M.E., Smith, T.L., Keillor, G.E. & Scrutchfield, W.L. (2000) Efficiency of spermatogenesis: a comparative approach. Animal Reproduction Science 60-61, 471-480.

Kornberg, R. D., & Lorch, Y. (1999). Twenty-five years of the nucleosome, fundamental particle of the eukaryote chromosome. *Cell, 98*, 285-294.

Kurohmaru, M., Kobayashi, H., Hattori, S., Nishida, T., & Hayashi, Y. (1994). Spermatogenesis and ultrastructure of a peculiar acrosomal formation in the muck shrew, Suncus murinus. Journal of Anatomy, 185, 503-509.

Laemmli, U. K. (1970). Cleavage of structural proteins during the assembly of the head of bacteriophage T4. Nature, 227, 680-685.

Lalli, M., & Clermont, Y. (1981). Structural changes of the head components of the rat spermatid during late spermiogenesis. American Journal of Anatomy, 160, 419-434.

Leblond C.P. & Clermont Y. (1952) Spermiogenesis of rat, mouse, hamster and guinea pig as revealed by the 'periodic acid-fuchsin sulfurous acid' technique.Am.J.Anat. 90, pp.167-216

Lombardi, J. (1998). Gamete and their reproduction. In J. Lombardi (Ed.), *Comparative Vertebrate Reproduction* (pp. 109-130). London: Kluwer Academic Publishers.

Manochantr, S., Sretarugsa, P., Chavadej, C., & Sobhon, P. (2004). Chromatin organization and basic nuclear proteins in the male germ cells of Rana tigerina. Molecular reproduction and development, 9999, 1-14.

Meistrich, M. L., Trostle-Weige, P. K., & Van Beek, M. E. (1994). Separation of specific stages of spermatids from vitamin A-synchronized rat testes for assessment of nucleoprotein changes during spermiogenesis. Biology of Reproduction, 51, 334-344.

Munoz, E.M., Fogal, T., Dominguez, S., Scardapane, L., Guzman, J., Cavicchia, J.C. & Piezzi, R.S. (1998) Stages of the cycle of the seminiferous epithelium of the viscacha (Lagostomus maximus maximus). The Anatomical Record, 252, 8-16.

Musser, G. G., & Carleton, M. D. (1993). Family Muridae. In D. E. Wilson & D. M. Reeder (Eds.), Mammal Species of the World (2 ed., pp. 501-755). Washington D.C.: Smithsonian Institute.

Oakberg, E. F. (1956). Duration of spermatogenesis in the mouse and timing of stages of the cycle of the seminiferous epithelium. American Journal of Anatomy, 99, 507-516.

Oko, R., & Clermont, Y. (1988). Isolation, structure and protein composition of the perforatorium of rat spermatozoa. Biology of Reproduction, 39, 673-687.

Oko, R., Moussakova, L., & Clermont, Y. (1990). Regional differences in composition of the perforatorium and of the outer periacrosomal layer of rat spermatozoa as revealed by immunocytochemistry. American Journal of Anatomy, 188, 64-73.

Ortavant, R. (1954). Contribution a' l'e'tude de las dure'e du processus spermatoge'ne'tique du be'lier a' l'aide de P32. Comptes Rendus Socie'te' de Biologie, 148, 804-806.

Ortavant, R. (1956). Autoradiographie des cellules germinales du testucule de be'lier. Dure'e des phe'nome'nes spermatoge'ne'tiques. Archives d'Anatomie Microscopique et de Morphologie Experimentale, 45, 1-10.

Ortavant, R. (1959). Spermatogenesis and morphology of the spermatozoon. In H. H. Cole & P. T. Cupps (Eds.), Reproduction in Domestic Animals (Vol. 2, pp. 1-50). New York: Academic Press.

Oud, J.J. & de Rooij, D.G. (1977) Spermatogenesis in the Chinese hamster. The Anatomical Record, 187, 113-124.

Paula, T.A.R., Chiarini-Garcia, H. & Franca, L.R. (1999) Seminiferous epithelium cycle and its duration in capybaras (Hydrochoerus hydrochaeris). Tissue & Cell, 31, 327-334.

Peirce, E.J. & Breed, W.G. (1987) Cytological organization of the seminiferous epithelium in the Australian rodents Pseudomys australis and Notomys alexis. Journal of Reproduction and Fertility, 80, 91-103.

Perey, B., Clermont, Y. & Leblond, C.P. (1961) The wave of the seminiferous epithelium in the rat. American Journal of Anatomy, 108, 47-78.

Platz, R. D., Grimes, S. R., Meistrich, M. L., & Hnilica, L. S. (1975). Changes in nuclear proteins of rat testis cells separated by velocity sedimentation. Journal of Biological and Chemistry, 250, 5791-5800.

Ravindranath, N., Dettin, L., & Dym, M. (2003). Mammalian testes: structure and function. In D. Tulsiani (Ed.), *Introduction to mammalian reproduction* (pp. 1-19). Boston: Kluwer Acadamic Publishers.

Redi, C.A., Garagna, S., Heth, G. & Nevo, E. (1986) Descriptive kinetics of spermatogenesis in four chromosomal species of the Spalax ehrenbergi superspecies in Israel. The Journal of Experimental Zoology, 238, 81-88.

Roosen-Runge, E. C., & Giesel, L. O. (1950). Quantitative studies on spermatogenesis in the albino rat. American Journal of Anatomy, 87, 1-30.

Russell, L.D., Ettlin, R.A., Sinha Hikim, A.P. & Clegg, E.D. (1990) Histological and histopathological evaluation of the testis, pp. 286 Vienna, IL, Cache River Press.

Schuler, H.M. & Gier, H.T. (1976) Duration of the cycle of the seminiferous epithelium in the prairie vole (Microtus ochrogaster ochrogaster). Journal of Experimental Zoology 197, 1-11

Schulze, W. & Rehder, U. (1984) Organization and morphogenesis of the human seminiferous epithelium. Cell and Tissue Research, 237, 395-407.

Sharpe, R. M. (1994). Regulation of spermatogenesis. In E. Knobil & J. D. Neill (Eds.), The Physiology of Reproduction (2nd ed., pp. 1363-1434). New York: Raven Press.

Sinha Hikim, A.P., Maiti, B.R. & Ghosh, A. (1985) Spermatogenesis in the bandicoot rat. I. Duration of the cycle of the seminiferous epithelium. Archives of Andrology, 14, 151-154.

Sinha Hikim, A.P., Rajavashisth, T.B., Sinha Hikim, I., Lue, Y., Bonavera, J.J., Leung, A., Wang, C. & Swerdloff, R.S. (1997) Significance of apoptosis in the temporal and stage-specific loss of germ cells in the adult rat after gonadotropin deprivation. Biology of Reproduction, 57, 1193-1201.

Sinha Hikim, A.P., Wang, C., Lue, Y., Johnson, L., Wang, H.-H. & Swerdloff R.S. (1998) Spontaneous germ cell apoptosis in humans: evidence for ethnic differences in the susceptibility of germ cells to programmed cell death. Journal of Clinical Endocrinology and Metabolism, 83, 152-156.

Smithwick, E.B., Young, L.G. & Gould, K.G. (1996) Duration of spermatogenesis and relative frequency of each stage in the seminiferous epithelial cycle of the chimpanzee. Tissue and Cell, 28, 357-366.

Tait, A.J. & Johnson, E. (1982) Spermatogenesis in the grey squirrel (Sciurus carolinensis) and changes during sexual regression. Journal of Reproduction and Fertility, 65, 53-58.

Wanichanon, C., Weerachatyanukul, W., Suphamungmee, W., Meepool, A., Apisawetakan, S., Linthong, V., Sretarugsa, P., Chavadej, J., Sobhon, P. (2001). Chromatin condensation during spermiogenesis in rats. *Science Asia, 27*, 211-220.

Ward, W. S., Partin, A. W., & Coffey, D. S. (1989). DNA loop domains in mammalian spermatozoa. Chromosoma, 98, 153-159.

Ward, W. S., & Coffey, D. S. (1991). DNA packaging and organization in mammalian spermatozoa: Comparison with somatic cells. Biology of Reproduction, 44, 569-574.

Weinbauer, G.F., Aslam, H., Krishnamurthy, H., Brinkworth, M.H., Einspanier, A. & Hodges, J.K. (2001) Quantitative analysis of spermatogenesis and apoptosis in the common marmoset (Callithrix jacchus) reveals high rates of spermatogonial turnover and high spermatogenic efficiency. Biology of Reproduction, 64, 120-126.

Wistuba, J.A, Schrod, A., Grewe, B., Hodges, J.K., Aslam, H., Weinbauer, G.F. & Luitjens, C.M. (2003) Organisation of seminiferous epithelium in primates: relationship to spermatogenic efficiency, phylogeny, and mating system. Biology of Reproduction, 69, 582-591.

Yanagimachi, R. (1994). Mammalian fetilization, chapter 5. In Knobil E. & J. D. Neill (Eds.), The physiology of reproduction, Second edition (pp. 189-317). New York: Raven Press.

Zweidler, A. (1978). Resolution of histones by polyacrylamide gel electrophoresis in the presence of nonionic detergents. *Method Cell Biology. 17*, 223-233.

OUTPUT OF RESEARCH PROJECT

1. List of Publications

1.1 Unusual germ cell organization in the seminiferous epithelium of a murid rodent from southern Asia, the greater bandicoot rat, *Bandicota Indica*. In International Journal of Andrology, 2004.

P. Worawittayawong[1, 2], C.M. Leigh[1], G. Cozens[3], E.J. Peirce[1], B.P. Setchell[1], **P. Sretarugsa**[2], A. Dharmarajan[3], W.G. Breed[1]

[1]Department of Anatomical Sciences, The University of Adelaide, Australia
[2]Department of Anatomy, Mahidol University, Bangkok, Thailand
[3]School of Anatomy and Human Biology, The University of Western Australia, Australia (เอกสารหมายเลข 1)

1.2 Chromatin organization and basic nuclear proteins in the male germ cells of the greater bandicoot rat, *Bandicota indica*.

We are preparing in manuscript for publication and will be submitted to Biology of Reproduction or Molecular Reproduction and Development.

2. Application

This study will provide the better understanding of spermatogenesis in *Bandicoda indica* especially, the process of chromatin condensation during spermiogenesis. Interestingly, the basic nuclear proteins, histones are present in all stages of spermatids and mature sperm as well. Moreover, the transition proteins (TPs) are also found in the epididymal sperm and their amount seem to be much higher than protamines. This is in contrast to the other mammal such as rat, mouse and human which TPs are absent in these species.

Apart from this academic contribution, I do expect that this project will give a chance to the young scientist to gain more experience as well as having a critical thinking in synthesizing and analysing the scientific information.

3. List of presentations

3.1 Oral Presentation:

3.1.1 Is the highly divergent sperm nuclear shape in bandicoot rats due to an unusual process of chromatin condensation?

***P Worawittayawong[1,2], P Sretarugsa[1]**, C.M. Leigh[2], W.G. Breed[2]

[1]Department of Anatomy, Mahidol University, Bangkok, Thailand
[2]Department of Anatomical Sciences, University of Adelaide, Adelaide, Australia
In the 3rd ASEAN Microscopy Conference and 19th Annual Conference of EMST on January 30th – February 1st, 2002 in Chiang Mai, Thailand (เอกสารหมายเลข 2)

3.1.2 Qualitative and Quantitative Production of Spermatozoa in the Asian Bandicoot Rat, *Bandicota indica*.

***P Worawittayawong[1,2]**, C Leigh[1], E Peirce[1], **P Sretarugsa[2]**, W Breed[1]

[1]Department of Anatomical Sciences, University of Adelaide, Adelaide, Australia
[2]Department of Anatomy, Mahidol University, Bangkok, Thailand
In the 49th AGM The Australian Mammal Society on 7-9 July 2003 at Sydney University, Australia (เอกสารหมายเลข 3)

3.2 Poster Presentation:

3.2.1 Is the highly divergent sperm nuclear shape in bandicoot rats due to an unusual process of chromatin condensation?

***P Worawittayawong[1,2], P Sretarugsa[1]**, C.M. Leigh[2], W.G. Breed[2]

[1]Department of Anatomy, Mahidol University, Bangkok, Thailand
[2]Department of Anatomical Sciences, University of Adelaide, Adelaide, Australia
In RGJ- Ph.D. Congress III on 25-27 April 2002 at Jomtien Palm Beach Resort, Pattaya, Chonburi (เอกสารหมายเลข 4)

3.2.2 A possible cause for the presence of vacuoles in the nucleus of spermatids and spermatozoa of the bandicoot rat (*Bandicota indica*)

***P Worawittayawong[1,2]**, C.M. Leigh[1], **P Sretarugsa[2]**, W.G. Breed[1]

[1]Department of Anatomical Sciences, University of Adelaide, Adelaide, Australia
[2]Department of Anatomy, Mahidol University, Bangkok, Thailand
In RGJ- Ph.D. Congress V on 23-25 April 2004 at Jomtien Palm Beach Resort, Pattaya, Chonburi (เอกสารหมายเลข 5)

APPENDIX

	I	J	A		5	2	9	B	Dispatch: 9.12.04	Journal: IJA	CE: Vd
	Journal Name			Manuscript No.					Author Received:	No. of pages: 10	PE: Valarmathi

เอกสารหมายเลข 1

international journal of andrology, (2004)

10.1111/j.1365-2605.2004.00529.x

Unusual germ cell organization in the seminiferous epithelium of a murid rodent from southern Asia, the greater bandicoot rat, *Bandicota Indica*

P. WORAWITTAYAWONG,*† C. M. LEIGH,* G. COZENS,‡ E. J. PEIRCE,* B. P. SETCHELL,* P. SRETARUGSA,† A. DHARMARAJAN‡ and W. G. BREED*

*Department of Anatomical Sciences, The University of Adelaide, Australia, †Department of Anatomy, Mahidol University, Bangkok, Thailand, and ‡School of Anatomy and Human Biology, The University of Western Australia, Australia

Summary

In the greater bandicoot rat, *Bandicota indica*, of south-east Asia, nine cell associations were documented in the testicular seminiferous epithelium. In about 10% of the tubule cross sections two or more cell associations occurred and, furthermore, some of the generations of germ cells within the cell associations were sometimes either out of phase, or missing, in the tubule cross sections. These features, together with the fact that this species has a highly pleiomorphic sperm head shape, are somewhat reminiscent of those of the seminiferous epithelium in humans and some other primates but not of common laboratory rodents. This species could thus be a good model for investigating irregular patterns of spermatogenesis in naturally occurring wild species of rodent.

Keywords: bandicoot rat, seminiferous epithelium, apoptosis

Introduction

In sexually mature, adult, males of most mammalian species germ cell production occurs in a highly regulated and organized way with the resultant spermatozoa having a uniform, and species-specific, shape. In species such as the laboratory rat and mouse, as well as in farm animals, the maturing germ cells within the testicular seminiferous epithelium are organized into a series of characteristic cell associations of various maturational stages that occupy the entire cross-sectional area of a seminiferous tubule. At any one point along a tubule, there is a change in the cell associations over time with the length of time it takes to pass through all of the cell associations resulting in a cycle of the seminiferous epithelium (Leblond & Clermont, 1952; Hess, 1990; Russell *et al.*, 1990). Furthermore, along the length of a tubule at any one time, different cell associations are present with the consequence that a wave of the seminiferous epithelium occurs (Perey *et al.*, 1961). In the human testis however, the germ cell organization is quite different as cross-sections of the seminiferous tubules display multiple cell associations including some that have an atypical composition of germ cell developmental stages (Clermont, 1964; Heller & Clermont, 1964). Moreover, adjacently located cell associations do not precede or follow each other consecutively in the cycle of the seminiferous epithelium (Heller & Clermont, 1964), although some, but not all, workers believe that a spiral wave is present (Schulze & Rehder, 1984; Johnson, 1994a). Tubule cross-sections with more than one cell association or stage of the cycle of seminiferous epithelium are also common in some other primates including apes and New World monkeys (Smithwick *et al.*, 1996; Weinbauer *et al.*, 2001; Wistuba *et al.*, 2003). Germ cell production in humans is also less efficient than that in laboratory rats (Johnson *et al.*, 1980, 2000) with apoptosis occurring in spermatogonia and

Correspondence: W.G. Breed, Department of Anatomical Sciences, The University of Adelaide SA 5005, Australia. E-mail: bill.breed@adelaide.edu.au

primary spermatocytes as well as in spermatids (Sinha Hikim *et al.*, 1997, 1998). Additionally, in humans, unlike in common laboratory rodents, the final form of the spermatozoon is highly pleiomorphic with some sperm having nuclear vacuoles (Bedford *et al.*, 1973; Fawcett, 1975).

Cell associations within the testes have been described for various rodent species besides common laboratory mice and rats, including hamsters (Clermont & Trott, 1969; Oud & de Rooij, 1977), prairie voles (Schuler & Gier, 1976), field voles (Grocock & Clarke, 1975, 1976), bank voles (Grocock & Clarke, 1976), grey squirrels (Tait & Johnson, 1982), mole rats (Redi *et al.*, 1986), Asian gerbils (Bilaspuri & Kaur, 1994), viscachas (Munoz *et al.*, 1998), capybaras (Paula *et al.*, 1999), lesser bandicoot rats (Sinha Hikim *et al.*, 1985), plains rats (Peirce & Breed, 1987) and hopping mice (Peirce & Breed, 1987). In all of these species, with the exception of the hopping mouse *Notomys alexis* (Peirce & Breed, 1987), a similar germ cell organization to that of the laboratory rat and mouse was found to occur.

A study of the sperm morphology of the three species of Asian bandicoot rats, genus *Bandicota*, has shown that, whereas lesser bandicoot rats have a similar sperm morphology to that of laboratory rats, this is not the case for the greater bandicoot rat, *Bandicota indica* where a very different, and highly variable, sperm head and nuclear morphology is present (Breed, 1993, 1998, 2004). Because of this highly divergent sperm head shape and the fact that these sperm, like those of humans, shows a high degree of pleiomorphism, we, in this study, ask two related questions. First, 'What is the organization of the seminiferous epithelium?' and secondly, 'Do adult males of this species, like humans, show unusually high levels of germ cell apoptosis?'

Materials and methods

Animals

Greater Bandicoot rats, *B. indica*, were collected in Thailand from near Maesod, Tak Province in October 2001 (n = 22, 11 females, 11 males) and in Supanburi Province in January 2003 (n = 21, 10 females, 11 males). After returning the animals to the laboratory at Mahidol University, Bangkok, they were anaesthetized and their sex, weight and reproductive condition was determined. In the 2001 sample, two of the 11 females were pregnant and two of the 11 males had sperm in the cauda epididymides, whereas in the 2003 sample seven of the 10 females were pregnant, another had recently ovulated, and all 11 males had sperm in the cauda epididymides.

Tissue preparation

From the males with sperm, small pieces of one testis and epididymis were removed and rapidly fixed in 3% glutaraldehyde/3% paraformaldehyde made up in 0.1 M phosphate buffer, pH 7.4, whereas the other testis was fixed whole using the same fixative. The tissue was then returned to The University of Adelaide, South Australia, where the small pieces of testes were post-fixed in 1% osmium, dehydrated and embedded in epoxy resin. Larger pieces of fixed tissue were removed from the whole testis, dehydrated and embedded in paraffin wax. From the epoxy resin-embedded testis samples, 0.5–1 µm thick plastic sections were cut and stained with toluidine blue. From the paraffin-embedded blocks, 6–8 µm thick sections were cut and stained with either H & E or PAS and haematoxylin.

Organization and frequency of stages of the seminiferous epithelium

The testicular seminiferous epithelium in both epoxy embedded and paraffin sections was analysed for the two animals with sperm collected in 2001 and four of the males collected in 2003. Nine cell associations were characterized, based on the appearance of the younger generation of spermatids within the seminiferous epithelium. The relative frequencies of the different cell associations, and the number of tubular cross-sections displaying more than one cell association, were determined in epoxy sections by scoring at least 130 tubular cross-sections from at least three different locations within the testis for each male.

Germ cell apoptosis

For determining the numbers and distribution of germ cells undergoing apoptosis terminal deoxynucleotide transfer-mediated dUTP nick end-labelling (TUNEL) was carried out on 6 µm thick paraffin sections using an ApopTag Peroxidase in situ apoptosis detection kit (Intergen Co., New York, USA) after 10-min incubation at room temperature for proteinase K digestion (see Lareu *et al.*, 2003).

Sperm morphology

For assessing the pleiomorphism in the sperm head nuclei, cauda sperm from four of the animals collected in January 2003 were placed on glass slides and then stained with dilute propidium iodide. The slides were viewed with an Olympus BH epifluorescent microscope using a 515 nm excitation filter and an IFK 90 nm barrier filter with an absorption wavelength of 535 nm and an emission wavelength of 617 nm. Photographs of the nuclei of cauda epididymal sperm were taken using an Olympus C-4040 zoom digital camera and 196–327 sperm randomly counted from each of these individuals and allocated to the various nuclear morphotypes.

Results

The body weights of the two 2001 individuals studied in detail with sperm were 655 and 561 g respectively and the average paired testes weight 2105 mg, whereas in the 2003 sample mean (±SE) body weight was 489 ± 55 g and paired testes weight 2.095 ± 287 mg (n = 7). As these testes

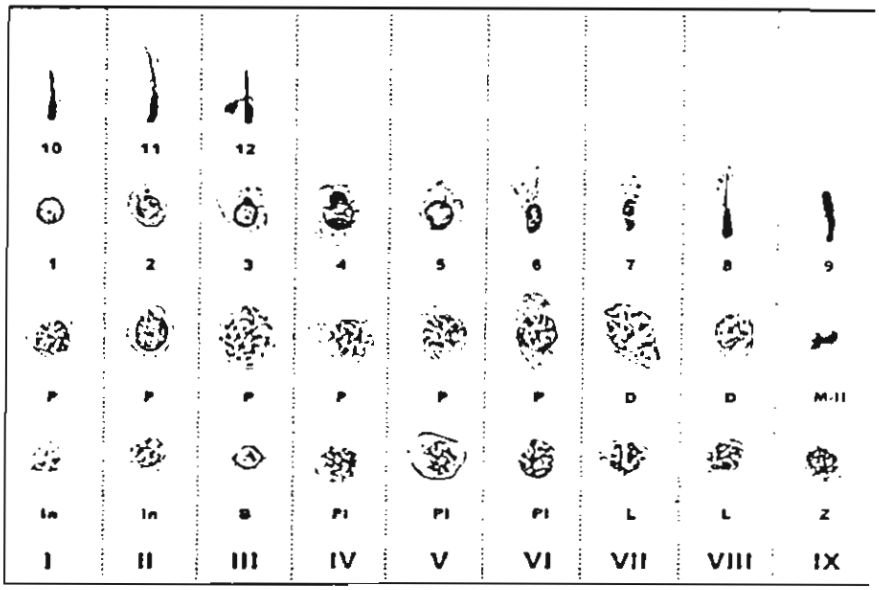

Figure 1. A map of the stages of the cycle of seminiferous epithelium in *Bandicota indica*, showing the phases of germ cell development Type A spermatogonia have been omitted In, B = intermediate, and B spermatogonia, PL = preleptotene; L = leptotene, Z = zygotene; P = pachytene; D = diplotene primary spermatocytes; M–II = meiosis II; 1–12 = steps of spermatid maturation (for more details see text and Figs 2 and 3).

weights are similar to those of mature male greater bandicoot rats caught previously (Breed & Taylor, 2000), and some females in both the 2001 and 2003 samples were pregnant, it is assumed that the males investigated were sexually mature.

Stages of the cycle of the seminiferous epithelium

The classification system used to determine the germ cell associations was that based on the morphological appearance of the younger generation of spermatids in the cell associations with Stage I beginning at the completion of the second meiotic division (see Russell *et al.*, 1990). The cycle of the seminiferous epithelium was divided into 9 cell associations or stages based on spermatid characteristics. In cycle Stages I–III one generation of pachytene primary spermatocytes and two generations of spermatids were present, whereas Stages IV–VIII had two generations of primary spermatocytes but only one generation of spermatids. Stage IX was characterized by the presence of meiotic figures in the older population of spermatocytes or by the presence of secondary spermatocytes.

Morphology and organization of the germ cells of the various cycle stages as seen in the toluidine blue-stained epoxy sections are described below (see Fig. 1 for summary). The cell associations were also identified in PAS and haematoxylin-stained paraffin sections, however cellular preservation and detail were not as good as in the plastic sections and thus the latter were used for describing the cell associations. Type A spermatogonia were present in all cell associations; they were flattened cells displaying extensive cytoplasmic contact with the basement membrane of the seminiferous tubule and had an ovoid nucleus that occupied a major portion of the cell.

Stage I was defined by the presence of small round spermatids without a visible Golgi complex or acrosomal vesicle (Fig. 2a). Type A and occasional intermediate spermatogonia or spermatogonia undergoing mitosis were present at the base of the seminiferous epithelium. The nuclei of intermediate spermatogonia were characterized by patches of heterochromatin around the nuclear envelope (Fig. 2a) whereas those of type A spermatogonia contained little heterochromatin. Pachytene primary spermatocytes had chromatin condensed into thick strands and, above them several layers of early spermatids with round nuclei were present. Situated between, and above, the round spermatids were groups of elongated spermatids in which there were intensely stained nuclei with acrosomes that were generally oriented towards the basement membrane (Fig. 2a).

Stage II was defined by the presence of round spermatids with a Golgi complex adjacent to the nucleus. Acrosomal vesicles or granules were present within the spermatid cytoplasm, but had little contact with the nuclear envelope (arrow – Fig. 2b). Intermediate spermatogonia were present. Round, pachytene primary spermatocytes contained large central, round nuclei with condensed, tightly packed, chromosomes. Early spermatids with central round nuclei were located above the pachytene primary spermatocytes and elongated late spermatids were present, with some of the nuclei having an apical extension (arrowhead – Fig. 2b) or an indented nuclear envelope (asterisk – Fig. 2b). The acrosomes of late spermatids were stained lighter than the nuclei and generally remained oriented towards the basement membrane.

Stage III was characterized by enlargement of the acrosome of the round spermatids. During this stage, the acrosome was round, attached to the anterior pole of the nucleus and spread over about 15° of the nuclear surface (Fig. 2c). Type B spermatogonia were present and characterized by having nuclei with an ovoid to round profile that displayed intensely stained chromatin along the nuclear envelope (arrowhead – Fig. 2c). There were two to three

COLOUR FIG.

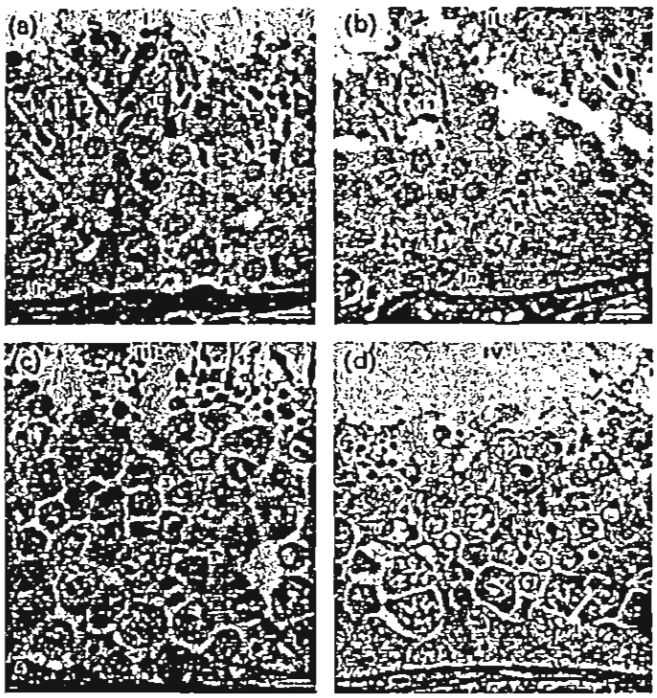

Figure 2. The stages of the cycle of seminiferous epithelium in *Bandicota indica* as shown in plastic sections stained with toluidine blue. (a)–(d) Stages I–IV respectively. A, In, B = A, intermediate, and B spermatogonia; Pl = preleptotene primary spermatocyte; L = leptotene primary spermatocyte; Z = zygotene primary spermatocyte; P = pachytene primary spermatocyte; D = diplotene primary spermatocyte; 1–12 = steps of spermatid maturation. All scale bars = 10 μm.

layers of pachytene primary spermatocytes that had round, heterochromatic, nuclei. Several layers of early round spermatids were located above the pachytene primary spermatocytes and along their nuclear envelopes in some regions there was intensely stained chromatin (Fig. 2c, arrow). The round spermatids were oriented in various directions, in some the acrosome was directed towards the basement membrane whereas in others it faced the lumen (Fig. 2c). In all round spermatids, the acrosome stained strongly with toluidine blue. Late spermatids had their heads located close to the luminal surface of the seminiferous epithelium. In these cells the chromatin was highly condensed and abundant residual bodies were present around the perimeter of the lumen of the seminiferous tubule (Fig. 2c) suggesting the shedding of considerable amounts of germ cell cytoplasm at this time.

In Stage IV the acrosome of the early spermatids was larger than that observed in Stage III and, in some cases, it had become somewhat oval in shape. It extended from 15° to about 45° over the nuclear surface. The spermatid nuclei were mostly round, with intensely stained chromatin along the nuclear envelope (arrow – Fig. 2d) although, in some, the nuclear envelope was flattened beneath the acrosome. These spermatids were located close to the lumen and oriented in various directions. During this stage, mitosis of Type B spermatogonia to form preleptotene primary spermatocytes occurred. The nuclei of the latter cells were generally round in shape, and contained lightly stained fine chromatin threads. Pachytene primary spermatocytes were larger than preleptotene primary spermatocytes and were irregular in shape. Late spermatids had been released into the lumen and were generally not evident although abundant residual bodies could still be seen close to the tubule lumen.

Stage V was characterized by spermatids having an acrosome that was crescent shaped and covered about a quarter of the anterior surface of the nucleus (Fig. 3a). Their nuclei were round or slightly ovoid with lightly stained chromatin. Many residual bodies remained near the luminal surface during this stage. The acrosome, which had reached its maximum size, was very intensely stained and in most cases oriented towards the basement membrane. Preleptotene primary spermatocytes, which were round with central nuclei and lightly stained chromatin, were generally present, whereas the pachytene primary spermatocytes, that were also present, had round nuclei with dense heterochromatin.

Some of the spermatids of Stage VI had nuclei that were a little bilaterally elongated. They were located near the lumen and had homogeneously stained chromatin. The acrosome

COLOUR FIG.

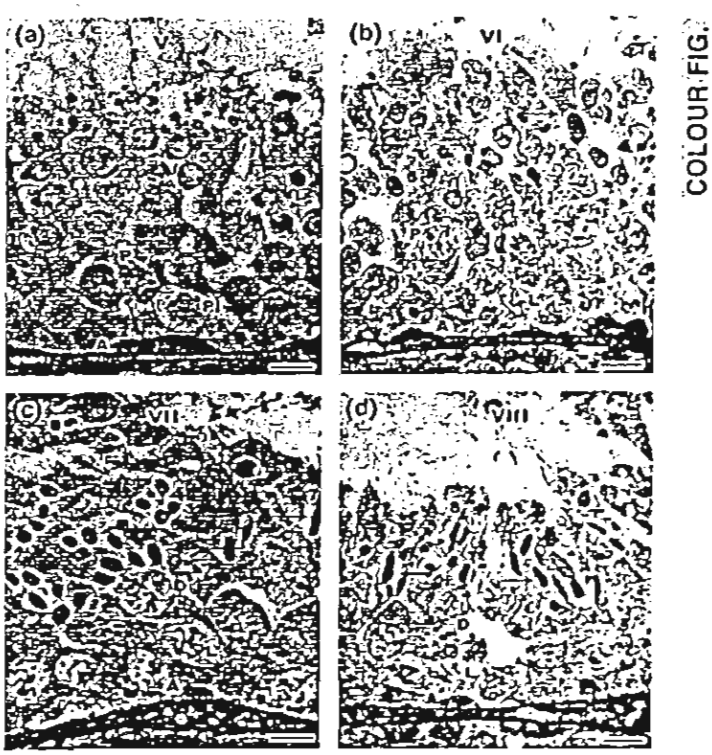

Figure 3. The stages of the cycle of seminiferous epithelium in *Bandicota indica* as shown in plastic sections stained with toluidine blue. (a)–(d) Stages V–VIII respectively. A, In, B = A, intermediate, and B spermatogonia, Pl = preleptotene primary spermatocyte; L = leptotene primary spermatocyte, Z = zygotene primary spermatocyte; P = pachytene primary spermatocyte, D = diplotene primary spermatocyte; 1–12 = steps of spermatid maturation. All scale bars = 10 μm.

was intensely stained and oriented towards the base of the tubule. In these cells the cytoplasm had migrated posteriorly (arrow – Fig. 3b) resulting in the acrosome being generally close to the plasma membrane. Leptotene primary spermatocytes occurred, which were round cells with large round nuclei and tightly packed threads of chromatin. Either pachytene, or occasionally diplotene, primary spermatocytes were present and generally ovoid in shape. Their nuclei were round and contained conspicuous chromatin threads.

In Stage VII, the spermatid nuclei were reduced in size compared with those in Stage VI and they stained more strongly with toluidine blue. They were generally oriented towards the basal lamina and the chromatin was condensed along the nuclear envelope (arrow – Fig. 3c). The acrosome covered the anterior region of nucleus and was deeply stained. Leptotene primary spermatocytes contained round central nuclei with thicker chromatin threads. Diplotene primary spermatocytes were irregular in shape, had spherical nuclei, and were larger in diameter than the pachytene primary spermatocytes at the previous stage. Their chromatin was loosely packed and most of the nucleus was only weakly stained (Fig. 3c).

Stage VIII had spermatids that were elongated and had more strongly stained chromatin than in the previous stage. They were embedded in recesses of the cell membrane of the Sertoli cells and oriented towards the basal lamina. Nuclear vacuoles could be seen (arrowhead – Fig. 3d). Most of the late spermatids had nuclei with apical extension(s) (arrows – Fig. 3d), and acrosomes that were lightly stained. Leptotene and diplotene primary spermatocytes had similar morphologies to those of Stage VII.

Stage IX began with the diplotene spermatocytes undergoing meiosis to form early round spermatids and ended with the completion of the second meiotic division. Zygotene primary spermatocytes were present and round in shape; the strongly stained nuclei showed more tightly packed chromatin than those of leptotene primary spermatocytes. The late spermatids were elongated and located near the lumen, and their chromatin had condensed along the nuclear envelope. The acrosome was strongly stained.

Frequencies (%) of the stages of cycle of the seminiferous epithelium

The frequency of each of the nine cell associations is presented in Table 1. The total number of seminiferous tubule cross sections counted was 1230 from six animals, two of which were collected in 2001 and the other four in 2003. Stage II occurred most often, with an average frequency of 28.5% (range 11.1–41.6%), whereas Stage VIII was the least frequent, and was observed in only three of six animals with a range of 1–3.7%. In three males (Bi 2–003, Bi 5–001, Bi 14–001) Stage II was the most frequent, whereas Stage V was the most common in Bi 7–003, Bi 8–003 and Bi 11–003. Although some variation in the most frequent cell associations was found between animals, in all cases Stages VII, VIII

Table 1. Number and frequency (%) of each germ cell association in seminiferous tubule cross sections of greater bandicoot rats

	Number and frequency (%) of tubules with typical cell associations									Total no. with typical cell associations	No. with atypical associations (%)	No. with multi-stage associations (%)
Animal no.	I	II	III	IV	V	VI	VII	VIII	IX			
Bi 5·001	25 (11.2)	65 (29.0)	36 (16.1)	45 (20.1)	21 (9.4)	8 (3.6)	4 (1.8)	0	20 (8.9)	224	18 (6.5)	34 (12.3)
Bi 14·001	22 (11.9)	77 (41.6)	36 (19.5)	23 (12.4)	19 (10.3)	6 (3.2)	1 (0.5)	0	1 (0.5)	185	62 (22.7)	26 (9.5)
Bi 2·003	26 (11.4)	76 (33.3)	25 (11.0)	47 (20.6)	15 (6.6)	14 (6.1)	4 (1.8)	3 (1.3)	18 (7.9)	228	6 (2.3)	32 (12.0)
Bi 7·003	10 (9.8)	21 (20.6)	14 (13.7)	20 (19.6)	22 (21.6)	11 (10.8)	0	1 (1.0)	3 (2.9)	102	12 (8.5)	27 (19.1)
Bi 8·003	7 (6.5)	12 (11.1)	16 (14.8)	16 (14.8)	26 (24.1)	24 (22.2)	2 (1.9)	4 (3.7)	1 (0.9)	108	22 (15.5)	12 (8.3)
Bi 11·003	11 (10.8)	20 (19.6)	17 (16.7)	12 (11.8)	25 (24.5)	10 (9.8)	6 (5.9)	0	1 (1.0)	102	21 (15.9)	9 (6.8)
Total (mean)	101 (10.6)	271 (28.5)	144 (15.2)	163 (19.1)	128 (13.5)	73 (7.7)	17 (1.8)	8 (0.8)	44 (4.6)	949	141 (11.5)	140 (11.4)

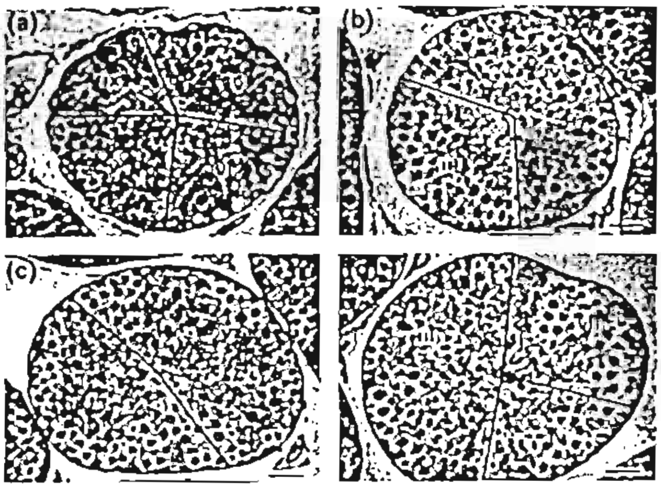

Figure 4. Seminiferous tubules of *Bandicota indica* testis containing more than one cell association in the same cross-section (a) Stages V, VI and IX, (b) Stages II and IV, (c) Stages I and V and (d) Stages III, IV and VII. All scale bars = 25 μm

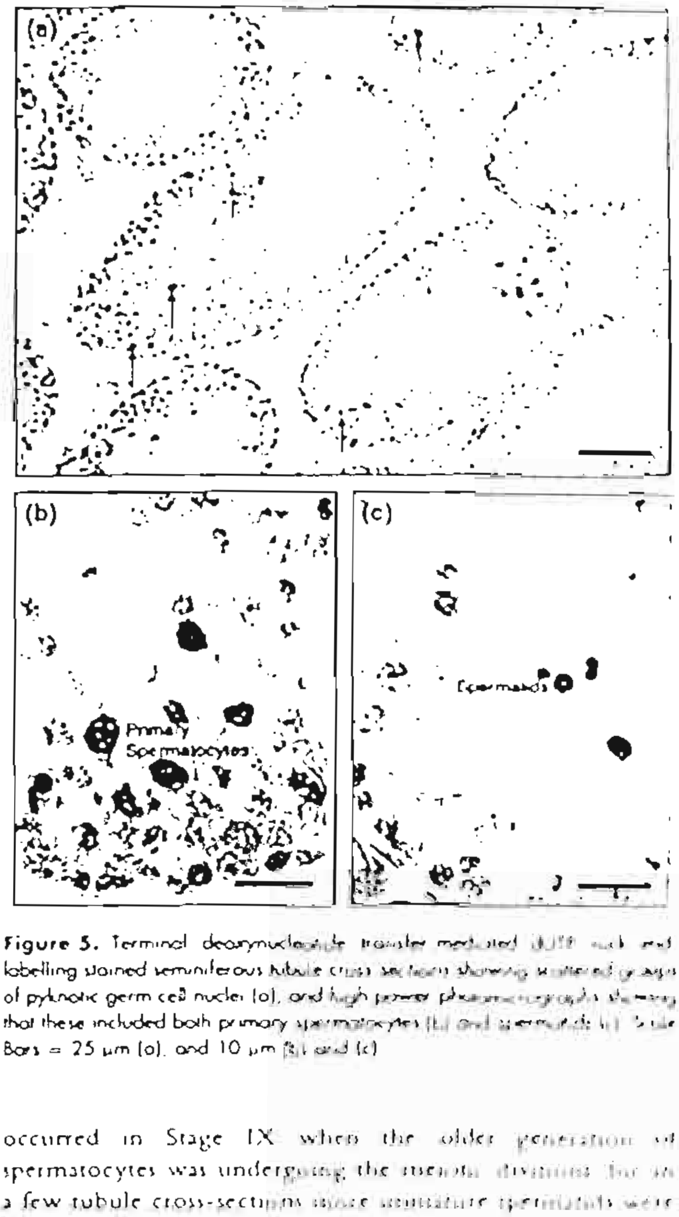

Figure 5. Terminal deoxynucleotide transfer mediated dUTP nick end labelling stained seminiferous tubule cross sections showing scattered groups of pyknotic germ cell nuclei (a), and high power photomicrographs showing that these included both primary spermatocytes (b) and spermatids (c). Scale Bars = 25 μm (a), and 10 μm (b) and (c)

and IX each comprised <10% of the total number of tubule cross sections and Stage I never exceeded 12% of the total.

In 140 of 1230 tubule cross-sections examined, more than one cell association was present in the tubule cross section. Such tubule cross-sections occurred with an average frequency of 11.4% (range 6.8–19.1% for the different individuals). The most common mixed cell associations in the tubule cross sections were either Stages I and IX, V and VI, or III and IV, but many combinations of cell associations (see Fig. 4a–d) were found to occur occasionally. Three, or even four, stages were present in a single cross section in 14 of the tubule cross-sections examined, e.g. in Bi 2-003 there were Stages V, VI and IX in one tubule cross section (see Fig. 4a).

In 141 of the 1230 tubule cross sections examined there was at least one germ cell population that was different from that normally seen within the cycle stage, with the result that atypical cell associations were present. Such associations occurred in an average of 11.5% (range 2.3–22.7%) of tubules examined for a particular individual. Animals Bi 8-003, Bi 11-003, and Bi 14-001 all had >15% tubule cross-sections with atypical cell associations (Table 1). Most abnormalities were associated with cell association IV. Normally in this stage there is no highly condensed spermatid population close to the lumen as recent release of spermatozoa had generally occurred. However, in some tubule cross sections, late spermatids were still present, and preleptotene primary spermatocytes were absent. In other cases of atypical cell associations a generation of germ cells was absent from the typical cell association (e.g. in Stage III where there were no late spermatids in the cross section of one tubule), or development of a spermatid population appeared to be delayed with respect to the other germ cell types present. For example, Step 9 spermatids generally occurred in Stage IX when the older generation of spermatocytes was undergoing the meiotic divisions but in a few tubule cross-sections more immature spermatids were seen to occur in conjunction with the meiotic figures.

The TUNEL results showed that occasional germ cells were undergoing apoptosis at the time the animals were killed. These cells either occurred singly or as small groups in a particular tubule cross section (Fig. 5a). Although the cells most frequently undergoing apoptosis were leptotene and zygotene primary spermatocytes (Fig. 5b), occasionally apoptotic spermatogonia and spermatids were also seen (Fig. 5c).

Nuclear pleomorphism of mature spermatozoa

Fluorescent microscopy, after staining with the DNA dye propidium iodide, indicated a range of different nuclear shapes occurred, the most frequent of which are shown in Fig. 6. Table 2 shows the frequency of the seven different nuclear morphotypes that were most commonly seen. It is clear that in all individuals a range of different nuclear shapes

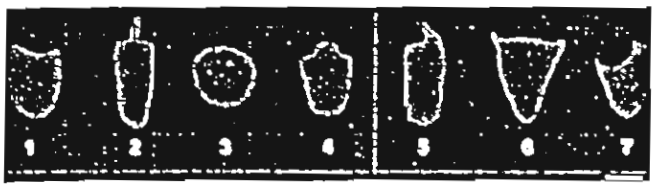

Figure 6. Fluorescence microscopy of nuclei of cauda epididymal sperm from one *Bandicota indica* adult male stained with propidium iodide showing highly variable nuclear shape. Scale bar = 2·8 μm.

were evident. In Bi 4-003 and Bi 7-003 morphotype 1 was the most frequent, whereas in Bi 6-003 morphotype 2 predominated, whereas in Bi 11-003 morphotype 3 was by far the most common.

Discussion

Although there is some basic knowledge of the oestrous cycle, pregnancy length and litter size of female greater bandicoot rats (Boonsong, 1984), and the sperm morphology of males (Breed, 1993; 1998), the organization of male germ cells in the testis has not been described for this species. In the present study we have found that the germ cell organization during the cycle of seminiferous epithelium in greater bandicoot rats is more variable that of both laboratory rodents and a closely related species, the lesser bandicoot rat (Sinha Hikim *et al.*, 1985).

In cross sections of seminiferous tubules of the laboratory rodents, as well as of the lesser bandicoot rat, the same cell association generally occupies an entire tubule cross section. In greater bandicoot rats, by contrast, this is sometimes not the case. In all of the individuals of this species that were investigated, around 10% of the tubule cross-sections contained two or more cell associations. In some of these multi-stage tubular cross-sections, the cell associations present were sequential in the cycle of the seminiferous epithelium, and thus represent the spatial transition from one stage to the next. Such an organization is consistent with a segmental arrangement of associations along the length of a tubule as occurs in the laboratory rat (Perey *et al.*, 1961; Russell *et al.*, 1990). In the other multi-stage cross sections however, cell associations adjacent to each other in the epithelium were non-sequential. The organization within these tubular cross sections therefore somewhat resembles that of humans (Clermont, 1963; Schulze & Rehder, 1984; Johnson, 1994b), and some other primate species (Chowdhury & Steinberger, 1976; Smithwick *et al.*, 1996; Wistuba *et al.*, 2003) in which cell associations are confined to smaller regions of the epithelium and may have a spiral wave, in contrast to that of common laboratory rodents or the other species of bandicoot rat, *B. bengalensis*.

The organization of the seminiferous epithelium in the testis of greater bandicoot rats also differs from that of the laboratory rodents and lesser bandicoot rats with respect to the constancy of germ cell composition of particular cell associations. Whereas in the latter species particular maturational stages of germ cells nearly always occur in synchrony with other specific maturational stages (Leblond & Clermont, 1952; Clermont, 1972), in the greater bandicoot rats between 2 and 23% (average 13%) of the tubule cross sections had at least one group of maturing germ cells within a cell association that was out of synchrony with the rest and, occasionally, a particular generation of germ cells appeared to be completely missing. Individual cell associations occupying smaller areas of the epithelium and the mixing of germ cells between associations at their physical boundaries may partially explain an increased incidence of atypical cell associations in this species, however it can not account for missing germ cell generations. Missing germ cell generations could reflect a lack of spermatogonial divisions during a particular cycle, or the death of an entire cohort of cells such that no cells of a particular type are encountered within a section of tissue. Why this might occur more often in this species however, remains to be determined.

In the atypical cell associations observed, the germ cell population most commonly out of synchrony with the other cell populations was the most mature spermatid population. The relatively common occurrence of elongated spermatids in stage IV indicates a delay in spermiation, although spermatids at an earlier step in spermiogenesis than that in a typical cell association also occurred. A delay or arrest in spermatid development, resulting in atypical cell associations,

Table 2. Numbers of sperm nuclei in the various different shape categories shown in Fig. 6 for four individual greater bandicoot rats

		Sperm nuclear shapes (see Fig. 6)[b]						
Animal no.	N°	1	2	3	4	5	6	7
Bi 4·003	289	92 (32%)	55 (19%)	29 (10%)	14 (5%)	35 (12%)	12 (4%)	52 (18%)
Bi 6·003	186	13 (7%)	73 (39%)	0	56 (30%)	26 (14%)	9 (5%)	9 (5%)
Bi 7·003	327	108 (33%)	0	26 (8%)	56 (17%)	26 (8%)	36 (11%)	75 (23%)
Bi 11·003	276	41 (15%)	14 (5%)	215 (78%)	0	6 (2%)	0	0

[a]Total number of sperm counted for each individual.
[b]Numbers refer to head shape shown in Fig. 6.

has been documented during the establishment of spermatogenesis in pubertal golden hamsters (Miething, 1998), but disappears as Leydig cell maturation is completed. However, both groups of male bandicoot rats we obtained were collected at the same place and time as pregnant females. Furthermore, since the body and testes weights were typical of sexually mature, adult males of the species (Breed & Taylor, 2000), we thus assume that these males were sexually mature and not just entering the onset of spermatogenesis. Another possible explanation for spermatid variability within an association in this species relates to the pleiomorphism observed in mature spermatozoa. Perhaps differences in the appearance of the elongated spermatid populations in some associations reflect variability in the nuclear form of the spermatozoa.

Several possible explanations have been put forward for the synchronous development of different generations of germ cells within a cell association, including interactions between the germ cells and Sertoli cells that regulate development, factors produced by more mature germ cell populations influencing the development of younger cell generations, and simultaneous activation of different developmental events in the germ cell lineage at a specific locality by periodic stimuli (Russell *et al.*, 1990). Whatever the cause, from its organization, it appears that maturation of germ cells within the seminiferous epithelium of the greater bandicoot rat is not be as tightly synchronized as that of common laboratory rats (Russell *et al.*, 1990) and lesser bandicoot rats (Sinha Hikim *et al.*, 1985). Furthermore, when TUNEL was carried out, it was found that occasional apoptotic cells, including spermatogonia, primary spermatocytes and spermatids, were scattered throughout the germinal epithelium. This is similar to the situation in human testes (Brinkworth *et al.*, 1997; Sinha Hikim *et al.*, 1998), but unlike that in the testes of laboratory rats and mice (Brinkworth *et al.*, 1995; Sinha Hikim *et al.*, 1997; Krishnamurthy *et al.*, 1998).

This study thus shows that this species of bandicoot rat, *B. indica*, has several features of the germ cell organization in the testis that differ from that of the laboratory rat and lesser bandicoot rats. In some regards they show some similarity to that of humans, apes and New World primates (Chowdhury & Steinberger, 1976; Johnson *et al.*, 1992; Johnson, 1994a; Smithwick *et al.*, 1996; Wistuba *et al.*, 2003). Greater bandicoot rats have previously been found also to have highly derived and pleiomorphic cauda epididymal sperm populations (Breed, 1993, 1998) and, in the present study, the pleiomorphic nature of the sperm nuclei was also confirmed. Furthermore, previous transmission electron microscope studies have shown nuclear vacuoles were sometimes present in spermatids and epididymal spermatozoa and that there is a variable response between the spermatozoa in chromatin dispersion when cauda spermatozoa are incubated in detergents (Breed, 1998). Therefore, the present observations, together with those made previously, indicate that some of the processes of germ cell maturation and the final form of the sperm of the greater bandicoot rat show some similarity to the situation in humans (Bedford *et al.*, 1973; Fawcett, 1975).

In conclusion, the greater bandicoot rat, that is a common and widespread species throughout much of south-east Asia (Corbett & Hill, 1992; Musser & Carleton, 1993), may turn out to be a useful model for investigations on the processes controlling spermatogenesis and sperm form because of the lack of tight synchrony in both germ cell maturation and final sperm form that occurs. Andrologists in south-east Asia may thus have a very useful model for probing questions on the regulatory processes of male germ cell morphogenesis and maturation both of which are extremely poorly understood phenomena at the present time (Sharpe, 1994).

Acknowledgements

This work was in part funded by a grant from the Thailand Research Fund through the Royal Golden Jubilee PhD Program (Grant No. PHD/00196/2541) and in part by the Australian Research Council and The University of Adelaide. We thank Leigh Clark for carrying out pilot work on TUNEL for apoptosis and Fiona Khor for initial studies on the germ cell associations of this species.

References

Bedford, J. M., Bent, M. J. & Calvin, H. (1973) Variations in the structural characters and stability of the nuclear chromatin in morphologically normal human spermatozoa. *Journal of Reproduction and Fertility* 33, 19–29.

Bilaspuri, G. S. & Kaur, R. (1994) Spermatogenic cells and stages of the seminiferous epithelial cycle in the Indian Gerbil Field Rat, *Tatera indica*. *Reproduction Fertility and Development* 6, 699–704.

Boonsong, P. (1984) Some biological aspects of the great bandicoot (*Bandicota indica* Bechstein). *Agricultural Research Journal* 2, 135–145.

Breed, W. G. (1993) Novel organisation of the spermatozoon in two species of murid rodents from southern Asia. *Journal of Reproduction and Fertility* 99, 149–158.

Breed, W. G. (1998) Interspecific variation in structural organisation of the spermatozoon in the Asian Bandicoot rats, *Bandicota* species (family Muridae). *Acta Zoologica* 79, 277–285.

Breed, W. G. (2004) The spermatozoon of Eurasian murine rodents: its morphological diversity and evolution. *Journal of Morphology* 261, 52–69.

Breed, W. G. & Taylor, J. (2000) Body mass, testis mass, and sperm size in murine rodents. *Journal of Mammalogy* 81, 758–768.

Brinkworth, M. H., Weinbauer, G. F., Schlatt, S. & Nieschlag, E. (1995) Identification of male germ cells undergoing apoptosis in adult rats. *Journal of Reproduction and Fertility* 105, 25–33.

Brinkworth, M. H., Weinbauer, G. F., Bergmann, M. & Nieschlag, E. (1997) Apoptosis as a mechanism of germ cell loss in elderly men. *International Journal of Andrology* 20, 222–228.

Chowdhury, A. K. & Steinberger, E. (1976) A study of germ cell morphology and duration of spermatogenic cycle in the baboon *Papio anubis*. *Anatomical Record* **185**, 155–170.

Clermont, Y. (1963) The cycle of the seminiferous epithelium in man. *American Journal of Anatomy* **112**, 35–51.

Clermont, Y. (1972) Kinetics of spermatogenesis in mammals: seminiferous epithelium cycle and spermatogonial renewal. *Physiology Reviews* **52**, 198–236.

Clermont, Y. & Trott, M. (1969) Duration of the cycle of the seminiferous epithelium in the mouse and hamster determined by means of 3H-thymidine and radioautography. *Fertility and Sterility* **20**, 805–817.

Corbett, G. B. & Hill, J. E. (1992) *The Mammals of the Indomalayan Region: A Systematic Review*, pp. 488. Oxford University Press, Oxford.

Fawcett, D. W. (1975) The Mammalian spermatozoon. *Developmental Biology* **44**, 394–436.

Grocock, C. A. & Clarke, J. R. (1975) Spermatogenesis in mature and regressed testes of the vole (*Microtus agrestis*). *Journal of Reproduction and Fertility* **43**, 461–470.

Grocock, C. A. & Clarke, J. R. (1976) Duration of spermatogenesis in the vole (*Microtus agrestis*) and bank vole (*Clethrionomys glareolus*). *Journal of Reproduction and Fertility* **47**, 133–135.

Hess, R. A. (1990) Quantitative and qualitative characteristics of the stages and transitions in the cycle of the rat seminiferous epithelium: light microscopic observations of perfusion-fixed and plastic-embedded testes. *Biology of Reproduction* **43**, 525–542.

Johnson, L. (1994a) A new approach to study the architectural arrangement of spermatogenic stages revealed little evidence of a partial wave along the length of human seminiferous tubules. *Journal of Andrology* **15**, 435–441.

Johnson, L. (1994b) Efficiency of spermatogenesis. *Microscopy Research and Technique* **32**, 385–422.

Johnson, L., Petty, C. S. & Neaves, W. B. (1980) A comparative study of daily sperm production and testicular composition in humans and rats. *Biology of Reproduction* **22**, 1233–1243.

Johnson, L., Chaturvedi, P. K. & Williams, J. D. (1992) Missing generations of spermatocytes and spermatids in seminiferous epithelium contribute to low efficiency of spermatogenesis in humans. *Biology of Reproduction* **47**, 1091–1098.

Johnson, L., Varner, D. D., Roberts, M. E., Smith, T. L., Keillor, G. E. & Scrutchfield, W. L. (2000) Efficiency of spermatogenesis: a comparative approach. *Animal Reproduction Science* **60–61**, 471–480.

Krishnamurthy, H., Weinbauer, G. F., Aslam, H., Yeung, C.-H & Nieschlag, E. (1998) Quantification of apoptotic testicular germ cells in normal and methoxyacetic acid-treated mice as determined by flow cytometry. *Journal of Andrology* **19**, 71–717

Lareu, R. R., Lacher, M. D., Bradley, C. K., Sridaran, R., Friis, R. R. & Dharmarajan, A. M. (2003) Regulated expression of inhibitor of apoptosis protein 3 in the rat corpus luteum. *Biology of Reproduction* **68**, 2232–2240.

Leblond, C. P. & Clermont, Y. (1952) Definition of the stages of the cycle of seminiferous epithelium in the rat. *Annals of the New York Academy of Science* **55**, 548–573.

Miething, A. (1998) The establishment of spermatogenesis in the seminiferous epithelium of the pubertal golden hamster (*Mesocricetus auratus*). In: *Advances in Anatomy, Embryology and Cell Biology*, Vol. 40. Springer, Berlin.

Munoz, E. M., Fogal, T., Dominguez, S., Scardapane, L., Guzman, J., Cavicchia, J. C. & Piezzi, R. S. (1998) Stages of the cycle of the seminiferous epithelium of the viscacha (*Lagostomus maximus maximus*). *The Anatomical Record* **252**, 8–16.

Musser, G. G. & Brothers, E. M. (1994) Identification of bandicoot rats from Thailand (Bandicota, Muridae, Rodentia). *American Museum Novitates* **3110**, 1–56

Musser, G. G. & Carleton, M. D. (1993) Family Muridae. In: *Mammal Species of the World*, 2nd edn (eds D. E. Wilson & D. M. Reeder), pp. 501–755. Smithsonian Institute, Washington, DC, USA.

Oud, J. J. & de Rooij, D. G. (1977) Spermatogenesis in the Chinese hamster. *The Anatomical Record* **187**, 113–124.

Paula, T. A. R., Chianni-Garcia, H. & Franca, L. R. (1999) Seminiferous epithelium cycle and its duration in capybaras (*Hydrochoerus hydrochaeris*). *Tissue & Cell* **31**, 327–334.

Peirce, E. J. & Breed, W. G. (1987) Cytological organization of the seminiferous epithelium in the Australian rodents *Pseudomys australis* and *Notomys alexis*. *Journal of Reproduction and Fertility* **80**, 91–103.

Perey, B., Clermont, Y. & Leblond, C. P. (1961) The wave of the seminiferous epithelium in the rat. *American Journal of Anatomy* **108**, 47–78.

Redi, C. A., Garagna, S., Heth, G. & Nevo, E. (1986) Descriptive kinetics of spermatogenesis in four chromosomal species of the *Spalax ehrenbergi* superspecies in Israel. *The Journal of Experimental Zoology* **238**, 81–88.

Russell, L. D., Ettlin, R. A., Sinha Hikim, A. P. & Clegg, E. D. (1990) *Histological and Histopathological Evaluation of the Testis*, pp. 286. Cache River Press, Vienna, IL, USA.

Schuler, H. M. & Gier, H. T. (1976) Duration of the cycle of the seminiferous epithelium in the prairie vole (*Microtus ochrogaster ochrogaster*). *Journal of Experimental Zoology* **197**, 1–11.

Schulze, W. & Rehder, U. (1984) Organization and morphogenesis of the human seminiferous epithelium. *Cell and Tissue Research* **237**, 395–407.

Sharpe, R. M. (1994) Regulation of spermatogenesis. In: *The Physiology of Reproduction*, 2nd edn (eds E. Knobil & J. D. Neill), pp. 1363–1434. Raven Press, New York.

Sinha Hikim, A. P. & Swerdloff, R. S. (1999) Hormonal and genetic control of germ cell apoptosis in the testis. *Reviews of Reproduction* **4**, 38–47.

Sinha Hikim, A. P., Maiti, B. R. & Ghosh, A. (1985) Spermatogenesis in the bandicoot rat. I. Duration of the cycle of the seminiferous epithelium. *Archives of Andrology* **14**, 151–154.

Sinha Hikim, A. P., Rajavashisth, T. B., Sinha Hikim, I., Lue, Y., Bonavera, J. J., Leung, A., Wang, C. & Swerdloff, R. S. (1997) Significance of apoptosis in the temporal and stage-specific loss of germ cells in the adult rat after gonadotropin deprivation. *Biology of Reproduction* **57**, 1193–1201.

Sinha Hikim, A. P., Wang, C., Lue, Y., Johnson, L., Wang, H.-H & Swerdloff, R. S. (1998) Spontaneous germ cell apoptosis in humans: evidence for ethnic differences in the susceptibility of germ cells to programmed cell death. *Journal of Clinical Endocrinology and Metabolism* **83**, 152–156.

Smithwick, E. B., Young, L. G. & Gould, K. G. (1996) Duration of spermatogenesis and relative frequency of each stage in the seminiferous epithelial cycle of the chimpanzee. *Tissue and Cell* **28**, 357–366.

Tait, A. J. & Johnson, E. (1982) Spermatogenesis in the grey squirrel (*Sciurus carolinensis*) and changes during sexual regression. *Journal of Reproduction and Fertility* **65**, 53–58.

Weinbauer, G. F., Aslam, H., Krishnamurthy, H., Brinkworth, M. H., Einspanier, A. & Hodges, J. K. (2001) Quantitative analysis of spermatogenesis and apoptosis in the common marmoset (*Callithrix jacchus*) reveals high rates of spermatogonial turnover and high spermatogenic efficiency. *Biology of Reproduction* **64**, 120–126.

Wistuba, J.A., Schrod, A., Grewe, B., Hodges, J. K., Aslam, H., Weinbauer, G. F. & Luttjens, C. M. (2003) Organisation of seminiferous epithelium in primates: relationship to spermatogenic efficiency, phylogeny, and mating system. *Biology of Reproduction* **69**, 582–591.

Received XX xxxxx 200x; revised XX xxxxx 200x; accepted XX 10 *xxxxx 200x*

ELECTRON MICROSCOPY SOCIETY OF THAILAND

3rd ASEAN Microscopy Conference

and

19th Annual Conference of EMST

January 30 - Feb [illegible] 2017

Chiang Mai [illegible]

Oral Presentation

J.E.M.S.T. Vol.16 No.1, pp 94-95, 2002
Printed in Thailand

P. Worawittayawong[1,2]
P. Sretarugsa[1]
C.M. Leigh[2]
W.G. Breed[2]

Is the Highly Divergent Sperm Nuclear Shape in Bandicoot Rats due to an Unusual Process of Chromatin Condensation?

[1] Department of Anatomy, Faculty of Sciences, Mahidol University, Bangkok, Thailand
[2] Department of Anatomical Sciences, Adelaide University SA 5005 Australia

The sperm head of mammals is largely composed of a nucleus and acrosome and in most murid rodents it is falciform in shape. Two southern Asian murids in the genus *Bandicota*, however, have evolved a unique sperm head that is conical with a small nucleus capped by a massive acrosome. In the present study we investigate the histochemistry of sperm chromatin during late spermiogenesis. For this, male *B indica* were collected in Thailand in September 1996 and January 2001. Testes were fixed in 3% buffered glutaraldehyde and either osmicated and stained with lead citrate and uranyl acetate, or fixed with alcoholic 3% phosphotungstic acid (PTA) overnight. In conventionally stained material chromatin appeared as large cords within which there were nuclear vacuoles with 50-90 nm electron-dense globules. PTA-stained material showed variable staining; some had peripheral electron-dense chromatin (Fig.1-4), suggesting lysine or thiol-rich nucleoproteins in these regions. How the chromatin is eventually packaged remains undetermined, but these observations indicate some unusual features of chromatin organization during late spermiogenesis; this may relate to the bizarre sperm head shape that eventually results.

Acknowledgement

This work was supported by Royal Golden Jubilee Thai Program, Thailand Research Fund.

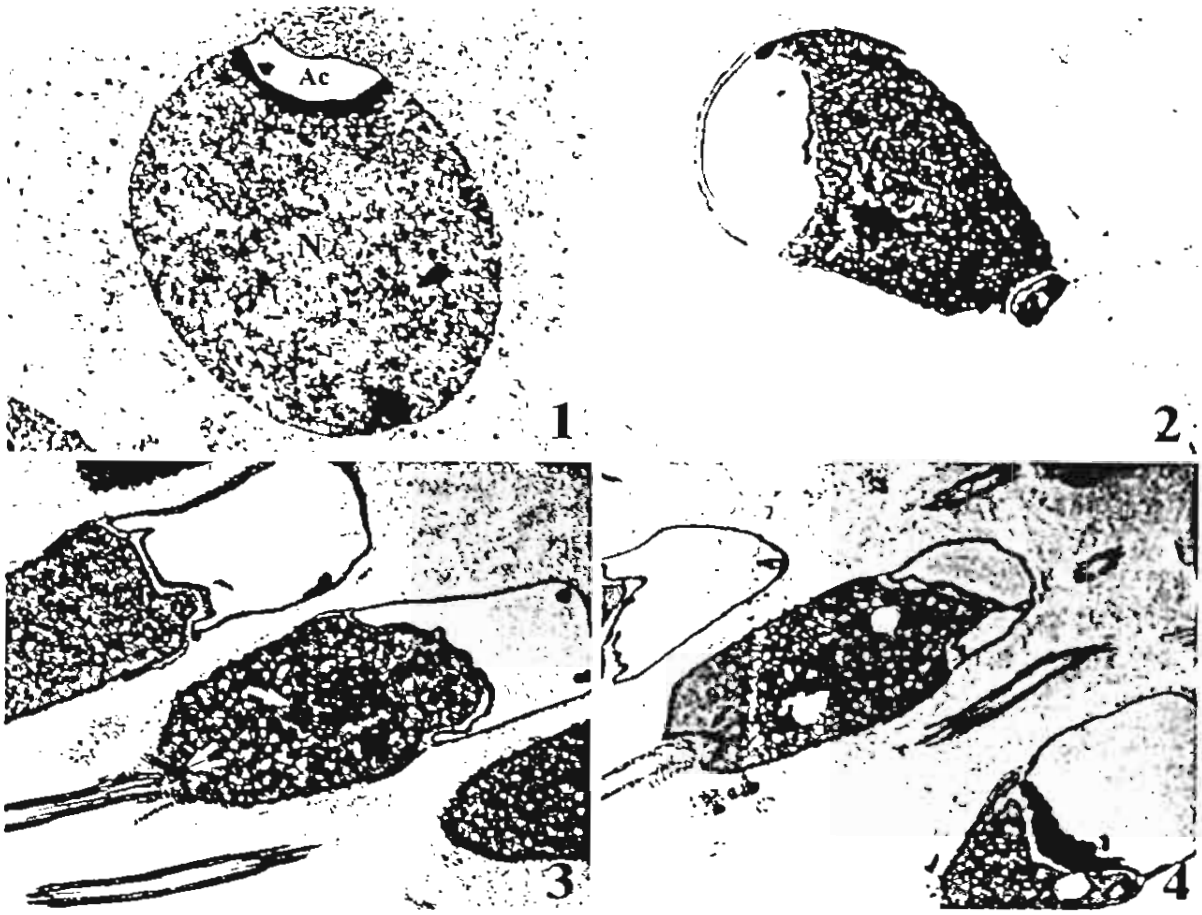

Fig.1 Early spermatid; dispersed chromatin in the nucleus (N) ; with strong PTA stained material under the acrosome (Ac).

Fig.2 Late spermatid; strong PTA stained chromatin in the posterior region of the nucleus; anteriorly a small localized (arrow) region of PTA positive material also occurs.

Fig. 3 Late spermatid or probable spermatozoan; strong PTA stained material in upper middlle part of nucleus (arrow) and near the basal plate (two arrows)

Fig. 4 Very late spermatid or probable spermatozoan; sperm nucleus with no PTA-staining except the region in basal plate (arrow)

ABSTRACTS

Forty-ninth AGM

The Australian Mammal Society

7-9 July 2003

Sydney University

Spoken papers pages 1-37
* Asterisks indicate the person delivering the paper

Poster papers pages 39-49

WIGGINS[1,2*], Natasha; McArthur[1,2], Clare; McLean[3], Stuart; and Boyle[3], Rebecca
[1]Cooperative Research Centre for Sustainable Production Forestry
[2]School of Zoology, University of Tasmania, GPO Box 252-05, Hobart, Tas, 7001
[3]School of Pharmacy, University of Tasmania, GPO Box 252-26, Hobart, Tas, 7001

EFFECTS OF TWO PLANT SECONDARY METABOLITES, CINEOLE AND GALLIC ACID, ON NIGHTLY FEEDING PATTERNS OF THE COMMON BRUSHTAIL POSSUM

Plant secondary metabolites (PSMs) can assist in a plant's defence against herbivory. The common brushtail possum (*Trichosurus vulpecula*) is a generalist folivore, adapted to consume a variety of plants. This enables them to encounter a wide range of PSMs, but each at low concentrations. We are interested in the behavioural responses of herbivores to PSMs, and what implications these responses have on their diet. The aim of this investigation was to determine patterns of feeding behaviour in brushtail possums in response to PSMs occurring in foliage they naturally consume.

We introduced two PSMs, cineole and gallic acid, into an artificial diet. Firstly, we tested whether possums altered their feeding behaviour in response to increasing levels of cineole. Diets contained three concentrations of cineole; zero, medium and high. Following this, possums were offered a choice PSM diet (cineole and gallic acid diets simultaneously) or a no-choice PSM diet (containing either cineole or gallic acid). With increasing cineole levels, possums ate less, had smaller feeding bouts, and had a lower rate of intake, but did not extend their total nightly feeding time. Possums offered the choice PSM diet compared with the no-choice diets, ate more, had larger feeding bouts, and tended to increase their rate of intake. These results indicate that PSMs not only constrain overall intake, but that possums alter their feeding behaviour in response to them. Altered feeding patterns may reduce the negative influence of PSMs on intake.

WORAWITTAYAWONG[1,2*], P., Leigh[1], C., Peirce[1], E., Sretarugsa[2], P., and Breed[1], W.
Bolliger Award Candidate
[1]Department of Anatomical Sciences, University of Adelaide
[2]Department of Anatomy, Mahidol University, Bangkok, Thailand

QUALITATIVE AND QUANTITATIVE PRODUCTION OF SPERMATOZOA IN THE ASIAN BANDICOOT RAT, *BANDICOTA INDICA*

The genus of the southern Asian murid rodent *Bandicota* is close to *Rattus*. Nevertheless, previous observations have shown that, in two species, highly divergent spermatozoa from those of *Rattus* occur in which there is generally a globular sperm head and very short tail. The present study on one of these species, *B. indica*, has quantitatively determined in 10 adult males (i) the variation in sperm head shape, and (ii) the organisation of the germ cells during maturation within the seminiferous epithelium. For the former approximately 100 cauda epididymal sperm from each individual were measured and allocated to one of several morphotypes and, for the latter, plastic sections of the testes were cut, stained with toluidine blue, and germ cell maturational stages determined in around 100 tubule cross sections from each individual.

The results showed that, although all sperm had pyriform or globular-shaped heads, there were invariably several different morphotypes present within the mature sperm population. Within the seminiferous tubules, 8 germ cell associations were recognised of varying abundance and sometimes germ cells out of synchrony with the typical cell association were found. These findings highlight that, in this species, sperm form shows marked heterogeneity as well as variable degrees of synchrony between the maturing germ cells within the cell associations. This suggests that the genetic control of sperm form has been relaxed such that synchrony of germ cell maturation does not occur and sperm pleiomorphism is evident in the mature spermatozoon population.

This work was sponsored by the Royal Golden Jubilee Thai Program, Thailand Research Fund.

RGJ - Ph.D. Congress III

เอกสารหมายเลข 4

การประชุมวิชาการ
โครงการปริญญาเอกกาญจนาภิเษก ครั้งที่ 3

25-27 เมษายน 2545
โรงแรมจอมเทียน ปาล์มบีช รีสอร์ท
เมืองพัทยา ชลบุรี

สกว
TRF

สำนักงานกองทุนสนับสนุนการวิจัย
The Thailand Research Fund

ISBN 974-7772-91-4

S3-P1

Is the Highly Divergent Sperm Nuclear Shape in Bandicoot Rats due to an Unusual Process of Chromatin Condensation?

P Worawittayawong[a, b], P Sretarugsa[a], CM Leigh[2] and WG Breed[b]
[a] *Department of Anatomy, Faculty of Sciences, Mahidol University, Bangkok, Thailand.*
[b] *Department of Anatomical Sciences[2], Adelaide University SA 5005 Australia.*

Objective

To investigate the histochemistry of sperm chromatin during spermiogenesis.

Methods

For this, male *B indica* were collected in Thailand in September 1996 and January 2001. Testes were fixed in 3% buffered glutaraldehyde and either osmicated and stained with lead citrate and uranyl acetate, or fixed with alcoholic 3% phosphotungstic acid (PTA) (2) overnight.

Results

The sperm head of mammals is largely composed of a nucleus and acrosome and in most murid rodents it is falciform in shape (1). Two southern Asian murids in the genus *Bandicota*, however, have evolved a unique sperm head that is conical with a small nucleus capped by a massive acrosome. In conventionally stained material chromatin appeared as large cords within which there were nuclear vacuoles with 50-90 nm electron-dense globules. PTA-stained material showed variable staining; some had peripheral electron-dense chromatin (Fig.1-4), suggesting lysine or thiol-rich nucleoproteins in these regions.

Conclusion

How the chromatin is eventually packaged remains undetermined, but these observations indicate some unusual features of chromatin organization during late spermiogenesis; this may relate to the bizarre sperm head shape that eventually results.

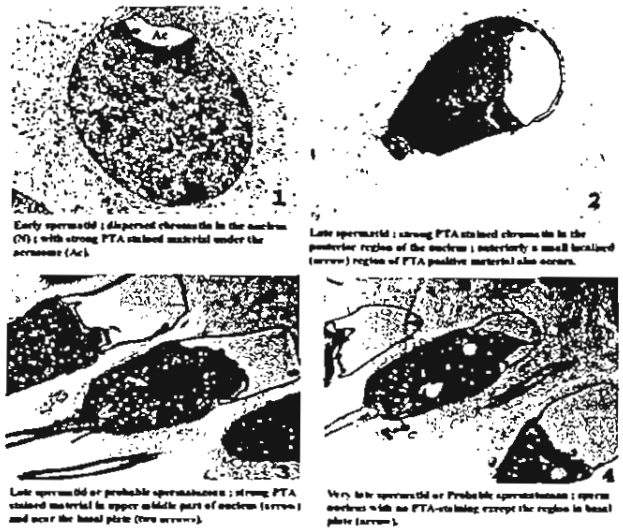

Keywords: sperm, bandicoot rat, chromatin, condensation.

References

1. WG Breed (1993) Novel organization of the spermatozoon in two species of murid rodents from Southern Asia. *J of Repro&Fer* 99, 149-58.
2. Jean-Luc Courtens and Maurice Loir (1981) A cytochemical study of nuclear changes in boar, bull, goat, mouse, rat, and stallion spermatids. *J of Ultrastructure Research* 74, 327-40.

RGJ - Ph.D. Congress V

เอกภาวิทยาเขต 5

การประชุมวิชาการ
โครงการปริญญาเอกกาญจนาภิเษก ครั้งที่ 5

23-25 เมษายน 2547
โรงแรมจอมเทียน ปาล์มบีช รีสอร์ท
เมืองพัทยา จังหวัดชลบุรี

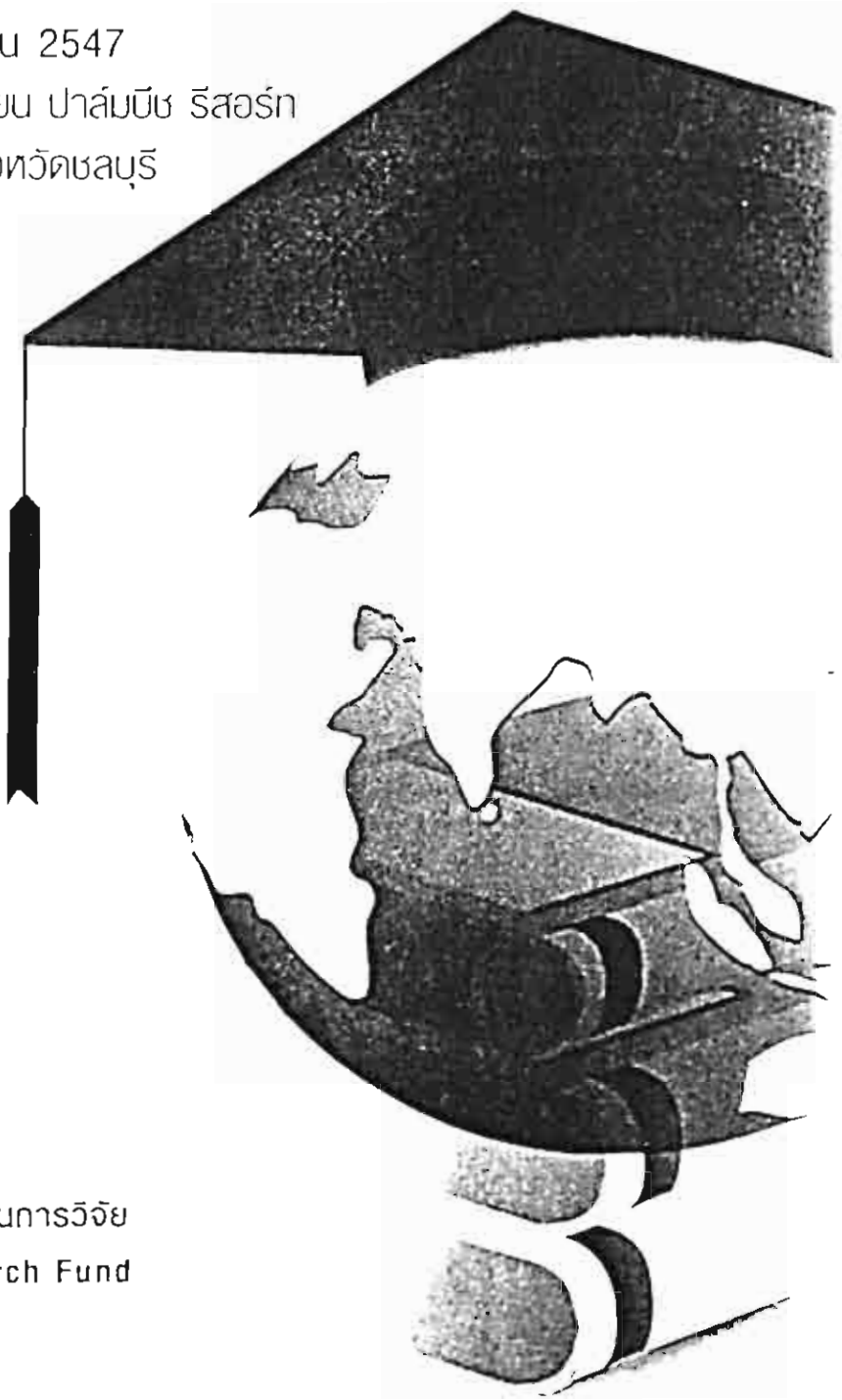

สกว
TRF

สำนักงานกองทุนสนับสนุนการวิจัย
The Thailand Research Fund

ISBN 974-9545-80-X

S3-P25

A Possible Cause for the Presence of Vacuoles in the Nucleus of Spermatids and Spermatozoa of the Bandicoot Rat (*Bandicota indica*)

P. Worawittayawong[a,b], C.M. Leigh[a], P. Sretarugsa[b] and W.G. Breed[a]

[a] *Department of Anatomical Sciences, Adelaide University SA 5005*

[b] *Department of Anatomy, Faculty of Sciences, Mahidol University, Bangkok, Thailand*

Objective

In this study we ask the following questions: what is the distribution of histones and transition proteins in the spermatid nuclei of the bandicoot rat, and do the nuclear vacuoles exhibit different proteins from the rest of the sperm chromatin?

Method

For routine TEM small pieces of testes were fixed in 2% glutaraldehyde, embedded in araldite, and stained in uranyl and lead citrate. For PTA staining testes were fixed in 4% glutaraldehyde, stained with 3% phosphotungstic acid (PTA) in 100% ethyl alcohol and embedded in Epon (1). For gold labeling with the antibodies to histones and transition proteins, pieces of testes were fixed in 0.5% glutaraldehyde, embedded in Lowicryl K4M, cut, and incubated in either a monoclonal anti-histone (H2A, H2B, H3, or H4) (2) or polyclonal anti-transition protein (TP1 or TP2) (3) antibody raised in rabbits. After washing, incubation in 10 nm gold conjugated goat antirabbit IgG was performed and distribution of gold particles determined.

Results

Routine TEM of spermatids showed that during chromatin condensation fibrillar chromatin with localized electron lucent regions with granules occurred. Further chromatin condensation then took place throughout most of the nucleus but the localized foci of electron lucent regions remained. Alcoholic PTA showed strong positive staining peripherally as well as in a localized area in the anterior region of the nucleus but this region did not appear to coincide with location of nuclear vacuoles. Observations of gold labeling with anti-TP1 showed abundant, widespread, labeling over the condensing chromatin but absence of labeling over the electron lucent nuclear vacuoles. Anti-TP2 and anti-H3 also labeled the condensing chromatin but not material in the nuclear vacuoles.

Conclusions

These results confirm that in the bandicoot rat condensing spermatid nuclei localized foci of electron lucent regions occur. These regions do not stain with alcoholic PTA nor does gold labeling with anti-TP1, anti-TP2, or anti-H3 antibodies occur over these regions unlike the rest of the condensing chromatin. We thus hypothesis that nuclear vacuoles may result from an absence of transition proteins being laid down during spermiogenesis, this may also be the case for vacuoles in human sperm nuclei.

Keywords: sperm, chromatin condensation, histone, Bandicoot rat

Selected References

1. Courtens, J. L. and Loir M. (1981). *J. Ultrast. Res.* 74: 322-326
2. Biggiogera, M., S. Muller, et al. (1992). *Micr. Res. Tech.* 20: 259-267
3. Oko, R. J., V. Jando, et al. (1996). *Biol. Reprod.* 54: 1141-1157.